

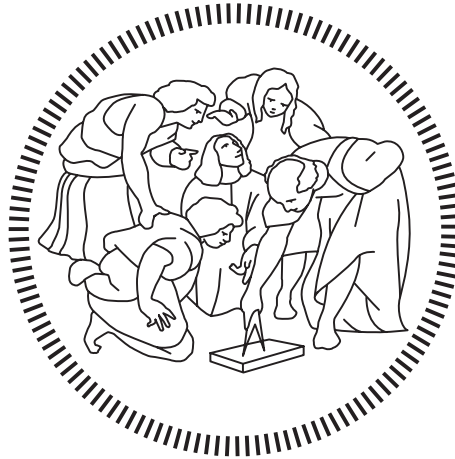
Politecnico di Milano

---

SCHOOL OF INDUSTRIAL AND INFORMATION ENGINEERING

Master of Science – Energy Engineering

Green Power System



## Hybridization of a CSP and PV Power Plant from an existing Coal Power Plant

Supervisor

Prof. Gianpaolo MANZOLINI

Co-Supervisor

Prof.ssa Cristina PRIETO RIOS

Candidate

Matteo CIRICILLO - 916740

---

Academic Year 2019 – 2020



# Acknowledgements

Questo lavoro è stato portato avanti con la speranza di ottenere un giorno non troppo lontano un mondo che si preoccupi veramente in che direzione sta prendendo e che rispetti e conviva con quelli che sono i ritmi della natura.

Dedicato a chi mi ha sempre supportato in questo lungo percorso di cinque anni e a chi come me condivide questa speranza per il nostro futuro.



# Sommario

Questa tesi è stata sviluppata con il proposito di dare visibilità e credibilità a nuove configurazioni di impianti ibridi basati su fonti rinnovabili.

Utilizzando come ipotesi di partenza l'utilizzo del ciclo di potenza di una già esistente centrale a carbone, si è convertito l'impianto in una soluzione ibrida CSP e PV.

Cercando di mantenere una produzione costante di 100 MW, si sono confrontate varie configurazioni: un impianto a torre solare munito di due torri, la soluzione ibrida citata, una configurazione ibrida di PV e sali fusi, implementando anche l'utilizzo di Carnot battery che sfruttasse gli eccedenti di produzione per alimentare il ciclo di potenza, ed infine una configurazione PV fornito di batterie LMO per garantire lo stesso tipo di funzionamento.

Utilizzando il software open source SAM (System Advisor Model) si sono calcolate le varie produzioni di energia elettrica nei vari impianti. Non prevedendo però il software configurazioni ibride, di due torri, o con produzione fissa costante, è stato necessario rielaborare i dati in uscita per ottenere risultati plausibili e coerenti con le ipotesi di partenza. A tal scopo sono stati utilizzati Excel e MATLAB, da cui poi sono stati graficati i risultati finali.

Con questi mezzi è stato possibile ottenere un impianto ibrido con fattore di capacità 74.7%, di cui 42.26% a pieno carico, e con una riduzione del LCOE del 22,3% rispetto a un impianto CSP e 7% rispetto ad un PV, utilizzati per lo stesso tipo di funzionamento.

La scelta di questo argomento per una possibile tesi è dovuta all'interesse rivolto al mondo delle rinnovabili e dell'innovazione ed in particolare al corso di Centrales Solares, condotto a Siviglia, oltre all'idea di utilizzare un software realmente utile in ambito lavorativo.



# Abstract

This work has been developed with the purpose of giving visibility and credibility to new hybrid plants configurations based on renewable sources.

Setting as a starting hypothesis the use of the power cycle of an already existing coal-fired power plant, the plant was converted into a hybrid CSP and PV solution.

Trying to maintain a constant production of 100 MW, several configurations have been compared: a solar tower system equipped with two towers, the aforementioned hybrid solution, a hybrid configuration of PV with molten salts, also implementing the use of Carnot battery that exploits the surplus production to feed the power cycle, and finally a PV configuration equipped with LMO batteries to guarantee the same type of operation.

Using the open source software SAM (System Advisor Model), the electricity productions of the plants were calculated. However, since the software did not provide with tools to deal with hybrid configurations, two towers, or with constant fixed production, it was necessary to re-elaborate the output data to obtain plausible results consistent with the initial hypotheses. For this purpose have been used Excel and MATLAB, from which final results have been plotted.

With those tools it has been able to obtain a Hybrid configuration with a Capacity factor of 74.7%, which 42.26% full load, with a LCOE reduction of 22,3% with respect a CSP plant and 7% to a PV one, both used in the same manner.

The choice of this topic for a possible thesis has to be found in the interest in the world of renewables and innovation and in particular to the Centrales Solares course, conducted in Seville, in addition to the opportunity to use real workplace renewable software.





# Table of Contents

<b>Acknowledgements .....</b>	<b>I</b>
<b>Sommario III</b>	
<b>Abstract V</b>	
<b>List of Figures .....</b>	<b>IX</b>
<b>Introduction 1</b>	
<b>Chapter 1 Possible alternatives .....</b>	<b>5</b>
1.1 Coal power plant conversion into CSP .....	5
1.2 Hybridization CSP and PV .....	6
1.2.1 Existent hybrid plants .....	6
<b>Chapter 2 Solar Energy.....</b>	<b>9</b>
2.1 Concepts.....	9
<b>Chapter 3 The three analysed technologies.....</b>	<b>17</b>
3.1 CSP .....	17
3.1.1 History of CSP.....	18
3.1.2 Components of CSP tower plant .....	20
3.2 PV .....	23
3.2.3 Histoy of PV .....	24
3.2.4 Componets of PV plant.....	28
3.3 Carnot battery plant.....	30
<b>Chapter 4 Technology compatibility.....</b>	<b>33</b>
4.1 Same aspects of the two technologies.....	33
4.2 Main differences .....	33
4.3 Possible outcome of the mix .....	34
<b>Chapter 5 Apology to Hybridation.....</b>	<b>35</b>
<b>Chapter 6 Used Software .....</b>	<b>39</b>
<b>Chapter 7 Case study.....</b>	<b>41</b>
7.1 Geographical location .....	41
7.1.1 Political and economical situation .....	42

7.2	Carbon plant model .....	42
7.2.2	Plant 1: Komati.....	43
7.2.3	Plant 2: Grootvlei .....	44
7.2.4	Plant 3: Camden .....	44
<b>Chapter 8</b>	<b>Implementation of the model .....</b>	<b>47</b>
8.1	Presentation of the analysed cases .....	47
8.1.1	Common hyphotesis .....	48
8.2	Solar Tower Plant .....	50
8.3	Solar Tower Plant + PV and Carnot battery .....	55
8.3.2	Solar Tower Plant.....	55
8.3.3	PV and Carnot battery .....	56
8.4	PV + molten salts and Carnot battery .....	59
8.5	PV + electrical storage.....	62
<b>Chapter 9</b>	<b>Results .....</b>	<b>65</b>
9.1	Solar Tower Plant .....	65
9.2	Solar Tower Plant + PV and Carnot battery .....	66
9.3	PV + molten salts and Carnot battery .....	68
9.4	PV + electrical storage.....	70
9.5	Summarised data output .....	72
9.6	Future development .....	74
<b>Conclusion</b>	<b>75</b>	
<b>Appendix I</b>		
<b>Acronyms</b>	<b>III</b>	
<b>Simbology</b>	<b>IV</b>	
<b>Bibliography</b> .....		<b>V</b>

# List of Figures

Figure 1-1 Irena Global energy transformation, a roadmap to 2050.....	3
Figure 1-1 Ouarzazate, Morocco, NOOR power plants.....	6
Figure 1-2 Dubai, United Arabs Emirates, Mohammed bin Rashid Solar Park.....	7
Figure 1-3 Atacama solar tower construction .....	8
Figure 1-4 NOOR Midelt, Hybrid solar plant [14] .....	8
Figure 2-1 Spectral radiation of a black body .....	10
Figure 2-2 AM explained graphically [18] .....	11
Figure 2-3 AM function of latitud [18].....	11
Figure 2-4 Componets of radiation [18] .....	12
Figure 2-5 Mean technologival values [15] .....	14
Figure 2-6 conductor, semiconductor, insulating materials behaviour .....	15
Figure 2-7 P-type and N-type Si doping.....	15
Figure 2-8 Adsorption bands [15].....	16
Figure 3-1 Different kinds of CSP technologies [20] .....	17
Figure 3-2 Giulio Parigi's burning mirrors, 1600, Uffizi Gallery, stanzino delle matematiche, Florence .....	18
Figure 3-3 Solar Motor Co. ....	19
Figure 3-4 Augustin Mouchot's Solar Generator (left), Frank Shuman's Parabolic Trough Plant in Egypt (right) .....	19
Figure 3-5 SEGS solar plants in the Mojave Desert (left), Solar Two (center), Solar furnace of Odeillo (right) .....	20
Figure 3-6 CSP total capacity, World 2008-2020 [25].....	20
Figure 3-7 Solar Tower CSP scheme [26] .....	21
Figure 3-8 Molten salt storage tanks.....	23
Figure 3-9 Bifacial cell in world market forecast [27] .....	24
Figure 3-10 from left to right: Edmond Becquerel, Willoughby Smith and Heinrich Hertz.....	24
Figure 3-11 Arco Solar, first commercial solar park, Hesperia, California .....	25
Figure 3-12 Global Renewable Cumulative Electricity Capacity Annual Percent Change [24] .....	26
Figure 3-13 PV total capacity, World 2008-2020 [25].....	26
Figure 3-14 Solar PV module cost 2010-2018 [29] .....	27
Figure 3-15 Differents solar panels characteristics [30] .....	28
Figure 3-16 I-V curves of a LR6-72PH-370M PV module (annex).....	29
Figure 3-17 Two axes configuration (left), one axis configuration (right).....	30
Figure 3-18 Schematic of PTES: a counterclockwise thermodynamic cycle is used to charge a thermal storage unit [32] .....	30
Figure 3-19 Malta Recuperative Bryton cycle (left) [36], Coal power plant scheme (right) [37, 36]	31
Figure 3-20 Pilot proget in Germany [37] .....	31
Figure 3-21 Phase 1 [37].....	32
Figure 3-22 Phase 2 [37].....	32
Figure 3-23 Phase 3 [37].....	32

Figure 5-1 Levelised cost of electricity and auction price trends for CSP, 2010-2022 [14] .....	37
Figure 6-1 National Renewable Energy Laboratory logo .....	39
Figure 6-2 System Advisor Model (SAM) first screen .....	40
Figure 7-1 Köppen-Geiger Climate Classification Map [48] .....	41
Figure 7-2 Komati power station .....	43
Figure 7-3 Residential houses built for the employees (left), View of the residential property with the .....	45
Figure 7-4 Simulation of the coal power plants disposal [65].....	46
Figure 8-1 Location and Resource data in SAM .....	48
Figure 8-2 Candem turbine data, Power Cycle in SAM .....	49
Figure 8-3 Lifetime Parameter in SAM .....	49
Figure 8-4 Financial Parameters in SAM.....	50
Figure 8-5 System Design in SAM (day) .....	50
Figure 8-6 System Design in SAM (night).....	51
Figure 8-7 Solar Multiple optimization in SAM Parametrics (day) .....	52
Figure 8-8 Heliostat Field in SAM (day) .....	53
Figure 8-9 Tower and Receiver Dimensions in SAM (day) .....	54
Figure 8-10 SAM results of the two simulation, day (left) and night (right) .....	54
Figure 8-11 Flow pattern and HTF type in SAM.....	56
Figure 8-12 SAM results of CSP simulation.....	56
Figure 8-13 Module and Inverter characteristics in SAM .....	57
Figure 8-14 PV design configuration.....	57
Figure 8-15 SAM results of PV simulation .....	58
Figure 8-16 PV design configuration.....	59
Figure 8-17 Tracking system.....	59
Figure 8-18 Modified costs in SAM.....	61
Figure 8-19 SAM results of PV simulation .....	61
Figure 8-20 PV design configuration.....	62
Figure 8-21 LMO Battery degradation in SAM.....	63
Figure 8-22 System Costs in SAM .....	63
Figure 8-23 SAM results of PV plus battery simulation .....	64
Figure 9-1 Power production in the two tower CSP plant (left), Daily Energy production in the two tower CSP plant (right) .....	65
Figure 9-2 Power production in summer (left) and winter, just before stop (right) .....	66
Figure 9-3 SAM PV power production .....	66
Figure 9-4 SAM production data summed up without any improvement (CSP + PV) (left), Power production of hybrid plant (orange) compared to original PV field production (black) (right).....	67
Figure 9-5 Daily Energy production in the hybrid plant.....	67
Figure 9-6 Energy produced by thermal storage (CSP + PV) in summer (left) and winter (right) ....	68
Figure 9-7 Power production in summer (left) and winter (right) .....	68
Figure 9-8 PV + molten salt plant production (orange) compared with PV electricity production in SAM (black) (left), Energy production by source (right) .....	69
Figure 9-9 Power produced by thermal storage in summer (left) and winter (right) .....	69
Figure 9-10 Power production in summer (left) and winter (right) .....	70
Figure 9-11 PV + LMO batteries production (blue) compared with PV electricity production in SAM (black) (left), Energy production by source (right).....	70

Figure 9-12 Power produced by LMO batteries in summer (left) and winter (right) .....71  
Figure 9-13 Power production in summer (left) and winter (right) .....71



# Introduction

Since the discovery of fire, the use of energy has always been a vehicle for change, improvement, progression. Over the centuries, the possibility of managing, storing and exploiting it at own advantage has brought to real revolutions in man's way of living and thinking.

As the first principle of thermodynamics states, Energy can be neither created nor destroyed, but is transformed from one form to another. Up to nowadays, the energy used has always been largely obtained by combustible sources, such as wood, coal, natural gas, oil and derivatives. Combustion is a chemical reaction of exothermic oxidation reduction, where one compound oxidizes while another reduces. In the case of fossil fuels, mainly hydrocarbons, the carbon oxidizes and the oxygen that feeds the reaction is reduced, with the formation of new compounds such as carbon dioxide and release of thermal energy that can be used to obtain work.

The over exploitation of this process which has been taking place since the first industrial revolution has led, as the scientific committee has been stating for more than half a century, to the production of a quantity of greenhouse gases greater than that which can be disposed of by our planet. Direct consequence is the increase of the average temperature and melting of glaciers, an increase in seas level and oceans acidity. “Carbon Dioxide levels are at their highest in 650.000 years”; “Nineteen of the twenty warmest years on record have occurred since 2001”; “In 2012, Artic summer sea ice shrank to the lowest enstent on record”; “Global average sea level has risen nearby 178 mm over the past 100 years” [1].

This contamination of the planet is not the only effect, during the process there is also the release in smaller quantities of other contaminants, which in high concentration poisons not only the area but also the population. “4.2 million deaths every year as a result of exposure to ambient (outdoor) air pollution; 3.8 million deaths every year as a result of household exposure to smoke from dirty cookstoves and fuels; 91% of the world’s population live in places where air quality exceeds WHO guideline limits” [2].

Thanks the awareness of these data since all over the past 30 years, the world has started to move, beginning in 1992 with the first United Nations Framework Conference on Climate Change (UNFCCC) where the need to intervene to limit greenhouse gas emission has been stated.

In 1997 it followed the Kyoto protocol, which has been active since 2005 and expects for a 5% reduction in greenhouse gas emissions by all member parties. The same script also defined operational tools, one of which is International Emission Trading (IET) which will create what is today the largest CO<sub>2</sub> market.

In 2015 the Paris agreement was signed, whose “central aim is to strengthen the global response to the threat of climate change by keeping a global temperature rise this century well below 2 degrees Celsius above pre-industrial levels and to pursue efforts to limit the temperature increase even further to 1.5 degrees Celsius. Additionally, the agreement aims to strengthen the ability of countries to deal with the impacts of climate change” [3]. Today ratified by 189 parts of the total 197 [3].

In line with these decisions, the production of energy from renewable sources has grown in recent years, from 156 billion kWh in 1990 to 1,645 trillion kWh in 2015 [4]. This sudden increase in the production of energy from alternative sources has also been made possible by the policies implemented in the OECD countries and in particular by Europe, with the liberalization of its energy market, or with incentives for the construction of new solar, wind and biomass plants; another strong point was the low price of the Asian workforce which allowed the beginning of the construction of components on a large scale and the exportation of these technologies, which are quick to install and put to work.

The increase in the percentage of energy produced from renewable sources, 26% of the global electricity share in 2018 according to IEA [5], has led to a decrease in the price of electricity. These technologies in fact exploit free sources available in nature, which do not need to be bought and / or stored, allowing a low production cost, limited to the construction and maintenance of the plant only and therefore guaranteeing its entry on the market as at a lower price.

However, the energy obtained from those sources are by their nature aleatory. The energy purchase system requires accurate information on the availability of production every 15 minutes, often difficult to guarantee by these technologies, causing problems of network stability.

In response to this need, reservoirs specifically prepared for the response are currently used. In absence of their availability, it is customary to activate auxiliary gas turbines used for this rapid response, however, thus increasing greenhouse gas emissions. Forecasts on solar and wind says they will contribute more than 85% of total electricity demand by 2050 [6]. Basically, a new storage system is needed for the future to come.



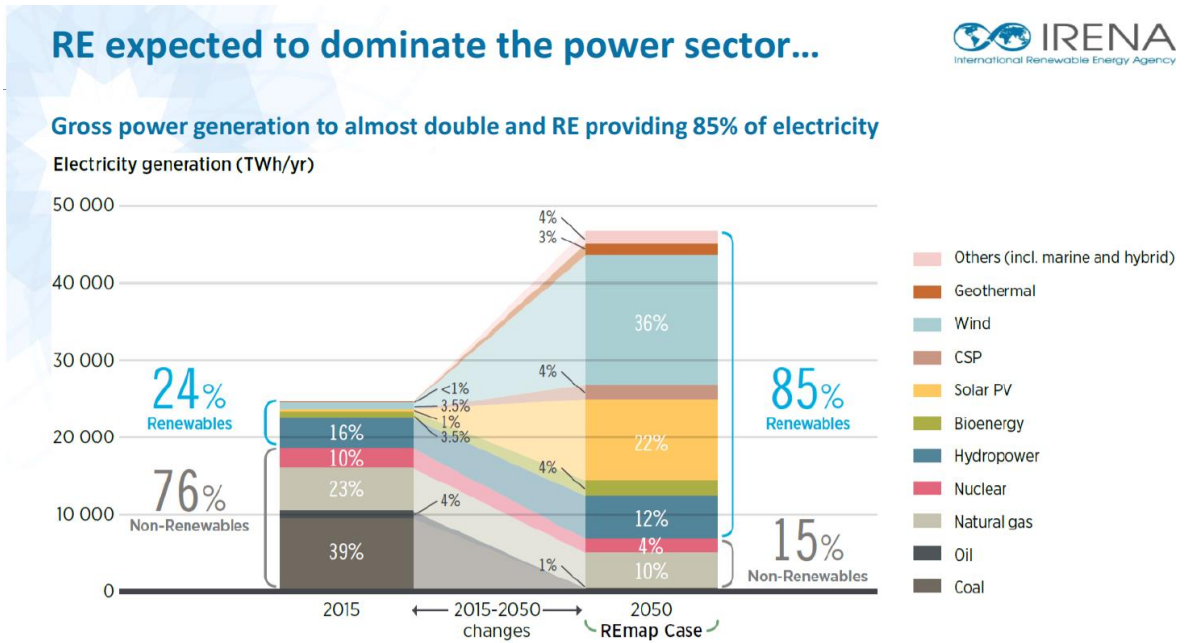


Figure 1-1 Irena Global energy transformation, a roadmap to 2050

Numerous studies are underway to solve this problem. A solution of current interest deals with the use of storage of electricity from renewable sources in batteries, technologically promising devices that allow a very rapid release response. However, despite the numerous improvements in this technology achieved in the last decade, the batteries are currently very expensive for such large quantities of stored energy, suffer greatly from temperature and operating cycle variations, and need to be replaced during the plant lifetime.

The subject of this thesis is an alternative solution to batteries, which allows to store energy from renewable sources, serving the grid and avoiding imbalances both in excess and in production defect, decreasing the emissions of carbon dioxide currently produced and proposing itself as a very new possible way to imagine energy management, for the first time in human history without the need for the use of combustible sources.



# Chapter 1 **Possible alternatives**

As anticipated in the introduction, this work not deals with an improvement of an existing technology, but with the hybridization of various technologies, existing since more or less time, with the aim of finding what nowadays is the ideal mix to satisfy the requests taken as a hypothesis, always maintaining economic competitiveness.

## **1.1 Coal power plant conversion into CSP**

With the current energy renewal plans to reduce emissions being carried out globally, the future for a highly polluting technology such as coal-fired power plants seem to have passed its golden years. Despite their quantity and operation, precisely designed to meet a large basic demand, and therefore intrinsically necessary at a time like today where energy demand is growing [7], thermodynamically efficient and within their limitation flexibles; the price of their emissions is becoming and will become too high in the coming years to maintain their current use status.

Europe is moving in a very ambitious way aiming to be "the first carbon-neutral continent" by 2050 [8] as mentioned in the EU Green Deal.

The disposal or the conversion of these complexes infrastructure surely will be an issue in the following years, therefore it seems obvious that starting to think already today what could be of the hundreds of plants and of the thousands of people who daily operate and work there, is the most correct thing to do to allow a gradual transition to a more sustainable environmental scenario. To guarantee a future for these people and try to keep a good amount of the plant structure parts, which in fact have not yet finished their useful life, a first solution has been studied in the recent years, it consist in the hybridization of coal-solar technologies mix, already thought to be implemented in some countries where solar irradiance is not a problem, like China, US, India, Australia, Chile, Suoth Africa, Jordania [9, 10].

That solution derives from the affinity of the carbon and the CSP technologies, similar in lot of parts, starting from the thermodynamical working cycle to the working fluid. The

difference that will bring a plus would be the implementation of a natural source instead of a fossil fuel one, presenting itself as reborn from its ashes, with new and modern emission standards.

## 1.2 Hybridization CSP and PV

A little variation of the typical CSP plant, already studied and in some places implemented to obtain the best of both technologies, is the hybridization of CSP and PV systems. It does not regard the coal power plant directly but would help in its conversion to a new renewable life, bringing it to limit or reduce to zero its direct emissions.

The advantages that the solar mix can obtain are innumerable. CSP can easily provide a constant load, permits large capacity storage and due to that is one if not the only one renewable technology that can be used and controlled, despite the weather conditions and during nighttime. PV as well known is cheaper than the previous one, so can be installed to cover the daytime production that is difficult to reach with the thermal plant, already working to reach enough energy storage for the nighttime.

### 1.2.1 Existent hybrid plants

Hybridization is a new way of thinking about power plants, today there are already some commercial plants with this concept. Here below are introduced four real examples of CSP and PV hybrid plants.

The first one is the plant complex of *NOOR I, II, III* and *IV*, four stages of a single big plant in Ouarzazate, Morocco. It has been active since 2016 and consists in two solar parabolic through plant of 160 MW and 3 hours of storage and 200 MW plant with 7 hours of storage, a 150 MW solar power tower plant with 7 hours of storage and a fourth part of 72 MW photovoltaic power station, planned to be completed at the end of 2020. With \$2.5 Billion construction cost and a site area of 2500 hectares (6178 acres), is one of the biggest plants of its kind existing in all over the world and its electricity production, with the cost 0.19 \$/kWh [9] manage to be competitive in its country without any problem.



Figure 1-1 Ouarzazate, Morocco, NOOR power plants

The second and very remarkable example that need to be mentioned is the *Noor 1 Energy* power plant, in Dubai, United Arabs Emirates. It is the fourth phase of Mohammed bin Rashid Solar Park projet and consists in the hybrid plat of 700 MW CSP: three subsections of 200 MW CSP through and one 100 MW solar tower with 15 hours of storage; plus 250 MW photovoltaic plant. The different technologies are been carried out by different companies and the project is still in construction.

The good work made between the government and the owner company has brought to a really low LCOE 7.03 ¢/kWh, based on 30 years of operation, guaranteeing in theory a really competitive construction price [10].



Figure 1-2 Dubai, United Arabs Emirates, Mohammed bin Rashid Solar Park

The third plant, Cerro Dominador, is in the desert of *Atacama*, Sierra Gorda, Chile. One of the places with the highest average irradiance on earth: 3500 kWh/m<sup>2</sup> at year DNI [11]. With its 110MW CSP and 17.5 hours of storage plus 100MW PV, since 2018 this plant has the capability to provide electricity in a manageable way all day long, adapting at the hourly consumption variations.

This project is part of a governative national plan of Chile for the development of renewable energy, with the objective to reach 20% of electric production from green sources in 2025. The construction, operation and maintainace helped not olny to provide clean energy but create about 2000 direct jobs and a lot of indirect one permitting a socioeconomic development of the region [12].





Figure 1-3 Atacama solar tower construction

Finally, Noor *Midelt* Phase 1 plant, “located 20km north of the town of Midelt in central Morocco, is expected to start towards the end of 2019, while delivery of the first electricity to the grid is planned from 2022” [13].

This project, which will have a total installed capacity of 800 MW, is the world’s first advanced hybridisation of CSP and PV technologies.

On completion, it will provide dispatchable solar energy during the day and until five hours after sunset for a record-low tariff at peak hours of *0.68 Moroccan dirhams per kWh* (about 7 USD cents) [14].

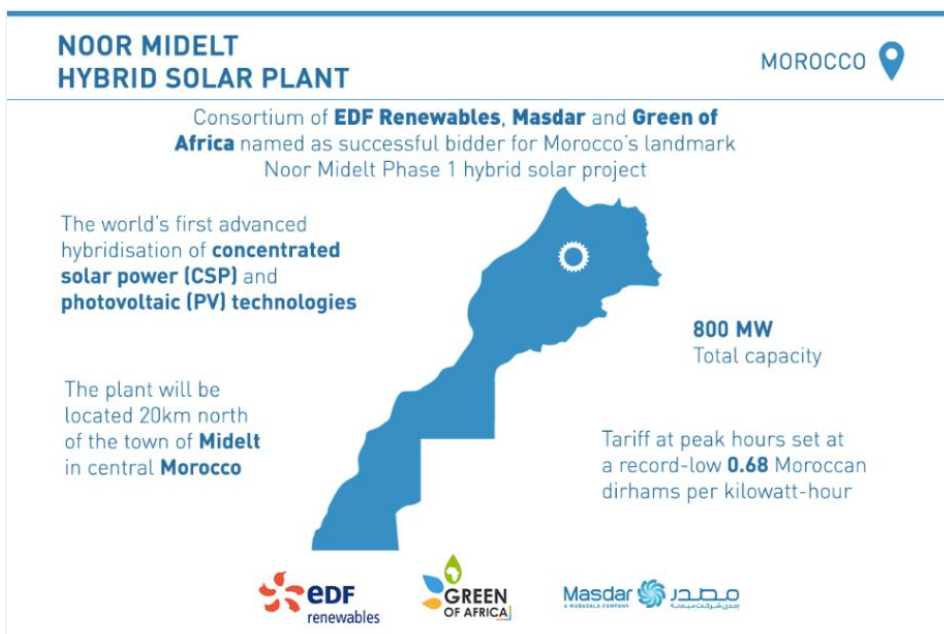


Figure 1-4 NOOR Midelt, Hybrid solar plant [14]

# Chapter 2    **Solar Energy**

Coming back to the principle of working of Solar plants is a date of fact that every second the sun releases  $3.845 \cdot 10^{20}$  MJ into space thanks to nuclear fusion of Hydrogen into Helium. But not all this energy can be utilised, the average intensity usable nowadays on Earth is about  $1367 \text{ W/m}^2$ , so the possibility linked of that amount of energy is not negligible [15]. Here below are explained the working principle and basic concepts of the studied subject.

## 2.1    **Concepts**

Before to enter in the details with the power plants is important to know the physics behind the technology utilised. Solar technologies can be divided in two big families:

- Solar thermal
- Photovoltaic

Both technologies have the same source, the sun light's energy. Light can be described as electromagnetic wave, which wavelength determines emission. In particular, the radiation of the sun can be approximated with the radiation of a black body emitting at  $5777\text{K}$ .

A black body is an idealized physical body that absorbs all incident electromagnetic radiation, regardless of frequency or angle of incidence. At thermal equilibrium (that is, at a constant temperature), a black body emits electromagnetic radiation called black-body radiation. The radiation is emitted according to Planck's law, meaning that it has a spectrum that is determined by the temperature alone, not by the body's shape or composition.

$$B_\nu(\nu, T) = \frac{2h\nu^3}{c^2 \left( e^{\frac{h\nu}{k_B T}} - 1 \right)} \tag{2-1}$$

$$c = \lambda\nu \tag{2-2}$$

$$B_{\lambda}(\lambda, T) = \frac{2hc^2}{\lambda^5 \left( e^{\frac{hc}{\lambda k_B T}} - 1 \right)} \quad 2-3$$

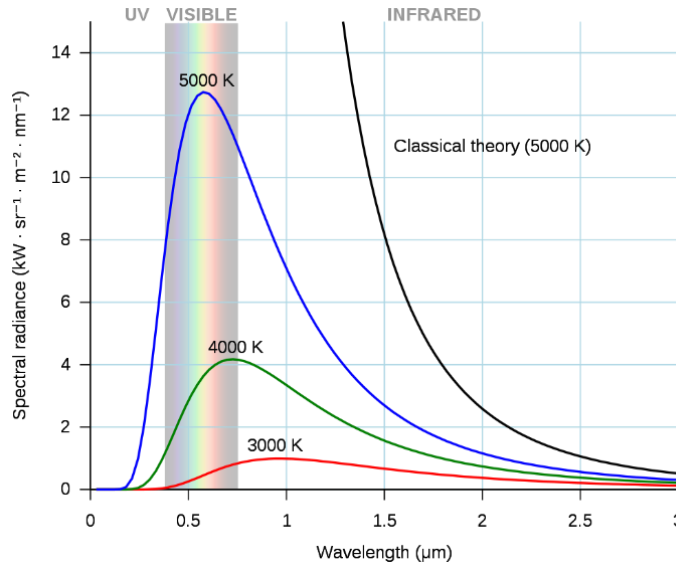


Figure 2-1 Spectral radiation of a black body

The total power emitted per unit area at the surface of a black body  $E_B$  may be found by integrating the black body spectral flux over all frequencies, and over the solid angles corresponding to a hemisphere above the surface.

$$E_B = \int_0^{\infty} d\nu \int d\Omega B_{\nu} \cos \theta \quad 2-4$$

The infinitesimal solid angle can be expressed in spherical polar coordinates:

$$d\Omega = \sin \theta \, d\theta \, d\phi \quad 2-5$$

So that:

$$E_B = \int_0^{\infty} d\nu \int_0^{\pi/2} d\theta \int_0^{2\pi} d\phi \sin \theta \cos \theta = \sigma T^4 \quad 2-6$$

Known as Stefan–Boltzmann law [16].

Each photon reaching the ground has to through the atmosphere. Its energy will inevitably decrease due to this passage. The longest is the path the higher are the losses. This phenomenon is named solar attenuation and it is taken into account using the air mass parameter [15].



The air mass coefficient defines the direct optical path length through the Earth's atmosphere, expressed as a ratio relative to the path length vertically upwards, i.e. at the zenith. The air mass coefficient can be used to help characterize the solar spectrum after solar radiation has traveled through the atmosphere. The air mass coefficient is commonly used to characterize the performance of solar cells under standardized conditions, and is often referred to using the syntax "AM" followed by a number. "AM1.5" is almost universal when characterizing terrestrial power-generating panels [17].

When the sun rays are perpendicular to the ground the zenith angle is null, it corresponds to AM=1, otherwise it is always bigger than one.

$$AM = \frac{1}{\cos \theta_z} = \frac{1}{\sin \gamma} \quad 2-7$$

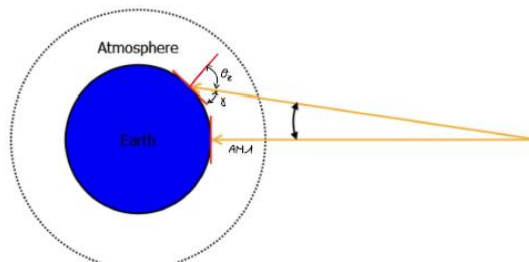


Figure 2-2 AM explained graphically [18]

So AM depends on  $\theta_z$ , which directly depends on the latitude of the geographical area, but also atmospheric conditions influence it, the higher the humidity the higher is the AM.

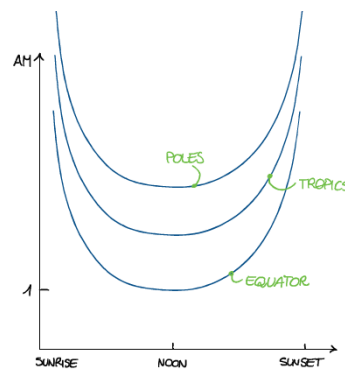


Figure 2-3 AM function of latitude [18]

Solar panels do not generally operate under exactly one atmosphere's thickness: if the sun is at an angle to the Earth's surface the effective thickness will be greater. Many of the world's major population centres, and hence solar installations and industry, across Europe, China, Japan, the United States of America and elsewhere (including northern India, southern Africa, Chile and Australia) lie in temperate latitudes. An AM number representing the spectrum at mid-latitudes is therefore much more common.

"AM1.5", 1.5 atmosphere thickness, corresponds to a solar zenith angle of  $z = 48.2^\circ$ .

The radiation hitting the surface is composed by three terms:

- Direct radiation
- Diffuse radiation
- Albedo (reflected radiation)

They can be summed under the assumption of homogeneous spectrum, because they have the same spectrum and are generated by a black body at the same temperature [19].

$$I_{tot} = I_{dir} + I_{diff} + I_{alb} \quad 2-8$$

$$I_{tot} = I_{DNI} \cos \theta_s + I_{diff} \frac{1 + \cos \beta}{2} + \rho * I_{alb} \frac{1 - \cos \beta}{2} \quad 2-9$$

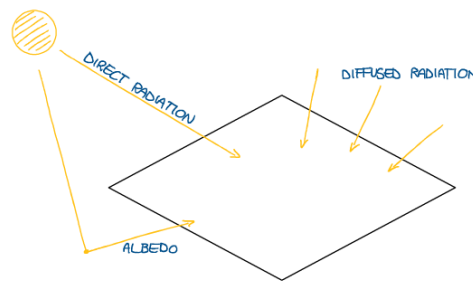


Figure 2-4 Components of radiation [18]

*Diffused radiation* is measured assuming that the radiation is homogeneously coming from the entire skyvault. It is due to scattering of radiation, photons pass through atmosphere (molecules and particles), the longer the path the higher is the wavelength diffused. This is the reason of red coloured sky at the sunset.

The *albedo*, instead, is generally negligible due to low reflectivity of surfaces and low view factor (panels and mirrors are usually sky oriented).

Solar thermal is a little more intuitive to understand compared to PV technology, it basically consist in concentrate the energy on a little area to increase its density per  $m^2$ . In this manner a heat transfer fluid is used to collect the thermal energy freed by this absorption in the receiver space. The energy obtained can be used to thermal porpoises, calefaction, or to produce electricity. If implemented, the thermal energy can also be stored in tanks and used when needed.

Anyway Solar thermal passes trough many more steps, including thermodynamical changing of states, it brings to many losses due to:

- Concentration efficiency
- Thermal efficiency
- Power cycle efficiency

The final efficiency of the system will be given by the chain product of the efficiencies.

Optical losses account for the difference between the solar power and the power absorbed by the tubes. They include the reflected and absorbed radiation by other protective layers different by the HTF tubes, superficial inaccuracies in the devices and not correct allineation with the hot spot [15].

Optical efficiency is a function of the glass trasmissivity, the receiver absorbance and the solar spectrum.

$$\eta_{sun \rightarrow HTF} = \frac{\dot{Q}_{rec}}{\dot{Q}_{sun}} * \frac{\dot{Q}_{HTF}}{\dot{Q}_{rec}} = \eta_{opt} * \eta_{th} \quad 2-10$$

$$\dot{Q}_{rec} = \dot{Q}_{sun} * \eta_{opt} = \tau_{glass} \alpha_{rec} G_{sun} A_{rec} \quad 2-11$$

*Thermal losses* account for the  $\Delta T$  between the receiver and the ambient temperatures.

Thermal efficiency is a function of the temperature and the properties of the material of the receiver.

$$\begin{aligned} \frac{\dot{Q}_{HTF}}{\dot{Q}_{rec}} &= 1 - \frac{\dot{Q}_{heat\ loss}}{\dot{Q}_{rec}} = 1 - \frac{\dot{Q}_{conv} + \dot{Q}_{rad}}{\dot{Q}_{rec}} = \\ &= 1 - \frac{h A_{rec} (T_{rec} - T_{amb})}{\dot{Q}_{rec}} - \frac{\sigma \epsilon_{rec} A_{rec} (T_{rec}^4 - T_{amb}^4)}{\dot{Q}_{rec}} \end{aligned} \quad 2-12$$

At the end, the energy transferred to the HTF is equal to the product of the receiver energy and the thermal efficiency

$$\tau_{glass} \alpha_{rec} G_{sun} A_{sf} - h A_{rec} (T_{rec} - T_{amb}) - \sigma \epsilon_{rec} A_{rec} (T_{rec}^4 - T_{amb}^4) \quad 2-13$$

Looking at the properties that the receiver should have to maximize  $\dot{Q}_{HTF}$  results:

- $\alpha_{rec}$  should be as high as possible to absorb the highest amount of solar irradiance
- $\epsilon_{rec}$  should be as low as possible to minimize radiative losses
- $T_{rec}$  should be as low as possible as both radiative and convective losses increase with it. This is a forst compromise in the plant operation due to the fact that the power block needs the higher value possible of  $T_{rec}$  to increase its efficiency.

Last but not least, looking at the previous formula can be noticed that to increase the heat absorbed by the HTF, instead of collection the solar power only using the receiver, a bigger collecting area made of reflective surfaces is better to be used, increasing the energy density reaching the receiver.

Concentration ratio is defined as:

$$CR = \frac{A_{solar\ field}}{A_{receiver}} \quad 2-14$$

$$\eta_{th} = 1 - \frac{hCR(T_{rec} - T_{amb})}{G_{sun}\eta_{opt}} - \frac{\sigma\epsilon_{rec}CR(T_{rec}^4 - T_{amb}^4)}{G_{sun}\eta_{opt}} \quad 2-15$$

The higher the concentration ratio the lower are the losses, so thermal efficiency increases meanwhile  $T_{rec}$  also increases. This second compromise is always related to the first one.

	Linear focus		Point focus	
	Parabola	Linear Fresnel	Solar Stirling	Solar Tower
Concentration ratio	~90	~160	>2500	~500-800
Nominal optical efficiency (%)	~76	~64	~80	~65-75
Yearly average optical efficiency (%)	~50 – 55	~35 – 40	~70	~57-65

Figure 2-5 Mean technological values [15]

Photovoltaic principles derive from the well-known photovoltaic effect. Solar energy as already said is just an electromagnetic signal composed by photons (energy carrier). Their energy depends on the wavelength  $\lambda$  and frequency  $\nu$ . High  $\nu$  and low  $\lambda$  photons have more energy.

$$E_{ph} = h\nu = \frac{hc}{\lambda} \quad 2-16$$

Depending on the energy transported, a photon hitting a material could be absorbed by electrons and then ejected as photoelectron if  $E_{ph}$  is higher than binding energy (photoelectric effect). The number of photons hitting the surface is not important, but the energy or equivalent frequency of individual photons.

*Photovoltaic effect* works in a similar way but instead of generating charged electrons it leads to creation of voltage and current in a material. Each material is composed by atoms bonded together without any  $\Delta V$ . electrons could be found in valence or conduction bands:

- Conduction band:  $e^-$  which create bonds between atoms are shared
- Valence band:  $e^-$  stays stick to the atom

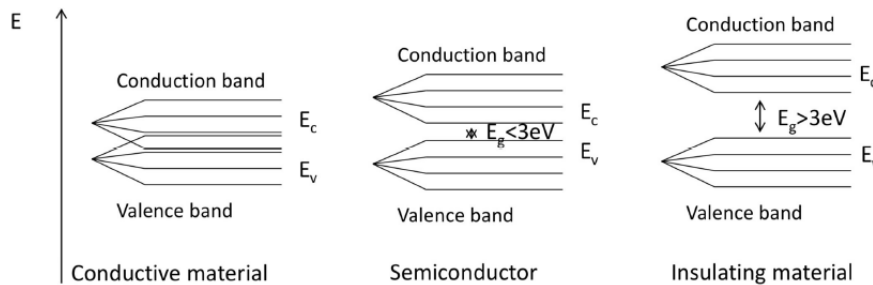


Figure 2-6 conductor, semiconductor, insulating materials behaviour

Energy level is different if  $e^-$  is in conduction or valence band, the goal is moving the band electrons to conduction bands so they can start moving generating current. The energy gap between valence and conduction depends on the material and its crystalline structure.

The most used material for PV cells is *silicon* (Si), a semiconductor, so a material with  $0 < E_g < 5$  that does not conduce at standard conditions. Its orbital representation is  $sp_3$  (contained in IV group).

Silicon excited by a photon would “release” an electron, but Si alone would simply heat up as its electrons would tend to recombine going back to its original state, for this reason Si has to be coupled with an external circuit in order to convert the movement in electricity.

Chemically the charged electron would recombine with its positive charged hole, to prevent it p-n junction has been developed.

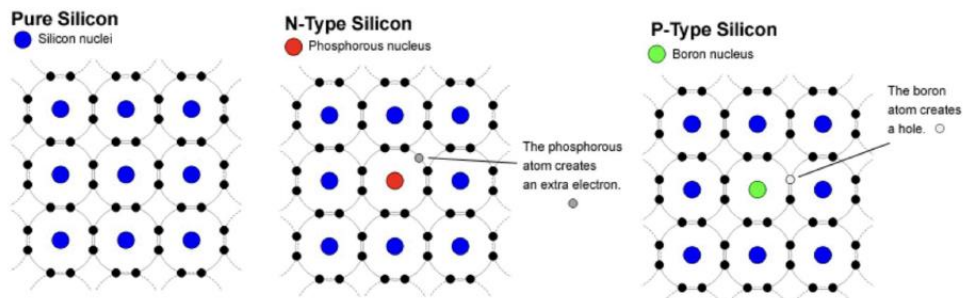


Figure 2-7 P-type and N-type Si doping

This material layout prevents recombinations and makes electrons available to the external circuit, at the end behaving like a diode. Silicon can be doped as n-dope and p-dope. The

total charge of both the configuration remains neutral but the final number of electrons is different.

*n-dope* uses phosphorous instead of some atoms of Si to add an additional electron into the structure (electrons are the major carriers), *p-dope* uses boron so that the valence band of it has a vacancy respect Si (holes are the major carriers). Coupling together the two materials a p-n junction is obtained.

Due to diffusion electrons will tend to go from n-dope to p-dope, looking for a more stable condition, and so holes (left from the moving charges) will tend to go in the opposite direction. That movement of electrons generates a current in the external circuit.

To decide how thick the n-layer should be the diffusion length is not enough to know the diffusion length. An important parameter is the adsorption length that is inverserlly proportional to the adsorption coefficient. This last changes for each semiconductor and strongly depend from the wavelength of incident light.

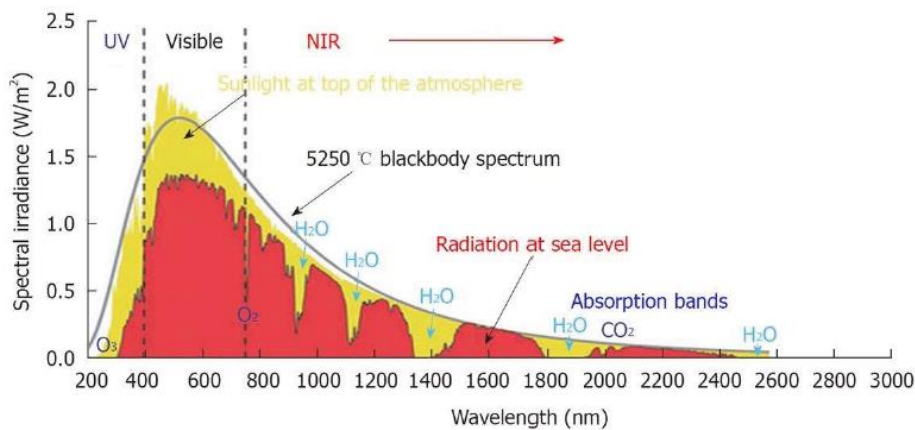


Figure 2-8 Adsorption bands [15]

A PV module is a device that directly convert sunlight into electricity, it does not require a Rankine cycle plant and its efficiency does not imply the carnot factor, but its conversion is limited by the Shockley-Queisser limit, which depends on the  $E_g$ .

To guarantee good performances is necessary not olny to orientate properly the modules and to use a sun following system, but is necessary to take into account and avoid the *shadow* produced between the modules themselves.

In case of heliostast it is also important to consider the blocking effect, or rather the *blocking* of the reflected sunlight directed to the tower by two neighbouring devices.

## Chapter 3 The three analysed technologies

In this chapter are presented, for each technology analysed, the working principles, a brief history introduction and a detailed description of the main plant components and functions.

### 3.1 CSP

Exists different kinds of CSP, solar collectors, solar tower, Fresnel, stirling engine, but all of them are based on optical technology, concentrating the sun, each in a different manner, in a hot spot used to heat or warm up a fluid. This fluid can be used as a working fluid used for heating houses or for industrial porpoises or as HTF in parabolic through or tower plants.

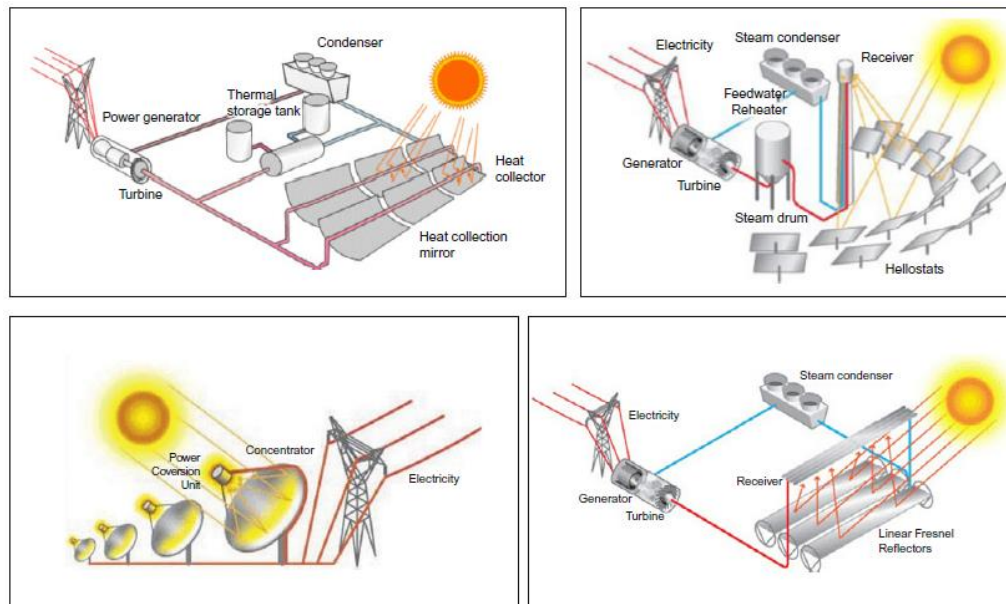


Figure 3-1 Different kinds of CSP technologies [20]

Nowadays the objective of these technology is to produce clean energy in a cheap way and so stirling engine, that have a very high cost ofprocution and maintenance has been abandoned.

*Solar tower* and *parabolic through* are the exploited between the four kinds, they have been largely studied and numerous commercial plants already exists.

Their advantage is that despite sun is an aleatory source they can be managed on the 24 hours, thanks to their storage system, mainly based on molten salts. The difference between the two of them is that in solar towers is easier to use a single fluid working as HTF and as storage one. In the other is necessary to use two different fluids to avoid big costs linked to the electric heating that would be required to maintain liquid the salts in the numerous km of pipeline during the night hours. Due to that reason in parabolic trough are used Fluid that solidify at lower temperature, but it limits the working maximum temperature to value much lower than tower.

A second big difference is that the first technology collects sun in a single spot using heliostats pointing at the receiver of the tower, where the fluid is heated up. The second one uses tubes to heat the HTF that pass through the parabolic fire or each collector, determining in that way a very huge pipeline, but also a higher capacity factor.

*Fresnel*, as the previous two technologies are modular, but due to the low temperature reachable are mainly used in industrial heat process production, and not to produce electricity.

### 3.1.1 History of CSP

The first relevant reference for concentrating solar energy might come from the III century B.C. when more historical sources writings state that during the battle of Syracuse between Roma and Greece, 212 B.C., *Archimedes* used some mirrors to try to burn the Roman fleet [21].



Figure 3-2 Giulio Parigi's burning mirrors, 1600, Uffizi Gallery, stanzino delle matematiche, Florence

After that episode and inspired by the mythical story of the battle, many are the scientists that during centuries tried to replicate the solar collector principles for the most different reasons.

A name that can be remembered is Augustin Mouchot who by 1866 had developed a parabolic trough solar collector and by 1875 presented a solar generator capable to provide a steam flow up to 140 liters per minute. After him, many others followed his steps like John



Ericsson or Aubrey Eneas who in 1892 founded the Solar Motor Company of Boston, the first solar energy company in the History, moved by the idea that the world would have run out of coal due to the industrial revolution [22].

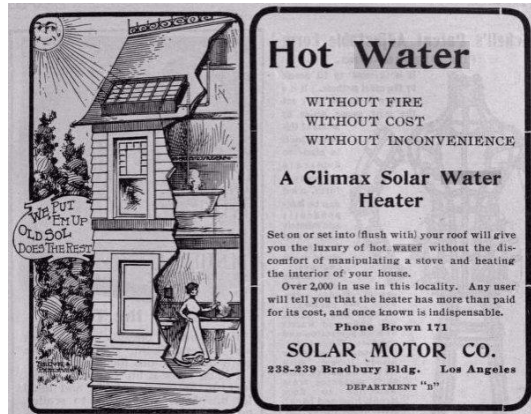


Figure 3-3 Solar Motor Co.

Another ambitious man trustfull of the future of this technology was Frank Schuman, that founded his own company, *Sun Power Company*, and after building a demonstration plant in Pennsylvania he went to Egypt (Maadi), where he built the world’s first solar thermal power plant between 1912 and 1913, consisting of 5 parabolic trough collectors and capable of producing 88 kW. His plan was to build a 200 MW parabolic trough plant in Egypt (the equivalent to the consumption in 1909) but due to the World War I, when he died, and the discovery of cheap oil in the 1930s the project was forgotten [21].

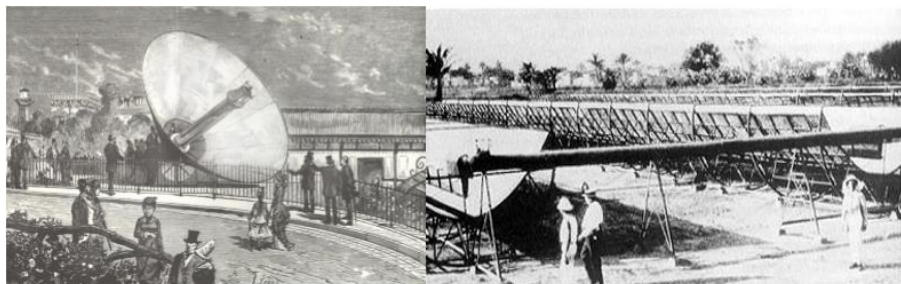


Figure 3-4 Augustin Mouchot’s Solar Generator (left), Frank Shuman’s Parabolic Trough Plant in Egypt (right)

The 1973 oil crisis favored the development of CSP between the 70s and the 90s. R&D centers were created for the development of CSP technologies where themain goal was to demonstrate the technical feasibility of generating electricity from the concentration of solar radiation.

Spain has been one of the first promoter of the development of this technology, starting with CESA 1 project, a solar tower with steam water as thermal fluid and a 1.2 MWe turbine with air cooling. And many others till Gemasolar, with its 19.9 MW of power and 15 hours of storage, operating since May 2011 [23].

But also the US in the ‘80s and ‘90s helped to improved the reliability of this technology with the palnts of Solar One, 10 MWe, used to test saturated steam solar receiver with molten salt storage and Solar Two to test a molten salt receiver with two tank molten salt storage using the same heliostat field as Solar One. And also with its from 14 MW in SEGS-1 to 80 MW in SEGS-IX in the Mojave Desert [20], construction 1984-1990, still operating.



Figure 3-5 SEGS solar plants in the Mojave Desert (left), Solar Two (center), Solar furnace of Odeillo (right)

For sake of curiosity is interesting to add that in France, by means of the Centre National de la Recherche Scientifique, different projects were developed like the solar furnace at Odeillo, the 2 MWe solar tower Themis 2 or the SRTA devices at Marseille and Ajaccio Universities [21].

Concerning nowadays production *Spain* led in cumulative CSP capacity. Globally, in 2018, CSP capacity totaled 5.5 GW [24], but as the trend in Figure 3-6 CSP total capacity, World 2008-2020 Figure 3-6 shows the amount is increasing.

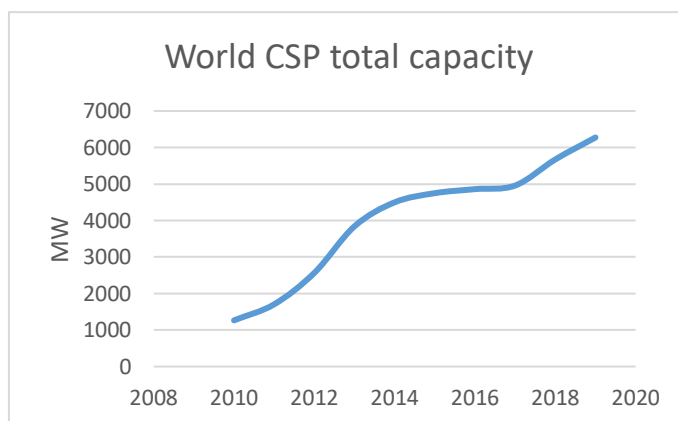


Figure 3-6 CSP total capacity, World 2008-2020 [25]

### 3.1.2 Components of CSP tower plant

CSP tower plant are usually oriented North-South direction at latitude higher than 35°. At lower latitudes, and so next to the equator, are usually built as surrounding field, where heliostats have same distance to the tower in each direction. They are basically made up by five components: heliostats, tower, receiver, storage system and power station.

A *heliostat* is a device that made up by of a reflective surface (mirrors), a support structure, drive mechanisms and a control and monitoring system. Following the movement of the Sun, its function is to concentrate the direct solar radiation on the receiver.

Each heliostat is made up of multiple mirror modules called facets. Each facet has a slight concave curvature (so slight that it is normally curved in the assembly) and is inclined with respect to the plane of the support structure to achieve, in this way, a better focus of the solar radiation reflected in the receiver limiting spillage.

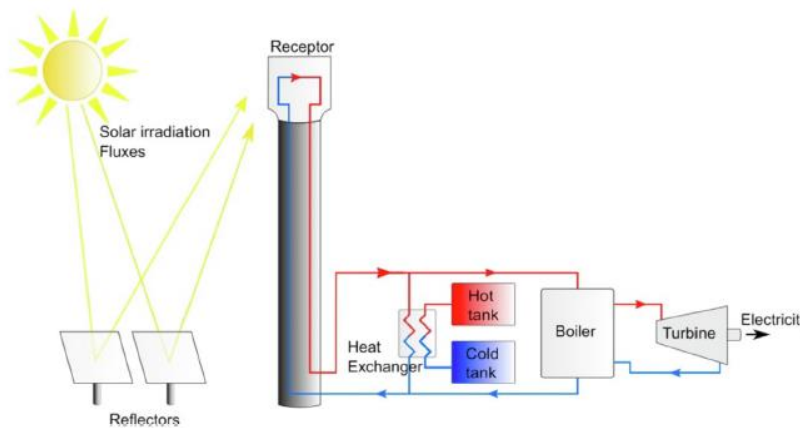


Figure 3-7 Solar Tower CSP scheme [26]

The most widely used reflective surfaces are glass mirrors, although high reflectivity polymer films can also be used.

The deployment of the heliostat field depends on the characteristics of the land, the size of the plant and the position of the receiver. As written before, the two possible positions are the deployment of the heliostat field around the tower (surrounding field) or on one side of the tower (North or South field, depending on the latitude of the site).

The receiver is the device where solar radiation is concentrated to obtain thermal energy that is transferred to the *HTF*. It is mainly formed by the absorption surface, the structure of the receiver and other auxiliary elements.

There are three typical receiver configurations:

- *External receivers*, in which the solar radiation reflected by the heliostat field falls directly on the absorbing surface. Its volume, its number of components and its costs are lower than in cavity receivers.
- *Cavity receivers*, in which radiation passes through an opening into a hollow box-shaped area, before reaching absorbent surfaces. In this type of receivers, the radiation losses are lower.

- *Volumetric receivers*, formed by a metallic or ceramic structure of various shapes, thus heating the fluid (usually air) that passes through its interior and achieving higher temperatures than the first two.
- *Solid particle receptors*, its main advantage over other configurations is that the radiation falls directly on the particles.

To ensure good performance of the heliostat field, the solar receiver must be installed at a certain height above the field. This is achieved by placing the receiver in a tower, which can be made of concrete (when it is greater than 100 m) or metallic (when it is less than 100 m). Its height is one of the most important parameters in the optimization process of the solar field. It is intended to be as small as possible. Normally the maximum distance of the tower heliostats is a function and a multiple of the same height.

Various heat transfer fluids can be used in tower systems [19]:

- *Water*. Saturated or superheated steam.
- *Molten salts*. They can be used directly as HTF and storage fluid, so they can be operated at their maximum temperature, which greatly reduces the amount of salts required.
- *Air*. It can work between 680 and 1300 °C, but it is a very bad thermal fluid due to its low  $C_p$ .
- *Liquid sodium*. It can work at very high temperatures. Its solidification temperature is lower than that of salts, it has better conductivity but worse  $C_p$ .

It is also important to differentiate the heat transfer fluid (HTF) and the energy storage fluid.

Molten salts are the most widely used technology as thermal storage fluid and is contained in the storage tanks, big thermal insulated vessels that are part of the storage system. Molten salts exist in various composition mixture, but the most common is the *60% wt  $NaNO_3$  and 40% wt  $KNO_3$* , the most suitable solution, thanks to good characteristics and price. It has low conductivity but can reach temperatures up to 560 °C.

The salts are contained in large *tanks*, about 35-50 m diameter and 15 m height. From the cold tank the flow is heated in the receiver (or by the HTF coming from the receiver), reaches the hot tank and is used to heat the cycle working fluid. After that it returns in the cold tank.



Figure 3-8 Molten salt storage tanks

The electric power generation system of a central receiver solar plant basically consists of the same elements of a conventional plant that works with the *Rankine cycle*, that is, a steam turbine group, compressor, pipes, heat exchangers, condensed steam recirculation pumps. The main difference is that in a solar plant the receiver is used instead of the boiler to heat transfer fluid.

### 3.2 PV

As said before, PV directly converts the energy of the sun light into electricity.

- First generation: based on silicon in mono and multi crystalline configuration.
- Second generation: amorphous silicon, cadmium telluride, gallium arsenite, copper inidium, selenide.
- Third generation: dye sensitized, quantum dots, organic cells.

No matter the technology used, all of them have the same limits: solar energy and material structure. PV cells present in the market are of first and second generation and covers the 99% of the share [15].

Nowadays *bifacial PV* is becoming mainstream with GW's of installed projects, they guarantee a higher energy production, also exploiting albedo and diffuse radiation on a bigger surface. LCOE of bifacial systems is competitive with monofacial systems now, even with initial cost adder of 5-6 ¢/W. Post-tariff, bifacial is a clear winner [27].



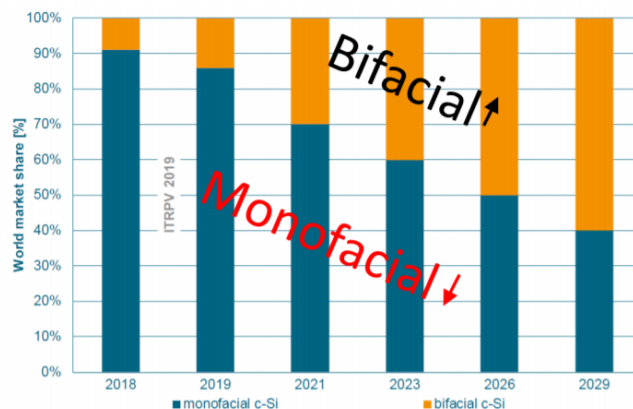


Figure 3-9 Bifacial cell in world market forecast [27]

### 3.2.3 History of PV

Solar PV power as we know it is no more than 60 years old, the discoveries that led to the solar cell began nearly 200 years ago. These discoveries about the properties of light and conductivity have made solar power what it is today [28].

Here is presented a timeline resumen of the evolution of this technology.

In 1839 a French scientist Edmond Becquerel first discovered the photovoltaic effect.

Willoughby Smith, an English electrical engineer, discovered the photoconductivity of selenium in 1873-1876.

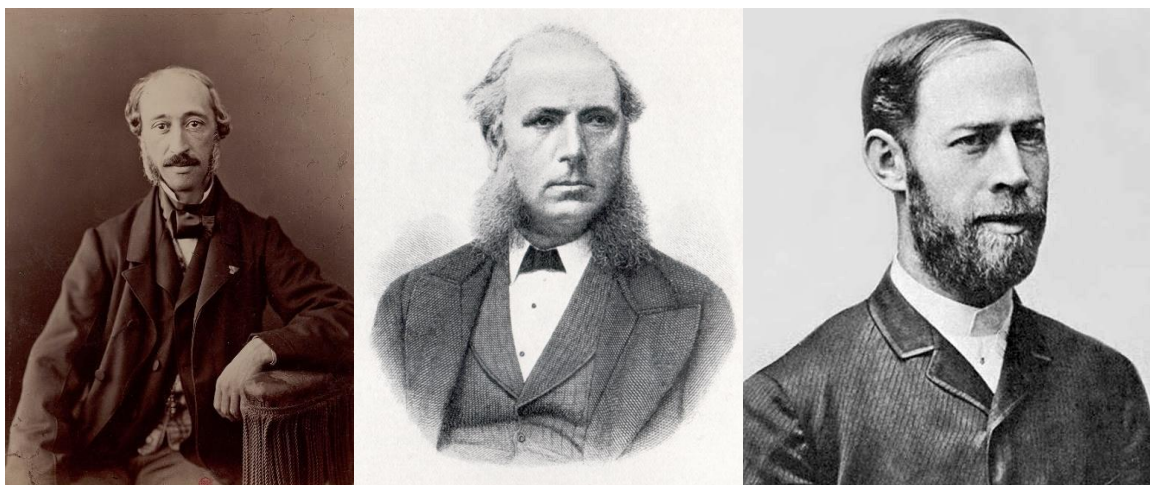


Figure 3-10 from left to right: Edmond Becquerel, Willoughby Smith and Heinrich Hertz

In 1883, in New York, inventor Charles Fritts created the first solar cell by coating selenium with a thin layer of gold. This cell achieved an energy conversion rate of 1-2%, while most modern solar cells nowadays work at an efficiency of 15-20%.

First to observe the photoelectric effect, was a German physicist, Heinrich Hertz in 1887. Contrary to expected results, Hertz found this process during experiments produced more

power when exposed to ultraviolet light, rather than more intense visible light. Albert Einstein later received the Nobel Prize for further explaining the effect.

In 1956 Western Electric began selling commercial licenses for its silicon PV technologies. Anyway, the prohibitive costs of silicon solar cells keep them from widespread market saturation. Only in the 1970s, when the demand for solar power increased, Exxon Corporation financed research to create solar cells made from lower-grade silicon and cheaper materials, pushing costs from \$100 per watt to only \$20-\$40 per watt, values that nowadays seems inconceivable. The federal government also passed several solar-friendly bills and initiatives and created the National Renewable Energy Laboratory (NREL) in 1977 [28].

The First Solar Park, Arco Solar, where created in in Hesperia, California, in 1982. This park generated 1 megawatt, or 1,000 kilowatts per hour, while operating at full capacity. This could power a 100-kilowatt lightbulb for 10 hours. In 1983, Arco Solar built a second solar park in Carrizo Plains, California. At the time, it was the largest collection of solar arrays in the world, containing 100,000 PV arrays that generated 5.2 MW at full capacity. While these plants fell into disarray with oil's return to popularity, they demonstrated the potential for commercial solar power production.

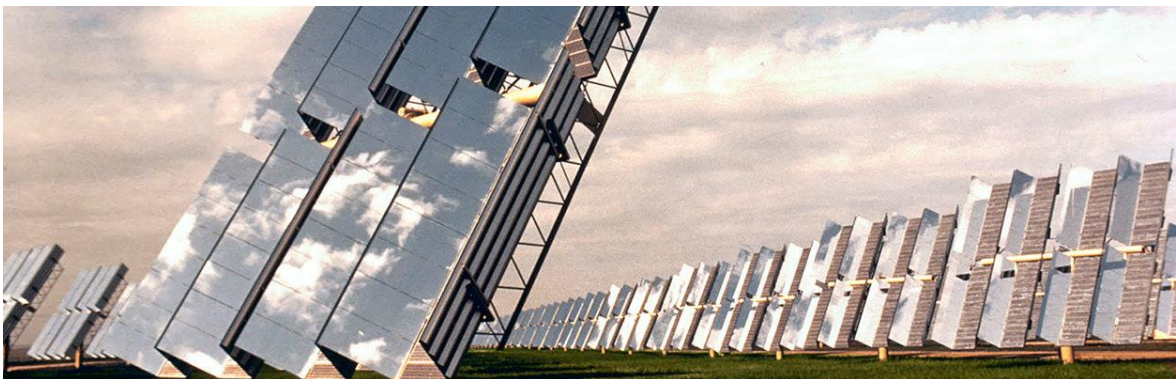


Figure 3-11 Arco Solar, first commercial solar park, Hesperia, California

In 1994, the National Renewable Energy Laboratory developed a new solar cell from gallium indium phosphide and gallium arsenide that exceeded 30% conversion efficiency. By the end of the century, the laboratory created thin-film solar cells that converted 32% of the sunlight it collected into usable energy.

As technology and efficiency of solar cells have increased, residential solar power has become more popular. DIY solar panels started hitting the market in 2005 and have become more prevalent with each new year.

Solar cells as thin as paper can now be manufactured using an industrial printer and made into products such as roof tiles or shingles. They have 20% power conversion efficiency,

and a single strip can produce up to 50 watts per square meter, making the cost of residential solar energy lower than ever [28].

Solar power has come a long way in the past 200 years, from observing the properties of light to finding new ways to convert it into power, but this technology shows no signs of slowing down.

Some numbers are shown in following figures. China continued to lead the world in cumulative renewable electricity capacity in 2018 where Global capacity increased by 25.4% [24]. Globally, cumulative capacity in 2018 totaled 480.6 GW for PV [24].

	Hydropower	Solar PV <sup>1</sup>	CSP	Wind	Geothermal	Biomass Energy	All Renewables
2009	3%	55%	60%	30%	5%	13%	8%
2010	4%	77%	62%	20%	2%	8%	8%
2011	3%	79%	31%	22%	1%	10%	9%
2012	3%	41%	53%	21%	4%	6%	9%
2013	5%	34%	46%	12%	2%	9%	8%
2014	4%	26%	18%	16%	5%	7%	8%
2015	3%	27%	7%	19%	5%	7%	9%
2016	3%	34%	2%	12%	4%	8%	9%
2017	2%	32%	2%	10%	3%	6%	9%
2018	2%	25%	10%	9%	5%	5%	8%
CAGR (2009-2018)	3%	36%	21%	14%	3%	7%	8%



Sources: IRENA, EIA, LBNL, and SEIA/GTM

Figure 3-12 Global Renewable Cumulative Electricity Capacity Annual Percent Change [24]

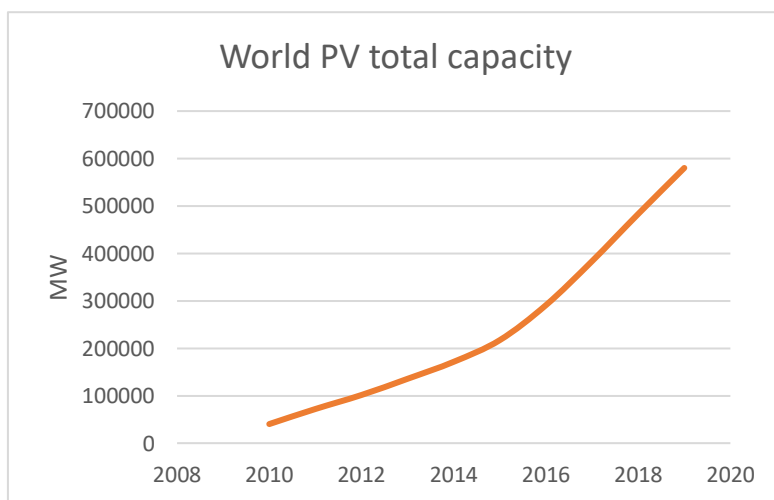


Figure 3-13 PV total capacity, World 2008-2020 [25]

For what regards prices, PV technology has no rivals nowadays. Maintaining the lowest price among renewables technology, as can be seen in the following figure.



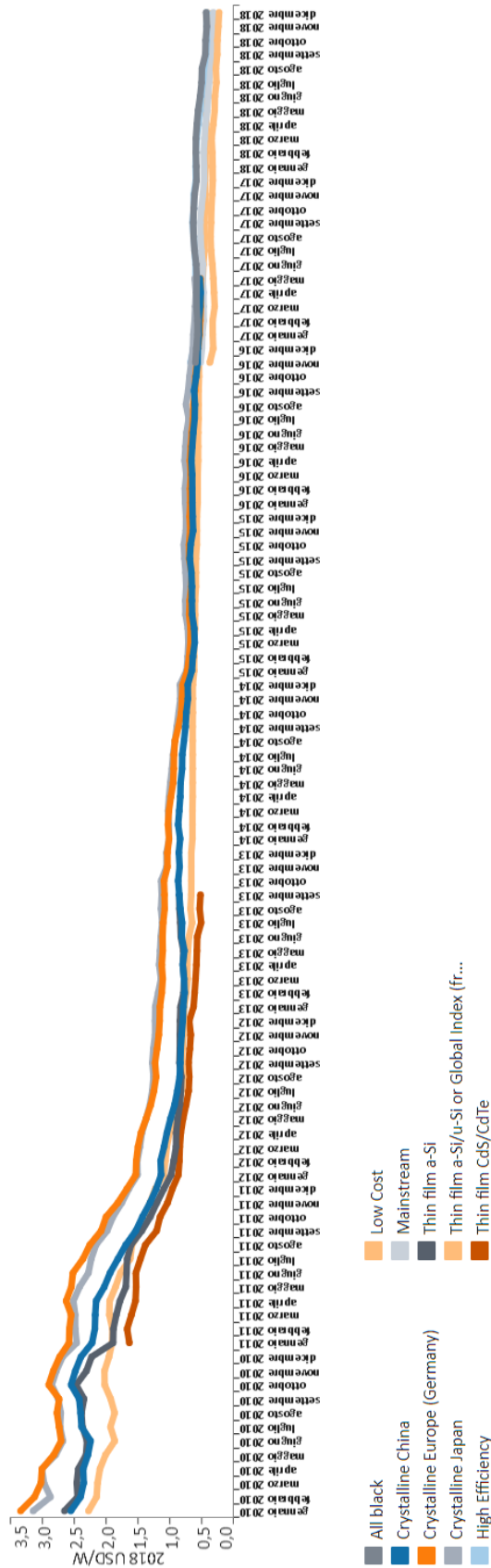


Figure 3-14 Solar PV module cost 2010-2018 [29]

### 3.2.4 Componets of PV plant

PV plant are a new but cheap and green solution to produce electricity during daylight. This plants are usually south oriented in the boreal emisphere and north oriented in the austral emisphere, in order to be always pointing at the sunlight, gaining the maximum energy available.

The four main componets of a PV power plant are:

- Module
- Inverte
- Tracker
- Battery

*Modules*, vulgarly called PV panels, can be made of different materials like crystalline silicon, thin film of cadmium telluride or amorphous silicon, depending of the efficiency, cost and generation size they are used in different fields, but 90% of the panels produced are crystalline silicon and generally their dimension are around the two meters squared each, to be easier to install.

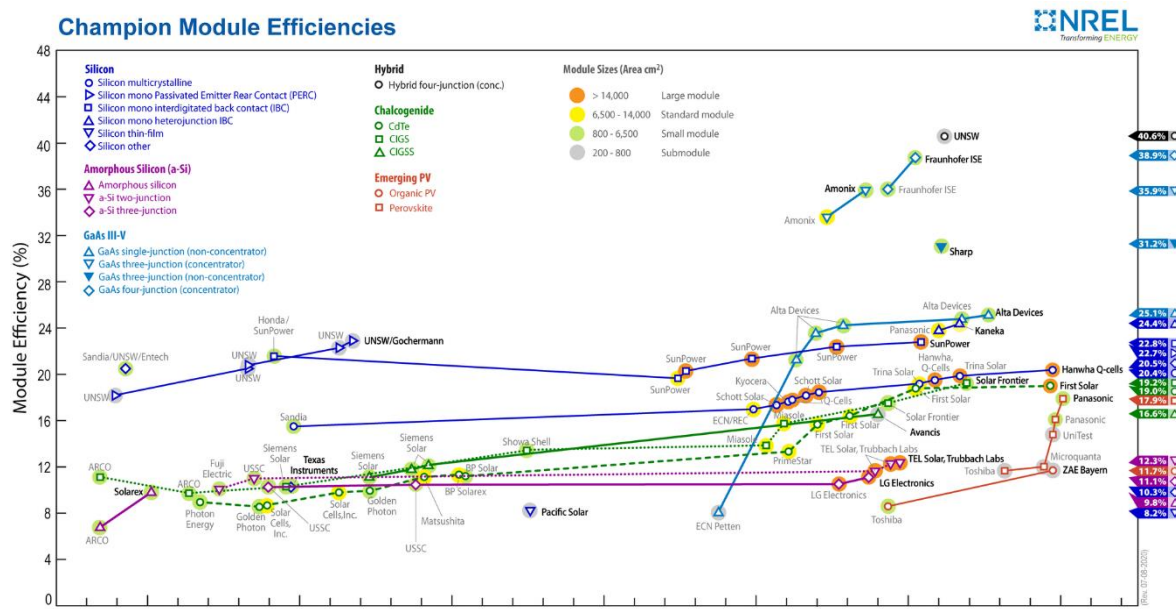


Figure 3-15 Differents solar panels characteristics [30]

PV panels produce normally at low current and low voltage, so in order to obtain a good power production they need to be organized in the field in series and parallels, always respecting the datasheet constraints. A serie of panels is called *string* and can not exceed the maximum voltage acceptable by a single panel. As well parallels panels current can not exceed the maximum current acceptable by a single one. Rule of thumb in designing a solar field is to use always the same kind of pannels, or at least the same kind in each subsection.

In case of not following that rule, the whole serie-parallel system would work as the worst present configuration possible. Another rule of thumb to avoid the same problem, and improve efficiency is to test singularly each module in site in order to put together the more similar ones and do not have performance losses. *Performances* also depends on ambient condition such temperature, humidity and altitude, effects can be seen on I-V curves.

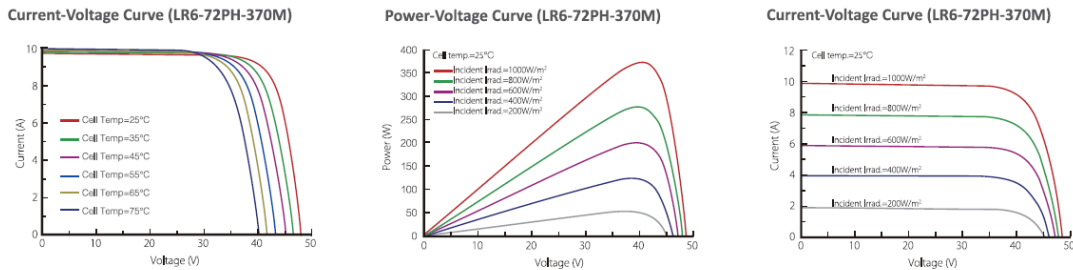


Figure 3-16 I-V curves of a LR6-72PH-370M PV module (annex)

The PV electricity production is direct current, and usually the pannels are in a floating grid till the first transformer, in order to minimize risks for the operators. Each subsection of serie-parallel of PV panels are connected to a transformer that innance the voltage, and so forth the series and parallels of transformers generate a hierachy till the desired voltage needed by the transformation center.

A *power inverter*, or inverter, is a power electronic device or circuitry that changes direct current (DC) to alternating current (AC). This device permits to shift from a production configuration to a transportation configuration. Inverters can be designed for indoor or outdoor conditions, but it is always preferable to keep them in a controlled enviroment in order to guarantee good performances and longer lifetime. The size of the inverter depends on the size of the plant, the production and the transformer center requirements.

As said in the chapter 2.1 PV technology use the sun energy to alterate the bound levels of its chemical componets to produce electricity, so to permits to meet the matching condition during operation trackers are used to follow the maximum power operating point, or to defocus in case of overproduction, regulation so the amount of energy reaching the surface of the module. The *tracking* can be on one or two axes, obiously the two axes are more precises but require a bigger investment and a bigger area to avoid blocking and shadowing between the differents arrays. Actually the one axis are the more used ones, due to low cost and really similar efficiency of the two ones, considering also their higher energy consumption.



Figure 3-17 Two axes configuration (left), one axis configuration (right)

*Batteries* are a PV field component not always present, but fundamental in some cases. Due to its high cost batteries are usually not implemented in residential or plant of little size. The purpose of use batteries is to have a more stable output electricity production, avoiding the big variation in the production that aleatory source provides. Always due to the high cost, around 300 €/kWh for big power plants [31], their use is limited at some hours of storage, just to cover some negative peak during the production period, but not enough to cover a nighttime period of demand.

### 3.3 Carnot battery plant

Nowadays, as specified in the previous chapter, storage electric energy in batteries is expensive but doable for short period, it is not for long periods; due to high costs, maintenance, replacement of batteries and pollution linked to their disposal.

Carnot Batteries are an emerging technology for the “*inexpensive*” and site-independent storage of electric energy at medium to large scale. They transform electricity into heat, store the heat in inexpensive storage media like water or molten salt and transform the heat back to electricity when required [32]. The cycle implemented to exploit the PTES could be of different kind: *Bryton*, *Recuperative Bryton*, *Rankine-Bryton*, *CO<sub>2</sub>*, *CHEST* [33].

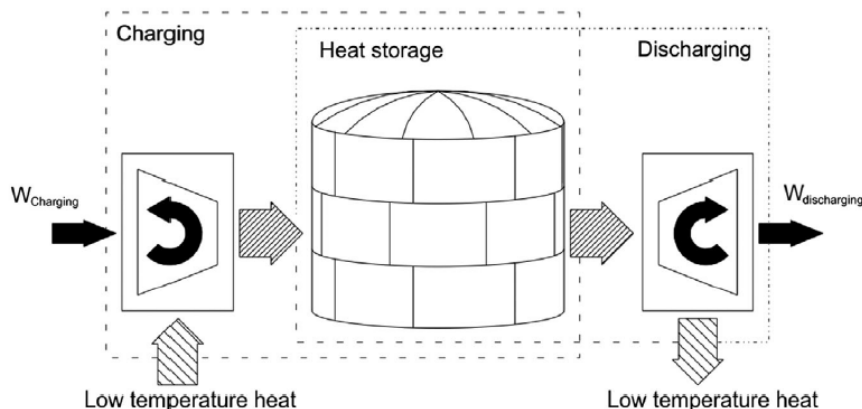


Figure 3-18 Schematic of PTES: a counterclockwise thermodynamic cycle is used to charge a thermal storage unit [32]

This new technology, based on CSP’s long-proven low-cost thermal energy storage using molten salts, as specified before as mix of sodium nitrate and potassium nitrate, promises a stable heat reservoir, used to drive a power block.

This heat in a CSP plant comes naturally from the sun irradiance, and is converted in electricity using a Rankine power cycle.

Because of the low cost compared to battery storage, the idea of building standalone thermal storage is not new. But nowadays the world’s largest steel producer, Arcelor Mittal, has begun to decarbonize steel making using thermal storage in slag and German research institute DLR has proposed siting thermal “batteries” of molten salt at decommissioned coal plants [34].

The interesting new idea developed by DLR is to generate, receive and deliver power back to the grid by utilizing the former coal plants existing infrastructure with the auxiliary implementation of salt thermal storage. Anyway when thermal storage is converted to electricity, the efficiency of the steam cycle in coal plants limits the conversion at a range of 40% losing a lot of energy due to the thermodynamical process. To solve this problem project's engineers have developed a new turbomachinery and a novel heat exchanger, which they are now engineering and manufacturing at full scale in a free-standing thermal storage plant in order to reach an efficiency around 60% (but using a *Recuperated Brayton cycle*), and implementing a four-tank storage to increase operating range [35].

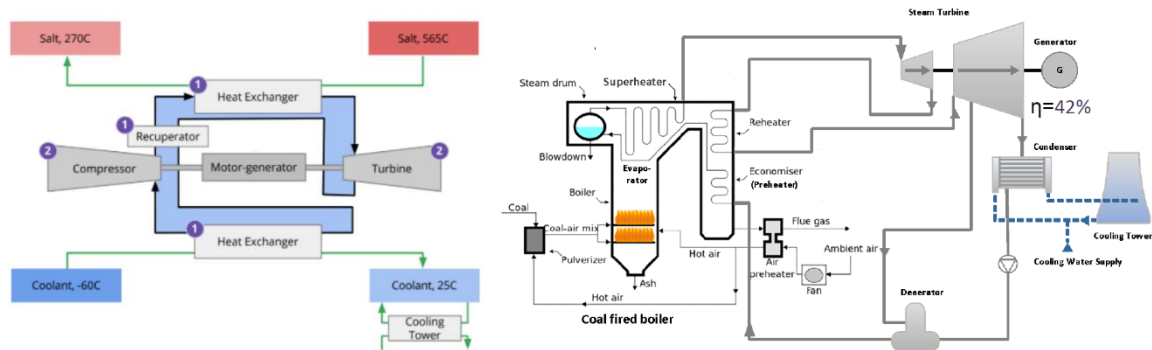


Figure 3-19 Malta Recuperative Bryton cycle (left) [36], Coal power plant scheme (right) [37, 36]

**Store2Power Pilot Project Germany**  
 Köln-Essen, 15 March 2019  
 RWE Power AG  
**Ground-breaking pilot project: thermal storage power plant to be built in Rhenish lignite area**  
 Announcements:  
 • RWE Power, DLR and Aachen University of Applied Sciences team up in development process  
 • Molten salt plant integrates renewables and conventional energy and creates future potential for power plant sites  
 • State of North Rhine Westphalia funds development with 42.9 million  
 RWE Power AG, DLR and FH Aachen currently analyzing techno-economic feasibility of converting a German lignite plant in the lignite region Rheinisches Revier into a storage plant by retrofit with a high temperature molten salt storage system to be charged with renewable electricity from the German grid. Supported with 2.9Mio Euro grant from state Government North Rhine Westphalia  
 Construction of pilot planned for 2021/22

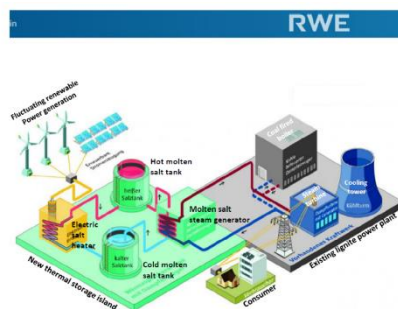


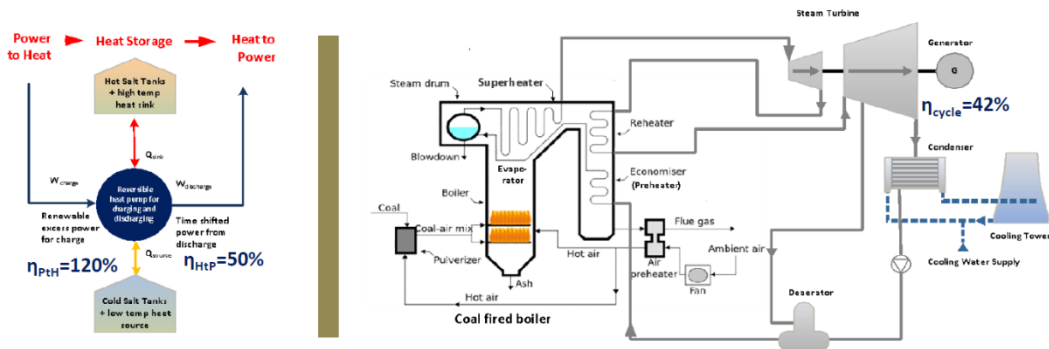
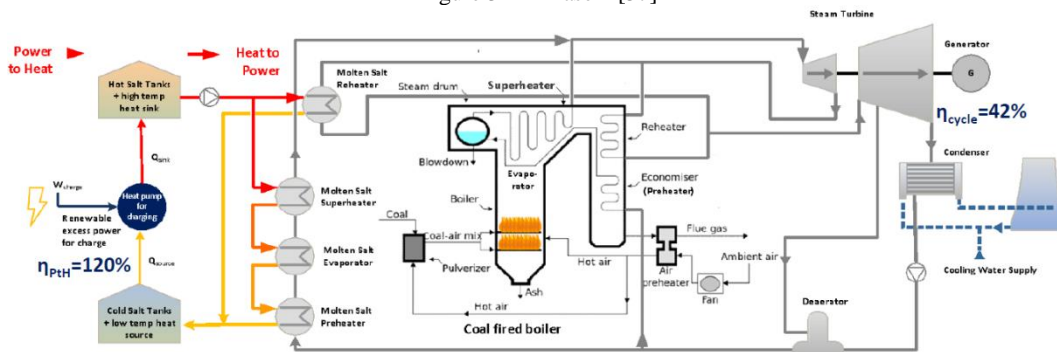
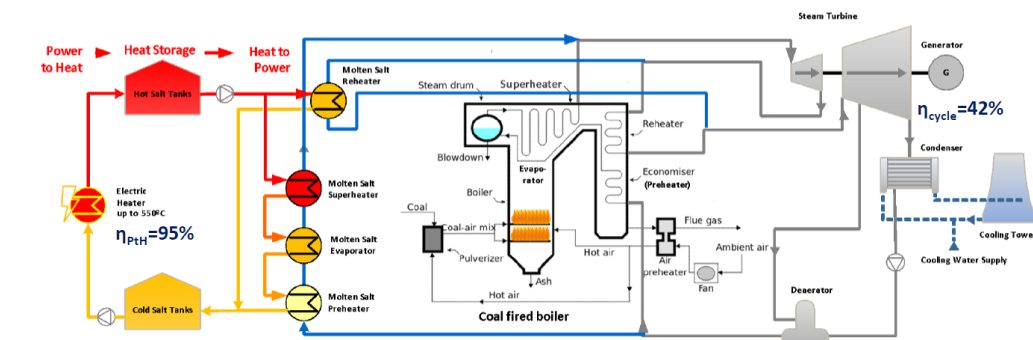
Figure 3-20 Pilot project in Germany [37]



So actually the ambitious plan of some company in Germany is to convert old coal power plants into giant batteries.

The step that they propose to follow are presented below and explained in the images:

- *Phase 1*) a pilot integration of molten salt storage in existing coal plant as proof of concept and efficiency roundtrip 40%.
- *Phase 2*) substitution of resistance heater by heat pump for charging proof of concept with an efficiency roundtrip 50%.
- *Phase 3*) pilot demonstration of reversible heat pump proof of concept efficiency roundtrip 60% [37].



## Chapter 4    **Technology compatibility**

To merge technologies, it always needs a common junction point. In this chapter are presented similarities, strongness and weakness points, compromises in their implementations.

### **4.1    Same aspects of the two technologies**

As well known, coal power plants exist since the first industrial revolution and provide almost all the baseload energy required by the global population. Since the climate change is a fact, many countries have pledged in significant changes, changes with the aim of *decrease* the *carbon footprint* of the human activity. Considering the amount of CO<sub>2</sub> emitted every year by this kind of technology many incentives as been proposed to accomplish their complete shut down in the next 30 years. So, the desire nowadays is to shift to renewables and carbon plants are an interesting asset to convert.

Considering the CSP plant, as said in the previous chapter, works with a *Rankine cycle*, so the power station is basically the same of a coal power plant.

Both work with water, have superheaters and reheaters, degassifier, condenser, feed and circulation pumps, that if still in good state can be reconverted to new life.

### **4.2    Main differences**

Both CSP and coal power plants need a heat source to work. The first works concentrating the solar light, the second burning fuel, so the first big difference between the two is the presence of the *boiler*, that depending on the plant can be a very big structure. While CSP does not need boiler but *heat exchangers*, a big *field* to put *collectors* and *storage tanks*. Second logical difference are specific areas in the plant, one dedicated to the coal, where the fuel is stored waiting to be used; the second one is the *ash dam*, where the solid residual of the combustion are disposed, in order to be treated, sold or directly put underground. They consist in a significant part of the plant that can be as big, if not even twice, the power station. CSP instead does not need these fields but requires a solar one (and depend on the kind of CSP also a tower receiver), and they are far bulkier ones, even 8 times the power station.

Other areas completely dedicated in CSP plant are the storage tanks previously described, and the containers needed to fill them after to have heat up the storage fluid.

### 4.3 Possible outcome of the mix

Coal power plants are usually located in industrial areas, isolated to the rest of the other buildings, also due to their high pollution emission. This is an advantage in the conversion to CSP, permitting to exploit all the neighboring area to add the concentrator system required. Carbon storage area can be converted in the thermal storage tank areas, optimizing the distance with the boiler, while ash dam area used for collectors. The boiler can be transformed in a big heat exchanger or can be maintained at minimum working load, implementing the CSP only to increase the temperature in the superheater and preheaters pipelines.

A more complex but even more effective merging could be the conversion of the plant in a hybrid one, employing CSP and PV. PV are a good auxiliary technology, because they can be dislocated and do not need to be close to the power station. Their cost is really low compared to CSP and so it could help to lower the overall *LCOE* of the hybrid plant. In this way the land area next to the power station can be optimized for the night energy demand storage, and if enough also for daily production. While surplus energy produced by PV is converted in heat using the *Joule effect*, so basically trough electrical resistances, and stored in tanks as concentration already does. Moreover, this procedure permits to increment the maximum temperature reachable in the molten salts, increasing efficiency and guaranteeing a no stop working service.

This transformation could give to dismantling intended plants a new life, decreasing the emission in the area, exploiting the remaining potential of the components, and continuing to serve as baseload. All using renewable energy, not only during dayperiod but also at night. The idea to convert a coal plant into a hybrid plant, can make it become a new kind of plant: a *storage plant*. Imaging the number of them around countries, it is simple to see the potencial of a storage plant fleet. Replacing the function of fast starting plants used to cover peaks demand. Once working together small changes in the fleet could adjust the grid with their effort alone, as France actually does with its nuclear power plants net.



## Chapter 5    **Apology to Hybridation**

Hybridization means merge two or more different types of power plant, especially to get better characteristics.

Hybrids exist ever since, as a logic consequence of study researches focused on development and improvement, but only in these late years are taking hold. That's probably due to energy market liberalization, that providing more option for the people that ask for a service, and to be competitive needs to be better than others, which was not the case with previous monopoly condition. Also shifting to renewables is probably giving voice to that subject, passing to a share of single technologies used in different cases, no new ones, aleatory for its intrinsic nature, and so needing to be merged to work consistently, efficiently and in a controllable manner all together.

Hybridization kinds that nowadays are under study are generally a *mix of renewable and fossil fuels solutions*. The goal is obtaining a good service producing with limited pollution, at a good price. Generally PV and wind plus lithium batteries and/or diesel; CSP plus turbogas or solar aided coal-fired power generation system (*SAPG*).

In particular the concept of hybridization of solar thermal energy and fossil fuels has been proposed and studied since *1970s*, but with recent necessity of clean energy storage the topic has found a new wave of success [38].

*SAPG* systems aim to lower emissions in existing coal plant, converting them in an low polluting hybrid, promising low costs, good efficiency and obviously low emissions [39]. Numerous studies have been published in the past three years, trying to give relevance to the subject, demonstrating that the fuel consumptions decreases considerably and plant flexibility improves [40, 41].

However hybrid solution renewables plus fossil fuels promises good results, it is possible not to be enough to this modern and fast changing world. That's the reason why full hybrid solution are now studied implementing as presented in the previous chapters, the use of PV technology and molten salts energy storage, taken singularly or helping a CSP plant, even PV used as a source of thermal energy [42, 43].

CSP used in a solar thermal power plant to generate electricity is often portrayed as competing with solar PV, but in fact, *CSP really competes with the other thermal power plants* like natural gas that supply dispatchable electricity.

PV is not dispatchable. PV only runs when the sun shines. CSP can be dispatched on demand, more like turning on a switch to get solar. So CSP doesn't compete with PV, if great amount of batteries are not present.

Although CSP makes solar electricity by harvesting sunlight like PV, it operates more like a conventional power plant. Once the sunlight is collected as heat, the “back end” – the power block – works the same as any other thermal energy power station.

CSP also runs on thermal energy. But instead of having to burn a fuel to generate the next few hours of electricity, CSP can harvest a pretty much endless supply of sunlight to store and deliver solar thermal energy. In contrast with a finite fuel like gas or coal or uranium that must be dug up from below the earth to use up by burning it to make electricity – this sunlight will be available above the earth for centuries.

Because of its ability to store solar energy thermally, CSP can deliver power on demand (so it's *dispatchable*), and it can be made available whenever it's wanted. In other words, CSP is solar power that can be switched on when needed — in the evening, before sunrise, or at whatever time the regional grid needs power [44].

A solar thermal power plant can respond to new demand within the same day. The speed of start-up is limited only by the time it takes to start the turbines, just as it does with other thermal power stations, about *20 minutes*.

This power block technology and the ability to store its solar energy thermally makes CSP a disruptive renewable technology. It can make the energy grid cleaner because it can actively replace fossil energy. Together with the other renewables, CSP plays a role in a cleaner new grid, and PV can only help it.

Like CSP, natural gas is dispatchable. But despite its green competitor, it's also not Climate-safe, dangerous and with an unpredictable volatile cost [45].

In 2017, the US National Renewable Energy Laboratory (NREL) has estimated that by 2020 electricity could be produced from power towers for 5.47 cents per kWh [46], but at the moment this price has not been reached yet, the times are not enough mature for such prices, but the direction that is taking that solution is not so far to reach it.

There is the deep necessity to change the public cocience on enegy value, because cheaper doesn't mean better, each technology has its own advantages.

Stability and dispachability are also need, and good integration with actual plants could help a *faster shift to full renewable EU 2050*, avoiding the desmantling of coal plant, helping instead their conversion, improving local development, saving lots of working places and maybe create others to the energivorous generetaions to come [47].

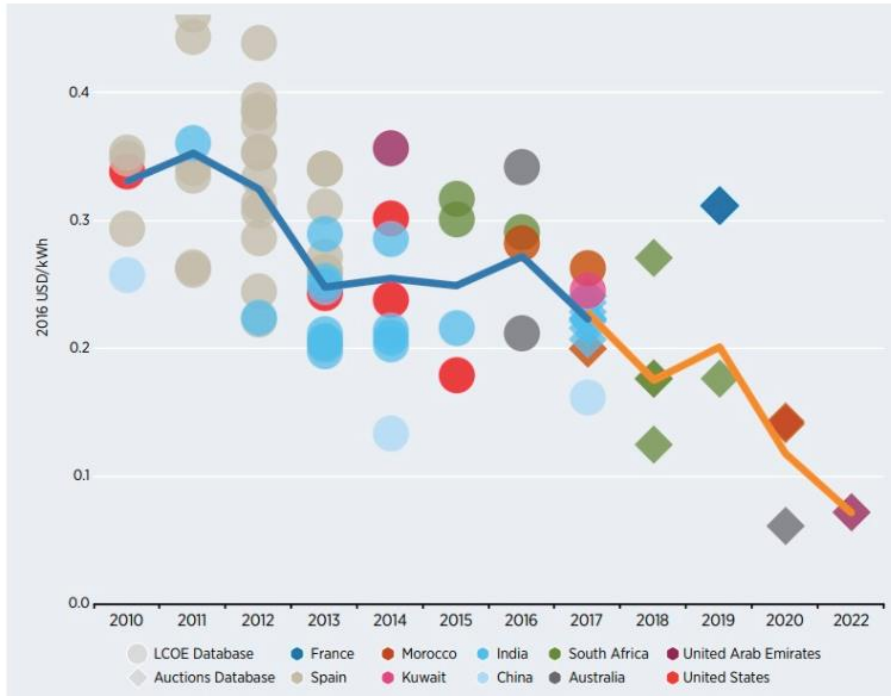


Figure 5-1 Levelised cost of electricity and auction price trends for CSP, 2010-2022 [14]



## Chapter 6 Used Software

To carry on the study, it has been used a free techno-economic software model, the System Advisor Model (SAM), developed by the National Renewable Energy Laboratory (NREL) a government-owned, contractor-operated facility, funded through the United States Department of Energy, version 2018.11.11. This software is generally used in the renewable energy industry to facilitates decision-making for project managers and engineers, policy analysts, technology developers and Researchers [66].



Figure 6-1 National Renewable Energy Laboratory logo

SAM can model many types of renewable energy systems, as:

- Photovoltaic systems, from small residential rooftop to large utility-scale systems
- Battery storage with Lithium ion, lead acid, or flow batteries for front-of-meter or behind-the-meter applications
- Concentrating Solar Power systems for electric power generation, including parabolic trough, power tower, and linear Fresnel
- Industrial process heat from parabolic trough and linear Fresnel systems
- Wind power, from individual turbines to large wind farms
- Marine energy wave and tidal systems
- Solar water heating
- Geothermal power generation
- Biomass combustion for power generation
- High concentration photovoltaic systems

In its architecture projects can be analysed with different financial models:

- Residential and commercial projects where the renewable energy system is on the customer side of the electric utility meter (behind the meter), and power from the system is used to reduce the customer's electricity bill.
- Power purchase agreement (PPA) projects where the system is connected to the grid at an interconnection point, and the project earns revenue through power sales. The project may be owned and operated by a single owner or by a partnership involving a flip or leaseback arrangement.
- Third party ownership where the system is installed on the customer's (host) property and owned by a separate entity (developer), and the host is compensated for power generated by the system through either a PPA or lease agreement.

During the current work, to obtain the first data to be analysed and restructured in new kind of hybrid plant, not modelled by the actual version of the software, are been used CSP power tower molten salt, PPA single owner (utility); and Photovoltaic (detailed), PPA single owner (utility).

Each model presents a common part linekd to Location and Resource, System Cost, Financial Cost, Lifetime, and for the CSP tower the Power Cycle. In sencod hand each model has its own subsection and design parameters.

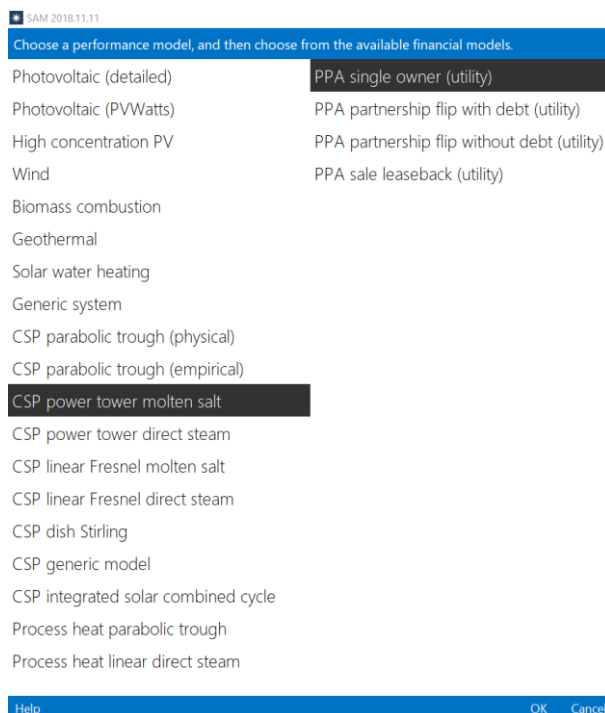


Figure 6-2 System Advisor Model (SAM) first screen

# Chapter 7 Case study

To choose a representative power plant the dimension and its production are not the only aspects to take into consideration. In this chapter other deeply import aspects are taken into account to choose the inical study plant.

## 7.1 Geographical location

Geographical data, latitude in particular, is necessary to obtain significant results. As introduces in the second chapter, the energy of the sun that can be exploited is a function of how the light reaches the ground, and so depending on the latitude can be more intense or variable during the year period.

CSP technology prefers very *sunny location* obviously, so best candidates where install a new plant are usually deserts, present in USA, maxico, south-east America, north and south Africa, middle east, Caspian area, China, India and Australia (BWh and BWk spots in the Figure 7-1 Köppen-Geiger Climate Classification Map ).

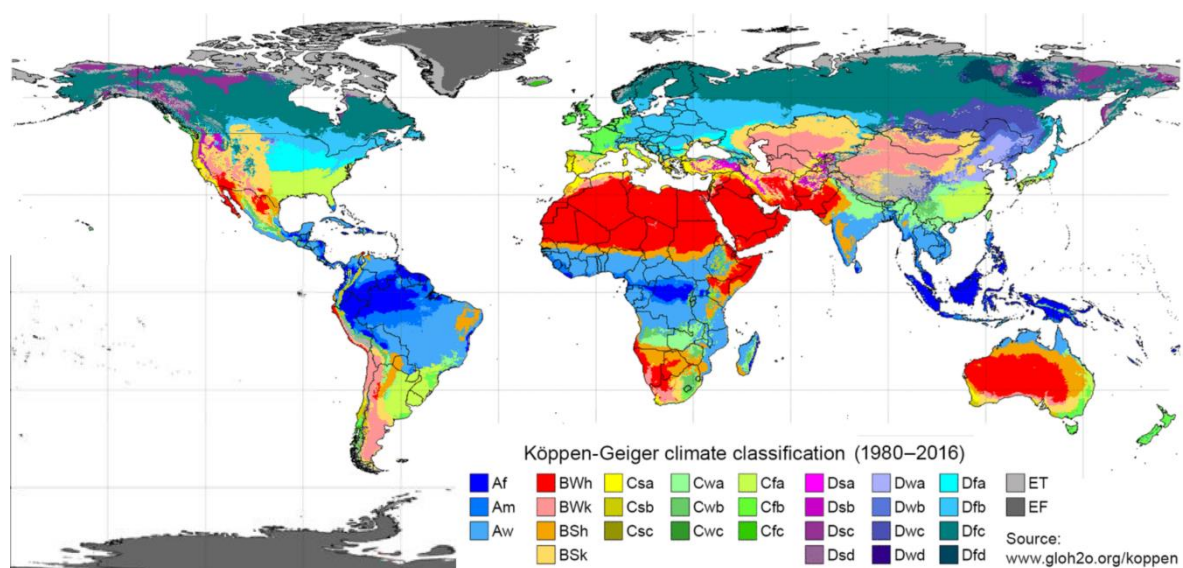


Figure 7-1 Köppen-Geiger Climate Classification Map [48]

Having found more data referring to the dimalting coal plants of South Africa and helping the technology the local development for not high industrialized areas, the choice fell on it.

### 7.1.1 Political and economical situation

South Africa is the second largest economy in Africa in terms of GDP (349.6 billion USD), after Nigeria [49]. As a regional manufacturing hub, it is the most industrialized and diversified economy of the continent, in fact it is an upper-middle-income economy, one of only eight such countries in Africa. However, rural and urban poverty still represent a significant problem. They are indeed the consequence of a peculiar kind of growth which resulted in a deep division between urban insiders and rural ‘outsiders’, and an uneven and selective incorporation of South Africa’s rural black population into the urban economy [50, 51].

While the average energy consumption per capita in most African countries ( $0.7 \text{ toe/capita}$ ) is well below the world average ( $1.86 \text{ toe/capita}$ ) and largely comparable to that of India, South Africa is characterized by an average energy consumption per capita equal to  $2.3 \text{ toe/capita}$ . The majority of the South African TPES is provided by coal, that accounts for 75%, imported oil (14%) and biofuel and waste (5%).

The high dependence on coal makes the country also very carbon-intensive, with energy related CO<sub>2</sub> emissions of  $7.4 \text{ ton}_{\text{CO}_2}/\text{capita}$ , higher than the world average of  $4.4 \text{ ton}_{\text{CO}_2}/\text{capita}$  and far higher than the regional average of  $0.9 \text{ ton}_{\text{CO}_2}/\text{capita}$  [52]. Given its coal-based energy economy, South African is one of the highest emitters of greenhouse gases when compared to other developing countries, whether this is measured in emissions per person or per unit of GDP. In accordance with the World Health Organization's guidelines, the air quality in South Africa is considered moderately unsafe: the country's annual mean concentration of PM<sub>2.5</sub> is  $25 \mu\text{g}/\text{m}^3$ , exceeding the recommended maximum of  $10 \mu\text{g}/\text{m}^3$ . Contributors to poor air quality in South Africa include the mining and agricultural industry and coal burning. Moreover, household air pollution from cooking and heating with solid fuels is responsible for 2.9 million deaths a year [53, 54, 55]. The share of the population that does not have access to electricity is 15.6% and this percentage rises to 29.7% if we consider the rural population only [56].

As reported on the INDC, the main focus for the near future is to increase the electricity production and switch to a low carbon economy in order to respond to climate change and obtain a sustainable economy and new labour for the growing country [57]. Plans are already be presented, and they consider disposing coal power plant, and build PV, Wind and CSP ones, depending on the natural resources of the chosen areas.

## 7.2 Carbon plant model

The three plants that provided the basis for the choice of data and hypotheses in the study are presented below.



## 7.2.2 Plant 1: Komati

Komati is situated about 37 km from Middelburg, 43km from Bethal and 40km from Witbank, via Vandyksdrift. The Planning started during the mid-1950 on the farm Koorfontein. The deed of transfer of the land was signed on 22 November 1957. Site levelling started in April 1958 and the first unit, Unit 5, was commissioned on 6 November 1961 and Unit 9, the last, in March 1966 [58].

During the mid-80's a decision was made to take out units and later the entire Power Station was out of service, mainly because of the surplus capacity, increasing of maintenance costs of the older plant and to be able to put newly built power stations, such as Majuba, in commercial service and make use of the guarantee period. It was also decided not to let the plant deteriorate but to conserve it properly to return it at a later stage. The conservation process was called mothballing.

In the early 2000's a decision was taken to return Komati Power Station to service to meet the growing demand of electricity and the power station was gradually brought back to service from about 2005, completing the project in 2012. In 2010 Komati ended up TOP in Plant Performance setting a new goal, name to "Be the Best of the Best in Generation" [59].



Figure 7-2 Komati power station

### General:

Komati was one of the first pulverised fuel firing stations and designed to generate 1000 MW with five units rated at 100 MW and four at 125 MW.

### Technical details:

Five 100 MW Units

Four 125 MW Units

Installed capacity: 1000 MW

Design efficiency of rated turbine MCR (%): 30.00%.

### **7.2.3 Plant 2: Grootvlei**

Grootvlei Power Station is situated near Balfour in Mpumalanga Province. The station was built in the late 1960's and was shut down in 1990 and then mothballed. The total station capacity is 1200 MW. The design of Grootvlei consists of 6 turbines of MAN design with Brown Boveri generators. The boilers are of Babcock design on 5 sets and a single Steinmuller design on unit 5. Boiler 5 has Loesche mills and the remaining units have BEC 8.5 E mills.

Each boiler has six mills, nominally five are required for full load. This was the first station of this size to have dry cooling and both direct (unit 5) and indirect cooling (unit 6). Unit 6 uses demineralised water as a cooling medium. The outside plant is generally classical Eskom design of that era with wet ashing and coal staithes supplying the coal via two incline conveyors to the boilers [60].

General:

Grootvlei's units 5 and 6 were the first test facilities for dry cooling in South Africa. Unit 6 has an indirect dry cooling system.

Technical details:

Six 200MW units

Installed capacity: 1 200MW

Design efficiency at rated turbine MCR (%): 32.90%.

### **7.2.4 Plant 3: Camden**

Load forecasting in the early 60's indicated that by the end of 1966 a new power station would be required. Toward the end of 1961 the chairman of the Electricity Supply Commission, Dr Reinhart Ludwig Straszacker, decided, after an economic investigation, that a station having an ultimate capacity of 1 600 MW consisting of eight 200 MW units should be considered.

Planning started early in 1962 with the issue of an enquiry for the supply of coal. Adjudication of ensuing tenders took into account, in addition to coal costs, such items as availability and cost of water, availability and cost of rail services and cost and feasibility of transmission lines, all in relation to the geographic position of the collieries concerned. So first unit was commissioned in April 1967 [61].

Camden became the starting point of the national power grid, consisting of a series of 400 kV lines which today interconnect the entire country. Power flowed from Camden over a high-voltage system, which was amongst the most extensive in the world. With the low cost of generation in the pithead power stations in the Transvaal (Mpumalanga) it was more

economical to supply those distant consumers in this manner than to build more coal-fired power stations in the Western Cape. The station's eight units were mothballed in 1990, but due to a sharp increase in the demand for electricity, the Eskom Board of Directors took a final decision in 2003 for the Return to Service (RTS) [62].



Figure 7-3 Residential houses built for the employees (left), View of the residential property with the power station in the background (right) [62]

Technical details:

Total station electrical capacity (8 sets)	1600 MW
Total boiler capacity (8 boilers)	1814.4 kg/sec
Total circulating water capacity (10 pumps)	73.242 m <sup>3</sup> /sec
Station efficiency	± 32.0%
Max. Total coal consumption	17440 metric tons/day

Description of Plant:

Turbine House:

Turbines	2 cylinder reaction type
Generators	200 MW rating
Manufacturer of turbo-generators	C A Parsons
Steam conditions at turbine shutdown valve	10.432 MPa, 538°C
Vacuum	6.77 kPa
Speed of generators	3000 r.p.m.
Generator Voltage	16500 volts

Boiler House:

Boilers (8) single drum, radiant furnace	Pulverised fuel furnace
Continuous rating	226.8 kg/sec
Boiler Manufacturers	International Combustion (Africa) Limited (ICAL)
Outlet Pressure	11.032 MPa
Outlet temperature	543°C
Calorific value of coal	24.65 MJ/kg (air dried value)

Coal Plant:  
 Coal sources Usutu South, West and East mines  
 Number of station coal straiths 4  
 Capacity of 4 straiths 72600 metric tons

Cooling Towers:  
 Cooling tower type Asbestos cement packed, natural draught, hyperbolic, film type  
 Number of towers 6  
 Capacity ± 581900 l/min  
 Height above sill 111.86 m  
 Diameter of top 54.25 m  
 Diameter of throat 49.99 m  
 Temperature drop 8.3°C

Water:  
 Main source Jericho Dam  
 Dam capacity Jericho 31000000 m3  
 Pipelines - Jericho to Camden 39 km  
 Main pipeline capacity 81.83 MI/day/pipe  
 Station consumption 109.1 MI/day

It is Eskom's intention to build a fleet of CSP plant, based on the learning attained from the construction and operation of the demonstration plant built in 2015. The capacity of such a fleet will be in accordance with, and in support of, the Integrated Resource Plan on South Africa [63]. As can be seen in the Transmission Development Plan 2018-2028 and 2019-2039, numerous simulation are already be done to dispose the coal plant in the next years and the idea is to substutue the electricity demand on green production, based on sun and wind [64, 65].

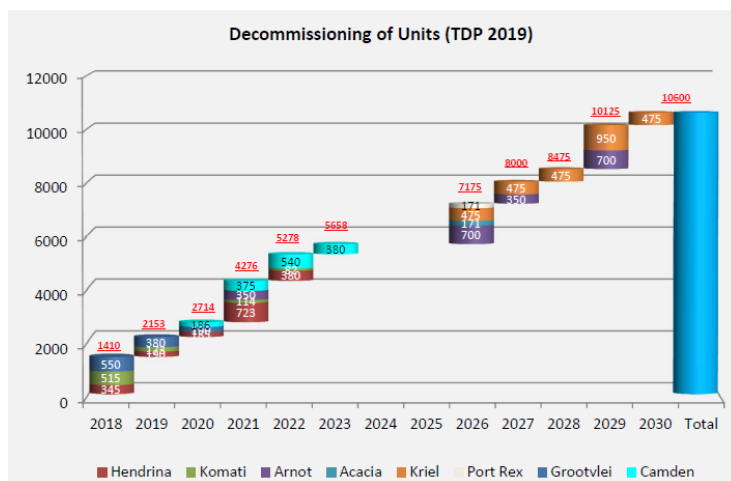


Figure 7-4 Simulation of the coal power plants disposal [65]

# Chapter 8 **Implementation of the model**

The eighth chapter contains the procedure followed for the different cases analysed during the study on SAM, the data implemented to obtain the results, and the way the SAM's results are being rearranged to obtain the final solution.

## **8.1 Presentation of the analysed cases**

The conducted work is a comparison between existing technologies and hybrid plants. It aims to provide information in favor of the hybrid configuration, in terms of produced energy, capacity factor, and LCOE.

Focus of the study are the technologies presented in Chapter 3:

- Solar Tower Plant
- Solar Tower Plant + PV and Carnot battery
- PV + molten salts and Carnot battery
- PV + electrical storage (batteries)

The goal is trying to provide a baseload power generation of 100 MW using only renewable sources, without any external help except the plant itself.

### 8.1.1 Common hypothesis

As anticipated in **Error! Reference source not found.**, the location has been chosen in order to use significative data from some real existing caol plants in South Africa. The location choosen between the three analysed in chapter 7.1 is Komati, with weather data downloaded from the database of Climate.OneBuilding, a global meteo database with 9,000 locations, proposed in the SAM wheather webpage [67, 68].

**Weather Data Information**

The following information describes the data in the highlighted weather file from the Solar Resource library above. This is the file SAM will use when you click Simulate.

Weather file:

---

**Header Data from Weather File**

Station ID	<input type="text" value="682970"/>	Latitude	<input type="text" value="-25.517"/>	DD	For NSRDB data, the latitude and longitude shown here from the weather file header are the coordinates of the NSRDB grid cell and may be different from the values in the file name, which are the coordinates of the requested location.
Data Source	<input type="text" value="ISD-TMYx"/>	Longitude	<input type="text" value="31.9"/>	DD	
Elevation	<input type="text" value="183"/> m	Time zone	<input type="text" value="GMT 2"/>		

---

**Annual Values Calculated from Weather File Data**

Global horizontal	<input type="text" value="5.24"/> kWh/m <sup>2</sup> /day	Average temperature	<input type="text" value="22.0"/> °C	<b>Optional Data</b>
Direct normal (beam)	<input type="text" value="3.87"/> kWh/m <sup>2</sup> /day	Average wind speed	<input type="text" value="2.0"/> m/s	Maximum snow depth <input type="text" value="0"/> cm
Diffuse horizontal	<input type="text" value="2.53"/> kWh/m <sup>2</sup> /day	*NaN indicates missing data.		Annual albedo <input type="text" value="-999"/>

Figure 8-1 Location and Resource data in SAM

One big hypothesis of the study, is giving new life to an existing coal plant structure, mantaning the power cycle and the turbine with its real data, taken from chapter 7.2.4, 7.2.4Plant 3: Camden. Hence, in *System Cost*, *Power Cycle* and *Turbine* costs are set to zero.

In order to be more real as possible, is as been considered a stop period of 15 days during winter, in particular as been chosen the worst 15 days of production for each case.

System Design Parameters:

- Power cycle estimated Net Output: 100 MW
- Cycle Thermal Efficiency: 32%
- Ambient Temperature: 31 °C
- Low Ambient Temperature: 10 °C
- High Ambient Temperature: 36 °C
- Cooling System Water Usage: 1262.73 kg/s
- Low HTF Temperature: 500 °C
- High HTF Temperature: 525 °C
- Power cycle Gross output determined by the hypothesis.
- Temperatures, Cycle Thermal Efficiency, Cooling System Water Usage, High HTF Temperature taken from Candem plant.
- Low HTF Temperature set as minimum by the SAM model.
- Ambient Temperature determined by dry temperature at P95.

System Design Parameters				
Power cycle gross output	111	MWe	Cycle thermal efficiency	0.412
Estimated gross to net conversion factor	0.9		Cycle thermal power	269.417
Estimated net output (nameplate)	99.9	MWe	HTF hot temperature	565 °C
			HTF cold temperature	290 °C

General Design Parameters					
Pumping power for HTF through power block	0.55	kW/kg/s	Cycle design HTF mass flow rate	650.5	kg/s
Fraction of thermal power needed for standby	0.2				
Power block startup time	0.5	hours			
Fraction of thermal power needed for startup	0.5				
Minimum turbine operation	0.2				
Maximum turbine over design operation	1.05				

User Defined Power Cycle ▾

User Defined Power Cycle Design Parameters					
Ambient temperature	31	°C	Gross power consumed by cooling system	0	%
Cooling system water usage	1262.73	kg/s	Gross power consumed by cooling system	0.0	MWe

Performance as Function of HTF Temperature, HTF Mass Flow Rate and Ambient Temperature					
Low, design, and high parameter values for input generation:					
Low HTF temperature	500	°C	Low normalized HTF m	0.3	
Design HTF temperature	565.0	°C	Design normalized HTF m	1.0	
High HTF temperature	525	°C	High normalized HTF m	1.2	
			Low ambient temperature	10	°C
			Design ambient temperature	31.0	°C
			High ambient temperature	36	°C

Figure 8-2 Candem turbine data, Power Cycle in SAM

In order to make a financial comparison, when permitted (all cases except PV + Battery), as been used the same financial model: *Constant IRR 11%*.

A *Lifetime* based on 25 years and a degradation rate of 0.02% each year.

System Performance Degradation	
Degradation rate	0.02 %/year
Applies to the system's total annual AC output.	
In Value mode, the degradation rate applies to the system's total annual kWh output for the previous year starting in Year 2. In Schedule mode, each year's rate applies to the Year 1 value. See Help for details.	

Figure 8-3 Lifetime Parameter in SAM

*Incentives* are not been taken into account.

All parameters not mentioned have been left by default.

The dimension of each plant has been set to cover 24h full production in the sunniest day of the year, in order to avoid defocusing and exemplifying the problem.

<b>Solution Mode</b>		IRR target <input type="text" value="11"/> % IRR target year <input type="text" value="20"/>		<b>Escalation Rate</b>	
<input checked="" type="radio"/> Specify IRR target	PPA price <input type="text" value="0.124"/> \$/kWh			PPA price escalation <input type="text" value="1"/> %/year	
<input type="radio"/> Specify PPA price				Inflation does not apply to the PPA price.	
<b>Analysis Parameters</b>					
Analysis period <input type="text" value="25"/> years		Inflation rate <input type="text" value="2.5"/> %/year		Real discount rate <input type="text" value="6.4"/> %/year	
				Nominal discount rate <input type="text" value="9.06"/> %/year	
<b>Project Tax and Insurance Rates</b>			<b>Property Tax</b>		
Federal income tax rate	<input type="text" value="21"/> %/year	Assessed percentage	<input type="text" value="100"/> % of installed cost		
State income tax rate	<input type="text" value="7"/> %/year	Assessed value	<input type="text" value="\$ 685,709,120.00"/>		
Sales tax	<input type="text" value="5"/> % of total direct cost	Annual decline	<input type="text" value="0"/> %/year		
Insurance rate (annual)	<input type="text" value="0.5"/> % of installed cost	Property tax rate	<input type="text" value="0"/> %/year		
<b>Salvage Value</b>					
Net salvage value <input type="text" value="0"/> % of installed cost		End of analysis period value <input type="text" value="\$ 0"/>			
<b>Project Term Debt</b>					
<b>Project Term Debt</b>					
<input type="radio"/> Debt percent	<input type="text" value="50"/> % of total cap. cost	<input checked="" type="radio"/> Equal payments (standard amortization)	Moratorium <input type="text" value="0"/> years		
<input checked="" type="radio"/> DSCR	<input type="text" value="1.3"/>	<input type="radio"/> Fixed principal declining interest			
Tenor	<input type="text" value="18"/> years	Choose "Debt percent" to size the debt manually as a percentage of total installed cost. Choose "DSCR" to size the debt based on cash available for debt service. See Help for details.			
Annual interest rate	<input type="text" value="7"/> %	For a project with no debt, set the either the debt percent or the DSCR to zero.			
Debt closing costs	<input type="text" value="450,000.00"/> \$	Be sure to verify that all debt-related costs are appropriate for your analysis: Debt closing costs, up-front fee, and debt service reserve account. Note that debt interest payments are tax deductible, so a project with more debt may have higher net after-tax annual cash flows than a project with less debt.			
Up-front fee	<input type="text" value="2.75"/> % of total debt				

Figure 8-4 Financial Parameters in SAM

## 8.2 Solar Tower Plant

First case analysed, and object of the comparison study is Solar Tower Plant.

<b>-Heliostat Field-</b>	
Design point DNI	<input type="text" value="965"/> W/m <sup>2</sup>
Solar multiple	<input type="text" value="3"/>
Receiver thermal power	<input type="text" value="808"/> MWt
<b>-Tower and Receiver-</b>	
HTF hot temperature	<input type="text" value="565"/> °C
HTF cold temperature	<input type="text" value="290"/> °C
<b>-Thermal Storage-</b>	
Full load hours of storage	<input type="text" value="6"/> hours
Solar field hours of storage	<input type="text" value="2"/> hours

Figure 8-5 System Design in SAM (day)

*DNI* determined with P95 in order to exploit the sun's energy as much as possible. *HTF hot and cold temperature* are been chosen as typical values, as explained in chapter 3.1.2 Components of CSP tower plant.



The *Solar Multiple* has been determined using the Parametric Simulations provided by SAM.

The overall steps for running Parametric Simulations are:

1. Set up parametric inputs by choosing parametric input variables and assigning values to them.
2. Choose output metrics.
3. Run parametric simulations.

After running the parametric simulations, SAM displays tables and graphs of the results on the *Parametric Simulations* page. This information can be used to choose an optimal value for an input variable, or export the data or graphs to explore relationships between input variables and results. Anyway these parametric simulation results are separate from the case results that appear on the *Results* page and once selected the optimal case it need to be set in the proper SAM label.

As can be seen in Figure 8-6 and Figure 8-7, the parameter that determined the *Solar Multiple* are *LCOE* minimum, *Capacity Factor* and *Annual Energy* maximum, *Tower Height* not exceeding 270m (structural limit). A problem met in the parametric analysis is the little amount of energy produced during the year and as a consequence the low capacity factor (place with low DNI). The problem has been solved considering the analysis based on two towers and two fields, using the same turbine, one working during the day and one during the night. Unfortunately SAM does not permit this type of configuration and the data has been reprocessed in Excel and MATLAB after to be extracted from the two cases solved individually.

*Full load hours of storage*, function of solar multiple, has been chosen to cover a 24h production during the sunniest day of the year (6 hours of storage for day period and 6 hours for night period in order to exemplify the calculation).

-Heliostat Field-	
Design point DNI	965 W/m <sup>2</sup>
Solar multiple	3.5
Receiver thermal power	943 MWt
-Tower and Receiver-	
HTF hot temperature	565 °C
HTF cold temperature	290 °C
-Thermal Storage-	
Full load hours of storage	6 hours
Solar field hours of storage	1.71429 hours

Figure 8-6 System Design in SAM (night)

	solarm ( )	lcoe_nom (cents/kWh)	capacity_factor (%)	annual_energy (kWh)	h_tower (m)
1	2	24.3786	20.1879	1.59162e+08	176.642
2	2.25	23.3217	22.8774	1.80365e+08	202.881
3	2.5	22.7389	25.2631	1.99174e+08	209.702
4	2.75	23.4614	26.2042	2.06594e+08	201.343
5	3	24.5794	26.7706	2.1106e+08	224.968
6	3.25	25.6173	27.1884	2.14354e+08	241.195
7	3.5	26.8216	27.5121	2.16905e+08	237.535
8	3.75	28.5225	27.2436	2.14789e+08	236.856
9	4	31.1564	26.2584	2.07022e+08	247.395
10	4.25	32.3373	26.5967	2.09689e+08	254.318
11	4.5	33.8646	26.638	2.10014e+08	254.454
12	4.75	35.9001	26.4154	2.08259e+08	272.245
13	5	37.8159	26.1913	2.06492e+08	278.323

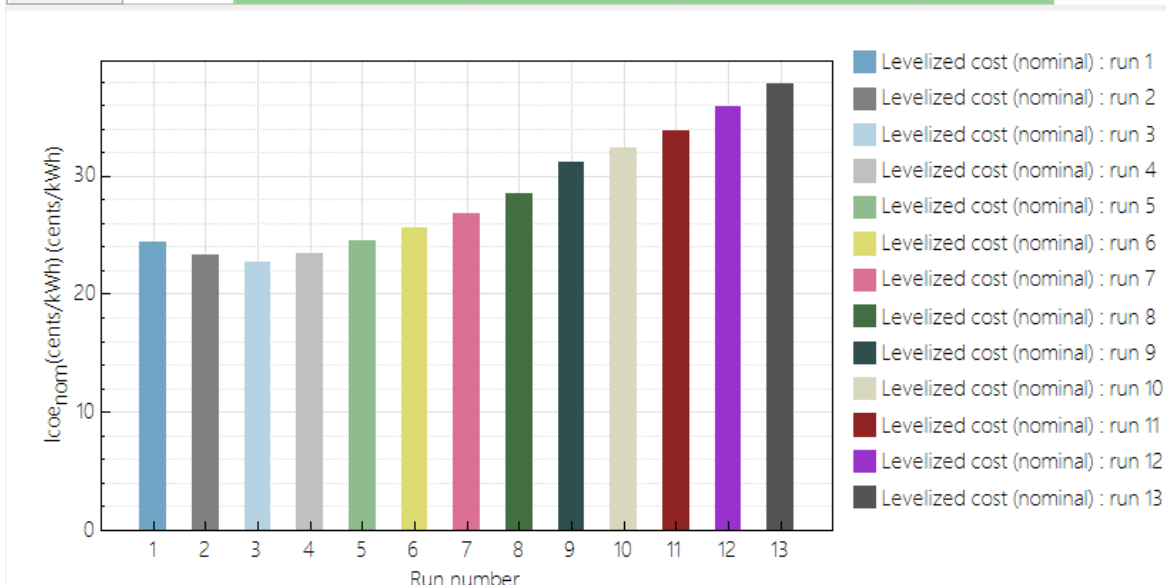


Figure 8-7 Solar Multiple optimization in SAM Parametrics (day)

*Heliostat field* is determined by an algorithm present in SAM, that looking for a optimum for its goal function determines the position of each single device.

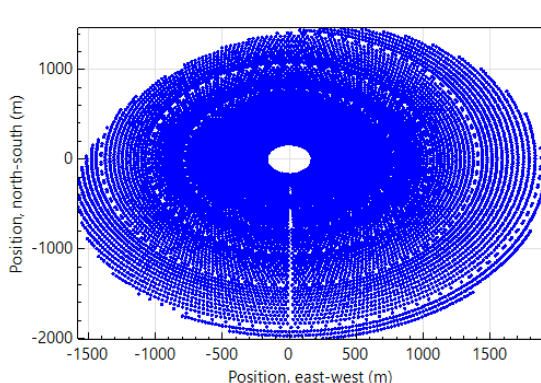
Heliostat properties as well as mirror reflectance and soiling have been taken from Datasheet, see Annex. While *Max heliostat distance to tower height ratio* has been determined in the same manner of Solar multiple, using parametric simulations.

### Heliostat Field

	X Position	Y Position
Import...	1873.93	-109.829
Export...	-1218.6	-700.827
Copy	79.6419	1438.35
Paste	1761.62	506.824
	195.319	-2008.53
	-782.589	1047.67
Heliostats:	230.275	1457.26
12059	1429.89	1003.68
	866.303	1374.56
	-928.572	920.768
	-798.871	-1749.6
	-1144.1	696.365
	400.000	1343.500

Generate heliostat layout using tower dimensions Calculate  
 Optimize heliostat layout and tower dimensions Calculate

Solar field geometry optimization calculates the number of heliostats above, and tower height, receiver height and diameter on Tower and Receiver page.



#### Optimization Settings

Initial optimization step size	0.06
Maximum optimization iterations	50
Optimization convergence tolerance	0.001

---

### Heliostat Properties

Heliostat width	12.96 m
Heliostat height	10.94 m
Ratio of reflective area to profile	0.97
Single heliostat area	137,529 m <sup>2</sup>
Image error (slope, single-axis)	1.53 mrad
Reflected image conical error	4.32749 mrad
Number of heliostat facets - X	4
Number of heliostat facets - Y	8
Heliostat focusing method	Ideal
Heliostat canting method	On-axis

### Heliostat Operation

Heliostat stow/deploy angle	8 deg
Wind stow speed	15 m/s
Heliostat startup energy	0.025 kWe-hr
Heliostat tracking power	0.055 kWe
Design-point DNI	965 W/m <sup>2</sup>

---

### Land Area

Non-solar field land area	45 acres
Solar field land area multiplier	1
Base land area	2306.34 acres
Total land area	2,351 acres
Total heliostat reflective area	1,658,461 m <sup>2</sup>

### Solar Field Layout Constraints

Max. heliostat distance to tower height ratio	9.5
Min. heliostat distance to tower height ratio	0.75
Tower height	229.307 m
Maximum distance from tower	2178.42 m
Minimum distance from tower	171.98 m

---

### Heliostat field availability

Edit losses... Constant loss: 0.0 %  
Hourly losses: None  
Custom periods: None

Curtailment and availability losses reduce the solar field output to represent component outages, soiling, or other events.

Mirror reflectance and soiling	0.948
Heliostat availability	0.99

Figure 8-8 Heliostat Field in SAM (day)

*Tower Receiver Properties* are obtained by the heliostat field optimization, while the *flow pattern of the HTF in the receiver* is obtained using parametric simulations. HTF is a mixture of 60% NaNO<sub>3</sub> and 40% KNO<sub>3</sub>.

53

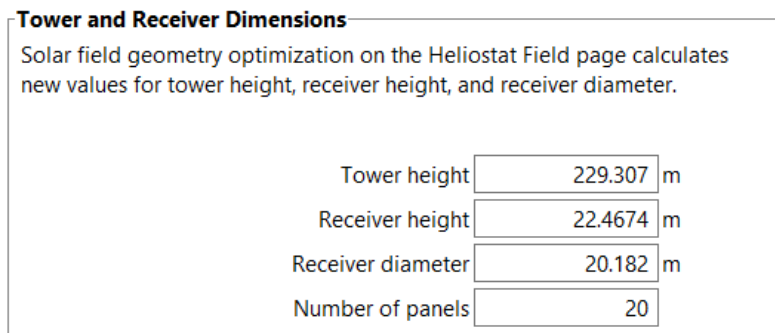


Figure 8-9 Tower and Receiver Dimensions in SAM (day)

*System control* and *TOD factor*, that give information on when the tower is producing electricity have been set working the first 12h of the day for day tower, and the second 12h for night tower (in order to exemplify the computations).

*System cost Thermal energy storage* for night tower has been increased by 15% to cover the cost of losses in the distance and the higher amount of pipeline to link the two towers in a single power station.

All parameters not mentioned have been left as default.

Metric	Value	Metric	Value
Annual energy (year 1)	271,083,136 kWh	Annual energy (year 1)	317,770,176 kWh
Capacity factor (year 1)	34.4%	Capacity factor (year 1)	40.3%
Annual Water Usage	15,363,146 m <sup>3</sup>	Annual Water Usage	16,445,995 m <sup>3</sup>
PPA price (year 1)	22.00 ¢/kWh	PPA price (year 1)	18.73 ¢/kWh
PPA price escalation	1.00 %/year	PPA price escalation	1.00 %/year
Levelized PPA price (nominal)	20.72 ¢/kWh	Levelized PPA price (nominal)	20.13 ¢/kWh
Levelized PPA price (real)	16.45 ¢/kWh	Levelized PPA price (real)	15.99 ¢/kWh
Levelized COE (nominal)	19.21 ¢/kWh	Levelized COE (nominal)	18.64 ¢/kWh
Levelized COE (real)	15.25 ¢/kWh	Levelized COE (real)	14.80 ¢/kWh
Net present value	\$39,883,272	Net present value	\$46,318,824
Internal rate of return (IRR)	11.00 %	Internal rate of return (IRR)	11.00 %
Year IRR is achieved	20	Year IRR is achieved	20
IRR at end of project	12.75 %	IRR at end of project	12.75 %
Net capital cost	\$633,290,496	Net capital cost	\$734,098,752
Equity	\$294,153,984	Equity	\$341,072,672
Size of debt	\$339,136,512	Size of debt	\$393,026,048

Figure 8-10 SAM results of the two simulation, day (left) and night (right)

Once ended the computations in SAM the hourly production has been taken and exported in Excel (with an implemented download tool), where the day and night production have been summed up. Here have been found the most productive day of the year and thanks to an iteration procedure have been found the correct number of *Full load hours of storage* needed to cover 24h of daily production in that day.

Subsequently these hourly data have been loaded on MATLAB, where the maximum production have been set at 106.397 MW each hour, and moving the excess on the subsequent hours. Computing the new total energy production the new LCOE and Capacity Factor have been calculated.

### 8.3 Solar Tower Plant + PV and Carnot battery

As anticipated, SAM does not permit a hybrid configuration study and the data has been reprocessed in Excel and MATLAB after to be extracted from the two cases solved individually. Here below are introduced the SAM configuration, in Chapter 9, Results, is presented the subsequent plotting of data.

#### 8.3.2 Solar Tower Plant

The procedure followed is the same presented in the chapter 8.2, Solar Tower Plant.

*DNI* determined with P95 in order to exploit the sun's energy as much as possible, 965 W/m<sup>2</sup>.

*HTF hot and cold temperature* are been chosen as tipycal values, as explaind in chapter 3.1.2 Components of CSP tower plant.

The *Solar Multiple* has been determined using the Parametric Simulations provided by SAM, choosing the one with *LCOE* minimum, *Capacity Factor* and *Annual Energy* maximum, *tower height* not exceeding 270m (structural limit).

*Full load hours of storage*, 13h, function of solar multiple, has been chosen to cover the production during the sunniest day of the year (24h sum of PV day production, CSP night production and PV carnot battery help in low production periods), always using a iteration procedure.

*Heliostat field* is determined by an algorithm present in SAM, that looking for a optimum for its goal function determines the position of each single device.

Heliostat properties as well as mirror reflectance and soiling have been taken from Datasheet, see Annex. While *Max heliostat distance to tower height ratio* has been determined in the same manner of Solar multiple, using parametric simulations, obtaining the same falue as the previous study.

Tower receiver properties are obtained by the heliostat field optimization, while the flow pattern of the HTF in the reciver is obtained using parametric simulations.

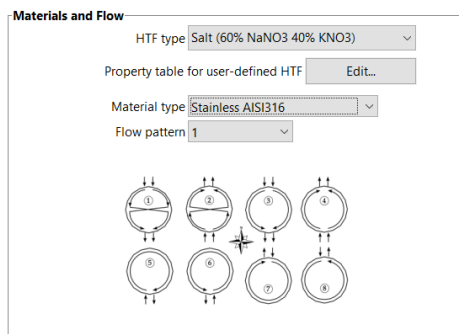


Figure 8-11 Flow pattern and HTF type in SAM

HTF is a mixture of 60% NaNO<sub>3</sub> and 40% KNO<sub>3</sub>.

*System control* and *TOD factor* have been set working during night hours.

*System cost of Thermal energy storage* for night tower has been increased by 15% to justify the cost of the electric heater used by the Carnot battery.

All parameters not mentioned have been left as default.

Metric	Value
Annual energy (year 1)	306,927,104 kWh
Capacity factor (year 1)	38.9%
Annual Water Usage	15,148,521 m <sup>3</sup>
PPA price (year 1)	18.81 ¢/kWh
PPA price escalation	1.00 %/year
Levelized PPA price (nominal)	21.58 ¢/kWh
Levelized PPA price (real)	17.14 ¢/kWh
Levelized COE (nominal)	19.97 ¢/kWh
Levelized COE (real)	15.86 ¢/kWh
Net present value	\$48,287,612
Internal rate of return (IRR)	11.00 %
Year IRR is achieved	20
IRR at end of project	12.75 %
Net capital cost	\$764,814,208
Equity	\$355,377,184
Size of debt	\$409,436,992

Figure 8-12 SAM results of CSP simulation

### 8.3.3 PV and Carnot battery

*Module* and *Inverter* properties as well as *module aspect* ratio have been taken from Datasheet, see Annex.

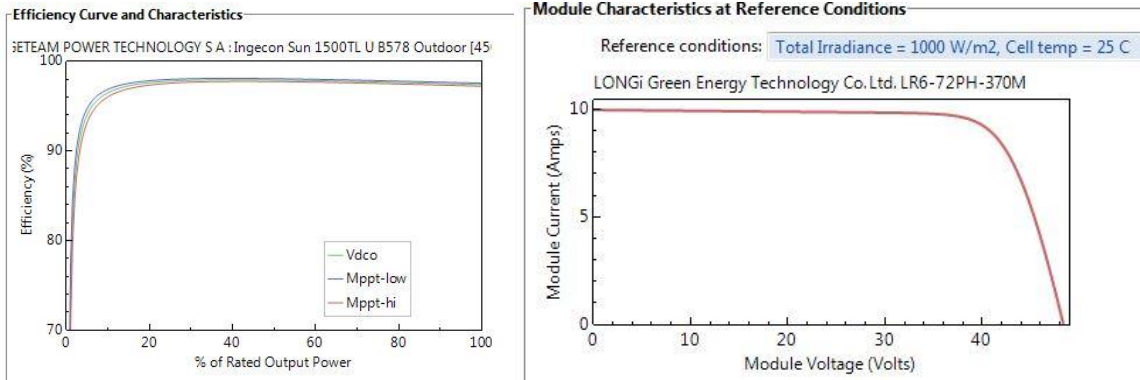


Figure 8-13 Module and Inverter characteristics in SAM

In *System Design* have been used the setting *Estimate Subarray 1 Configuration* with a desired array size of 235 MW<sub>DC</sub>, that gives automatically the number of necessary PV modules in serie and parallel to guarantee the voltage and current limits of the devices chosen. Quantity of power chosen in function of daily production of 106.397 MW each hour of the day (24h total, CSP + PV + Carnot battery), working as normal PV producing directly electric power during daylight and using the excess to charge the molten salts tanks using the electrical heater. This energy stored is used after that in night hours thanks to the ex coal power plant turbine.

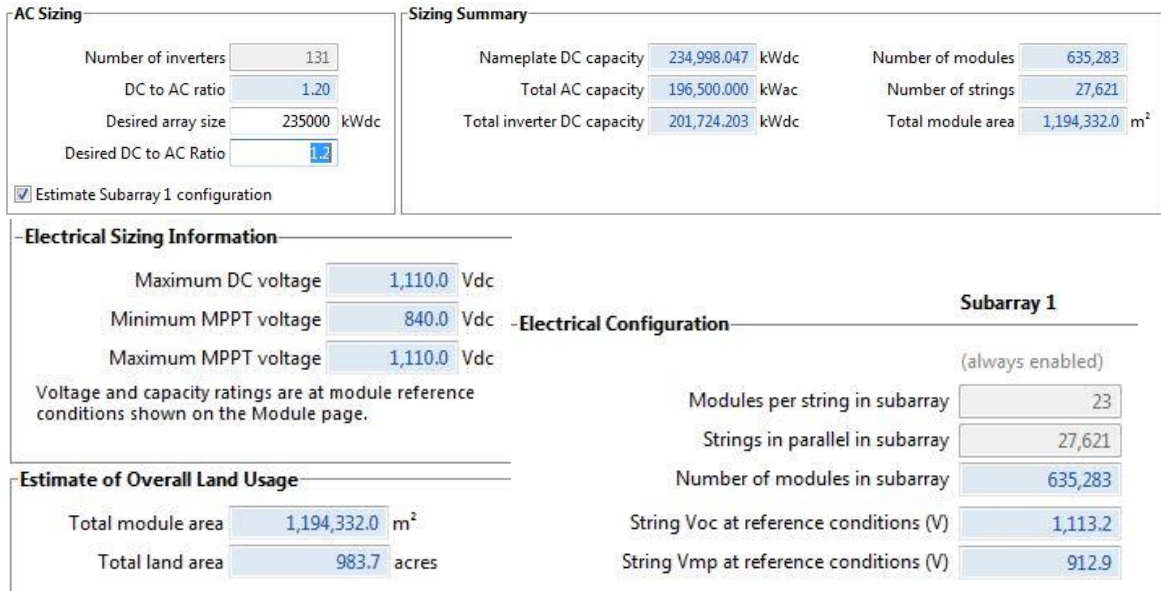


Figure 8-14 PV design configuration

Tracking orientation have been set on one axis.

*System control* and *TOD factor* have been set working all day long, in order to cover the electrical power demand during the daylight period using the PV technology, and using the stored heat to cover the low sun period through the day and the nighttime period using the thermal energy storad in molten salts.



System Cost of land have been set to the same cost of CSP land.

All parameters not mentioned have been left as default.

Metric	Value
Annual energy (year 1)	363,950,208 kWh
Capacity factor (year 1)	17.7%
Energy yield (year 1)	1,549 kWh/kW
Performance ratio (year 1)	0.80
PPA price (year 1)	8.75 ¢/kWh
PPA price escalation	1.00 %/year
Levelized PPA price (nominal)	9.47 ¢/kWh
Levelized PPA price (real)	7.52 ¢/kWh
Levelized COE (nominal)	8.94 ¢/kWh
Levelized COE (real)	7.10 ¢/kWh
Net present value	\$18,940,562
Internal rate of return (IRR)	11.00 %
Year IRR is achieved	20
IRR at end of project	13.07 %
Net capital cost	\$270,381,376
Equity	\$119,368,088
Size of debt	\$151,013,296

Figure 8-15 SAM results of PV simulation

Once ended the computations in SAM the hourly production have been taken and exported in Excel, where the PV production have been separated in electrical and thermal, electrical set to max production of 100 MW and the excess have been moved to electric energy to thermal storage to electric energy again.

- Electric to thermal efficiency 95%
- Thermal to electric efficiency 32% (turbine efficiency)
- Transformer efficiency 98%

Subsequently these data have been loaded on MATLAB, where the maximum production of the sum of CSP, PV and Carnot battery have been set at 106.397 MW each hour and moving the surplus on the subsequent hours.

After to have defined the new total energy production the new LCOE and Capacity Factor have been calculated.



### 8.4 PV + molten salts and Carnot battery

The procedure followed is similar to the one presented in the chapter 8.3. This study, one of a kind, is not covered in SAM configurations. As for the previous hybrid cases, the data has been reprocessed in Excel and MATLAB after to be extracted from the original PV production.

Module and Inverter properties as well as module aspect ratio have been taken from Datasheet, see Annex.

In System Design the setting *Estimate Subarray 1 Configuration* with a desired array size of 750 MW<sub>DC</sub> has been used, that gives automatically the number of necessary PV modules in serie and parallel to guarantee the voltage and current limits of the devices chosen. Quantity of power chosen in function of daily production of 106.397 MW each hour of the day (24h total, PV + Carnot battery), working as normal PV producing directly electric power during daylight and using the excess to fill the molten salts tanks using the electrical heater. The energy stored is used after that in night hours thanks to the ex coal power plant turbine.

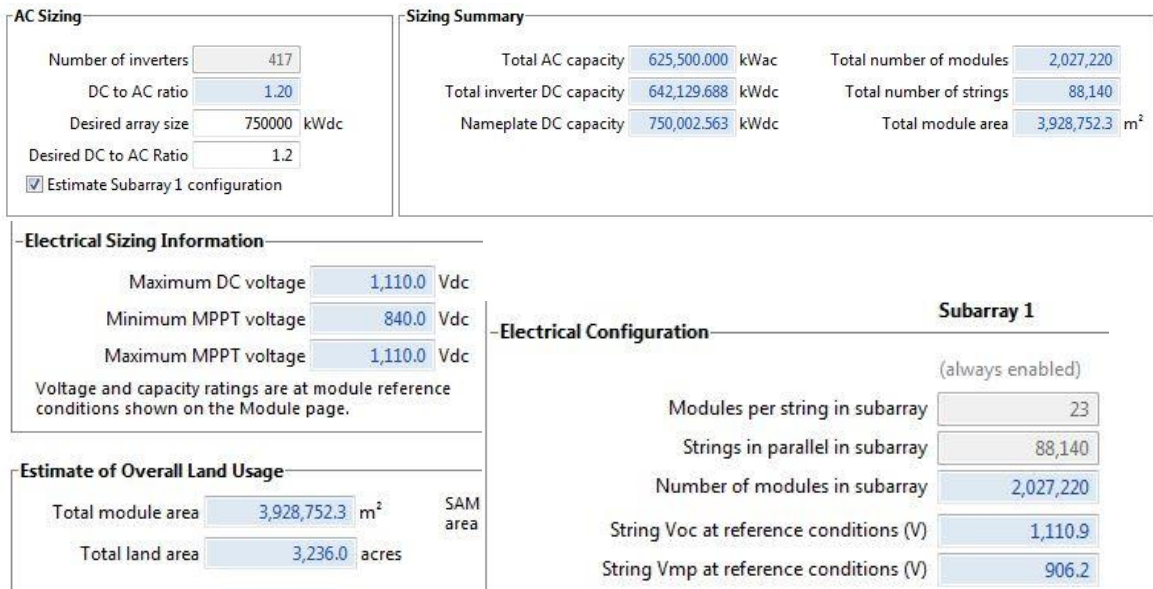


Figure 8-16 PV design configuration

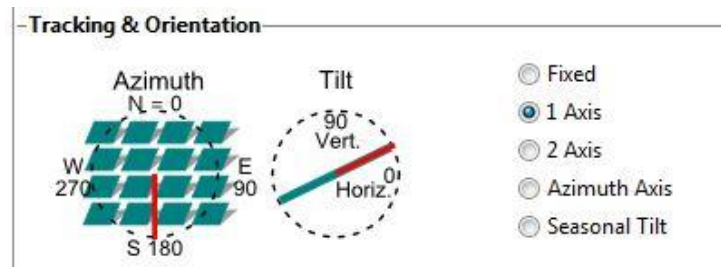


Figure 8-17 Tracking system

Tracking orientation has been set on one axis.

*System control* and *TOD factor* have been set working all day long, in order to cover the electrical power demand during the daylight period using the PV technology, and using the stored heat to cover the low sun period through the day and the nighttime period using the thermal energy stored in molten salts.

*Full load hours of storage*, function of PV production, but not present in SAM configuration has been chosen to cover a fictitious 11.9 h production during the sunniest day of the year (24h sum of PV day production and PV Carnot battery in nighttime). It has been taken into account adding the *System cost, Thermal energy storage* of a TES storage system, to the fixed costs of the PV plant (the normal cost plus a 15% more to cover the cost of the heater and heat exchanger).

Moreover, contingency percentage has been increased to 5%, middle between CSP and PV ones. Maintenance cost has been increased by a 10% of the CSP maintenance cost. System Cost of land has been set to the same cost of CSP land.

Direct Capital Costs							
Module	2,027,220 units	0.4 kWdc/unit	750,002.6 kWdc	0.35	\$/Wdc	\$ 262,500,880.00	
Inverter	417 units	1,500.0 kWac/unit	625,500.0 kWac	0.06	\$/Wdc	\$ 45,000,152.00	
			\$	\$/Wdc	\$/m <sup>2</sup>		
Balance of system equipment			94,084,376.00	0.20	0.00	\$ 244,084,896.00	
Installation labor			0.00	0.13	0.00	\$ 97,500,328.00	
Installer margin and overhead			0.00	0.06	0.00	\$ 45,000,152.00	
						Subtotal	
						\$ 694,086,400.00	
-Contingency							
				Contingency	5 % of subtotal	\$ 34,704,320.00	
						<b>Total direct cost</b>	
						\$ 728,790,720.00	
Total Installed Cost							
The total installed cost is the sum of the direct and indirect costs. Note that it does not include any financing costs from the Financial Parameters page.						<b>Total installed cost</b>	\$ 917,802,624.00
						Total installed cost per capacity	\$ 1.22/Wdc
Operation and Maintenance Costs							
		First year cost		Escalation rate (above inflation)			
Fixed annual cost	Value	0	\$/yr	0 %		In Value mode, SAM applies both inflation and escalation to the first year cost to calculate out-year costs. In Schedule mode, neither inflation nor escalation applies. See Help for details.	
Fixed cost by capacity	Value	20	\$/kW-yr	0 %			
Variable cost by generation	Value	0	\$/MWh	0 %			

Indirect Capital Costs				
	% of direct cost		\$/Wdc	\$
Permitting and environmental studies	0		0.01	0.00
Engineering and developer overhead	0	+	0.08	0.00
Grid interconnection	0		0.03	0.00
<b>-Land Costs-</b>				
Land area	3,235.982	acres		
Land purchase	\$ 10000/acre	0	0.03	0.00
Land prep. & transmission	\$ 0/acre	0	0.02	0.00
<b>-Sales Tax-</b>				
Sales tax basis, percent of direct cost	80	%	Sales tax rate	5.0
				%
				\$ 29,151,628.00
<b>Total indirect cost</b>				<b>\$ 189,011,888.00</b>

Figure 8-18 Modified costs in SAM

All parameters do not mentioned have been left as default.

Metric	Value
Annual energy (year 1)	1,161,542,656 kWh
Capacity factor (year 1)	17.7%
Energy yield (year 1)	1,549 kWh/kW
Performance ratio (year 1)	0.80
PPA price (year 1)	10.13 ¢/kWh
PPA price escalation	1.00 %/year
Levelized PPA price (nominal)	10.97 ¢/kWh
Levelized PPA price (real)	8.71 ¢/kWh
Levelized COE (nominal)	10.37 ¢/kWh
Levelized COE (real)	8.23 ¢/kWh
Net present value	\$68,428,992
Internal rate of return (IRR)	11.00 %
Year IRR is achieved	20
IRR at end of project	13.03 %
Net capital cost	\$992,460,928
Equity	\$440,822,816
Size of debt	\$551,638,080

Figure 8-19 SAM results of PV simulation

Once ended the computations in SAM the hourly production have been taken and exported in Excel, where the PV production have been separated in electrical and thermal, electrical set to max production of 100 MW and the excess have been moved to electric energy to thermal storage to electric energy again.

- Electric to thermal efficiency 95%
- Thermal to electric efficiency 32% (turbine efficiency)
- Transformer efficiency 98%

Subsequently these data have been loaded on MATLAB, where the maximum production have been set at 106.397 MW each hour and moving the surplus on the subsequent hours. After to have defined the new total energy production the new LCOE and Capacity Factor have been calculated.

## 8.5 PV + electrical storage

Last but not least the extreme comparison in case on only PV production with battery.

*Module* and *Inverter* properties as well as *module aspect* ratio have been taken from Datasheet, see Annex.

In *System Design* have been used the setting *Estimate Subarray 1 Configuration* with a desired array size of 370 MW<sub>DC</sub>, that gives automatically the number of necessary PV modules in serie and parallel to guarantee the voltage and current limits of the devices choosen. Quantity of power chosen in function of daily production of 100 MW each hour of the day (24h total, PV + energy stored in LMO battery), working as normal PV producing directly electric power during daylight and using the excess to fill the electric batteries, energy used after that in night hours and not sunny periods during the day.

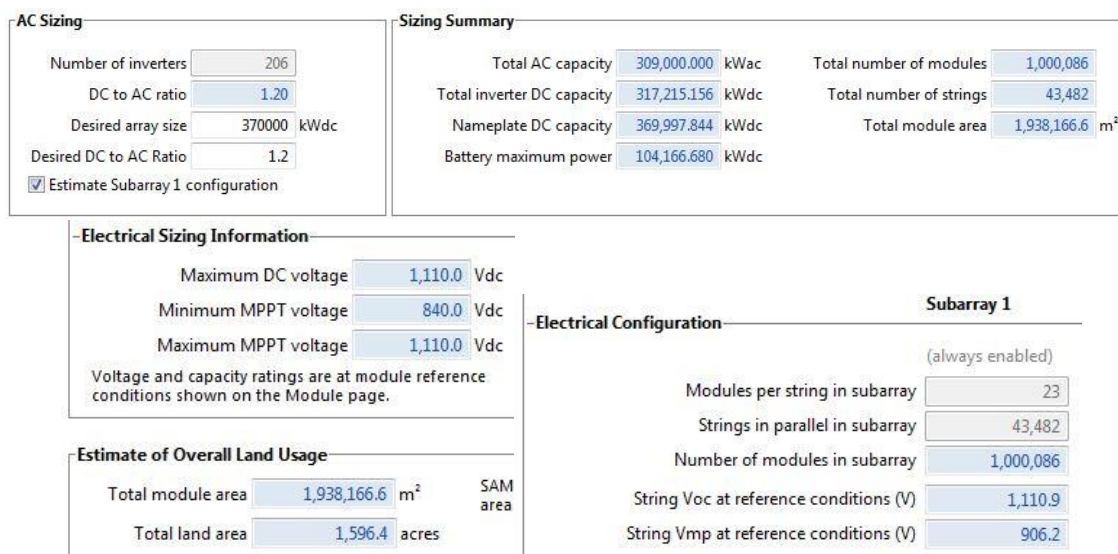


Figure 8-20 PV design configuration

Tracking orientation have been set on one axis.

*System control* and *TOD factor* have been set working all day long, in order to cover the electrical power demand during the daylight period using the PV technology, and using the batteries to cover the low sun period through the day and the nighttime period.

*Hours of storage*, function of PV production, has been chosen to cover a 12.2 h production during the sunniest day of the year (24h sum of PV day production and PV Carnot battery in nighttime) plus a 10%, power output 100 MW. Sostitution of LMO batteries have been considered each time 50% of capacity drop is reached.



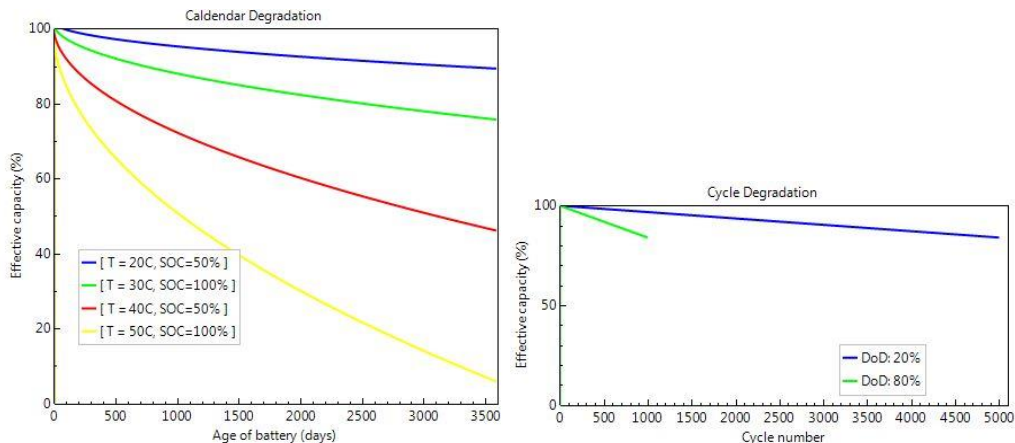


Figure 8-21 LMO Battery degradation in SAM

Direct Capital Costs							
Module	1,000,247 units	0.4 kWdc/unit	370,002.2 kWdc	0.35 \$/Wdc		\$ 129,500,760.00	
Inverter	206 units	1,500.0 kWac/unit	309,000.0 kWac	0.06 \$/Wdc		\$ 22,200,130.00	
Battery DC capacity	1,323,234.3 kWh	103,377.7 kW	300.00 \$/kWh	600.00 \$/kW	=	\$ 458,996,864.00	
Balance of system equipment			\$ 0.00	\$/Wdc 0.20	\$/m <sup>2</sup> 0.00	\$ 74,000,440.00	
Installation labor			\$ 0.00	0.13	0.00	\$ 48,100,284.00	
Installer margin and overhead			\$ 0.00	0.06	0.00	\$ 22,200,130.00	
Subtotal						\$ 754,998,592.00	
-Contingency							
				Contingency	4 % of subtotal	\$ 30,199,944.00	
<b>Total direct cost</b>						<b>\$ 785,198,528.00</b>	
Indirect Capital Costs							
		% of direct cost		\$/Wdc	\$		
Permitting and environmental studies		0		0.01	0.00	\$ 3,700,021.75	
Engineering and developer overhead		0		0.08	0.00	\$ 29,600,174.00	
Grid interconnection		0		0.03	0.00	\$ 11,100,065.00	
-Land Costs							
Land area	1,548.876 acres						
Land purchase	\$ 10000/acre	0		0.03	0.00	\$ 26,588,822.00	
Land prep. & transmission	\$ 0/acre	0		0.02	0.00	\$ 7,400,043.50	
-Sales Tax							
Sales tax basis, percent of direct cost		100 %		Sales tax rate	5.0 %	\$ 39,259,928.00	
<b>Total indirect cost</b>						<b>\$ 117,649,056.00</b>	
Total Installed Cost							
The total installed cost is the sum of the direct and indirect costs. Note that it does not include any financing costs from the Financial Parameters page.						<b>Total installed cost</b>	\$ 902,847,616.00
Total installed cost per capacity						\$ 2.44/Wdc	
Operation and Maintenance Costs							
	First year cost		Escalation rate (above inflation)				
Fixed annual cost	Value 0 \$/yr		0 %			In Value mode, SAM applies both inflation and escalation to the first year cost to calculate out-year costs. In Schedule mode, neither inflation nor escalation applies. See Help for details.	
Fixed cost by capacity	Value 13 \$/kW-yr		0 %				
Variable cost by generation	Value 0 \$/MWh		0 %				
Battery replacement cost	Value 500 \$/kWh		0 %				

Figure 8-22 System Costs in SAM

Contingency percentage have been increased to 4%, ad default PV plus battery plant.

System Cost of land have been set to the same cost of CSP land.

All parameters not mentioned have been left as default.

Metric	Value
Annual energy (year 1)	572,485,952 kWh
Capacity factor (year 1)	17.7%
Energy yield (year 1)	1,547 kWh/kW
Performance ratio (year 1)	0.80
Battery efficiency (incl. converter + ancillary)	NaN
PPA price (year 1)	10.00 ¢/kWh
PPA price escalation	1.00 %/year
Levelized PPA price (nominal)	10.83 ¢/kWh
Levelized PPA price (real)	8.60 ¢/kWh
Levelized COE (nominal)	15.87 ¢/kWh
Levelized COE (real)	12.61 ¢/kWh
Net present value	\$-281,840,896
Internal rate of return (IRR)	-5.39 %
Year IRR is achieved	20
IRR at end of project	-0.34 %
Net capital cost	\$952,408,576
Equity	\$719,023,744
Size of debt	\$233,384,848

Figure 8-23 SAM results of PV plus battery simulation

Once ended the computations in SAM the hourly production have been taken and exported in Excel, where the PV production have been separated in direct electrical production and electrical storage. In entering and exiting the batteries an overall efficiency of 93% have been considered. Subsequently these data have been loaded on MATLAB, where the maximum production have been set at 100 MW each hour and moving the excess on the subsequent hours where batteries are fully discharged.

After to have defined the new total energy production the new LCOE and Capacity Factor have been calculated.

Land Area, as for each PV field analysed, has been considered 2.1 hectares each MW installed, as tipycal rule of thumb [69].

# Chapter 9 Results

After to be reprocessed using the excel and matlab tools, the the data coming from the four cases are now plotted to be discussed.

## 9.1 Solar Tower Plant

As anticipated in chapter 8.2 the the data obtained in SAM have been reodered. The production of day and night tower summed up bring to a good result in terms of constancy. Producing 593.6 GWh during the year, with a capacity factor of 70.67% in the 8400 working hours, 39.6% full load.

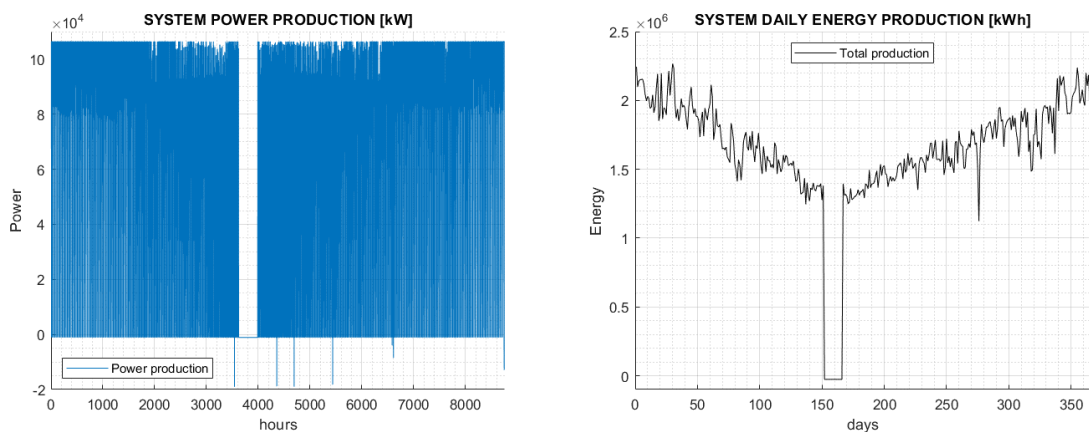


Figure 9-1 Power production in the two tower CSP plant (left), Daily Energy production in the two tower CSP plant (right)

The big hole in production in the chart represents the 15 days of *turbine maintenance stop*, while the negative spikes that arrive almost to -2kW are due very rainy days, in which the molten salts are to be maintained at temperature higher that 290°C in order not to solidify, and so a lot of electric energy is used in the heater.

Looking the data at a higher level of aggregation can be rapidly noticed that the production decreases, as expected, during the summer period.

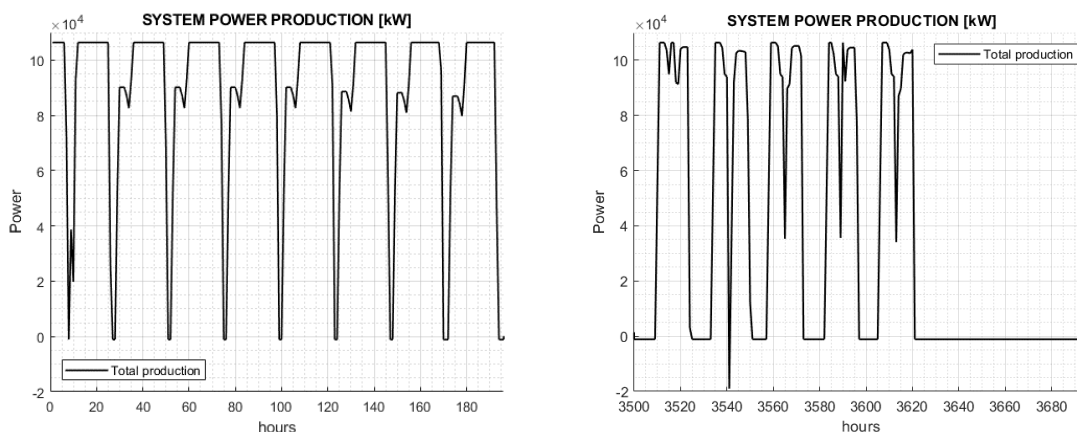


Figure 9-2 Power production in summer (left) and winter, just before stop (right)

In Figure 9-2 are shown the production trends, more constant during summer days, with little decrease during the morning, probably due to some shadow present in the area; and a more rough production during winter. The flat line on the right represent the turbine shutdown mentioned in the hypothesis. Duck curve in witer is present, deep but short.

## 9.2 Solar Tower Plant + PV and Carnot battery

The size of PV plant has been determined in order to have a 100 MW production during daylight and use the surplus to heat up the molten salts tanks, obtaining a 24h production with the help of CSP plant in the sunniest day of the year. To convert electrical energy in thermal storad energy, and again in electric energy the step and procedure *drain a lot of entropy*, enlowering the exergy, and so the whole work. This brings to an overdimensioned PV field needed to cover the production holes.

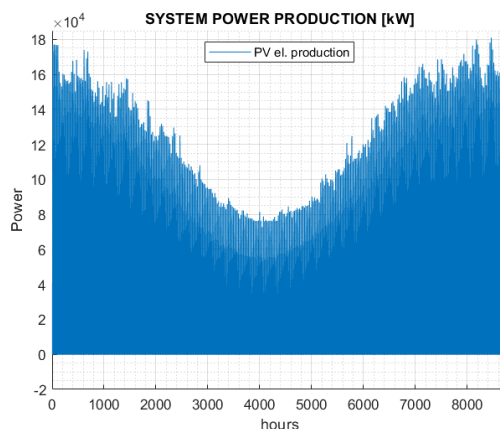


Figure 9-3 SAM PV power production

Here below are presented the sum of SAM datas collected by the CSP and PV prower production results. As can be easily noticed the distribution of energy in time is not uniform and the are spikes of over production.



To solve the problem the surplus energy have been stored in tanks and used in the following hours, in order to flat the production to 106.397 MW. The fianl result is present in Figure 9-4 **Error! Reference source not found..**

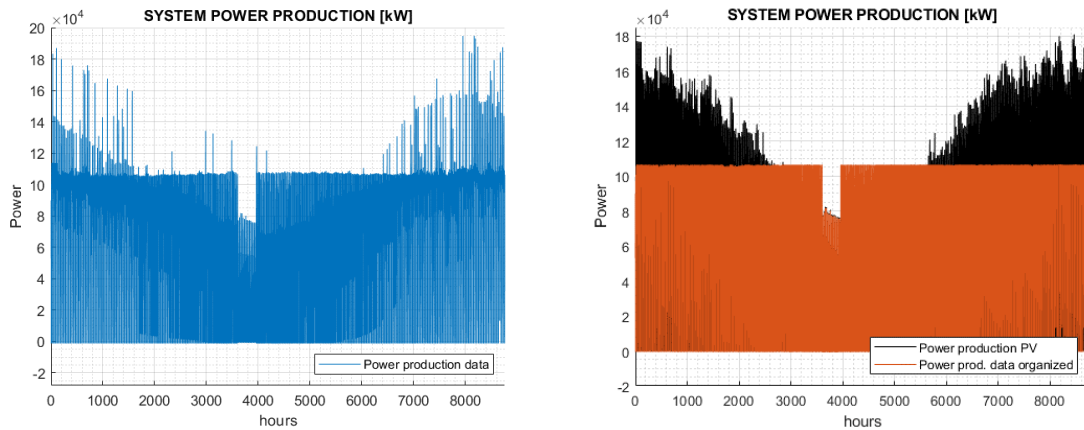


Figure 9-4 SAM production data summed up without any improvement (CSP + PV) (left), Power production of hybrid plant (orange) compared to original PV field production (black) (right)

In this way the hourly production is guaranted during 42.26 % of the year considering the turbine shutdown. *Very good result* corindering that LCOE and land area decreases compared with the two tower CSP plant.

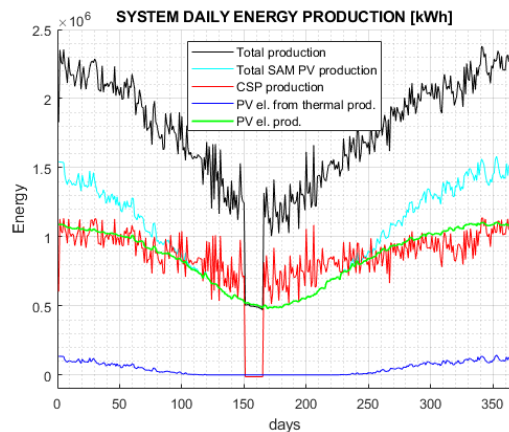


Figure 9-5 Daily Energy production in the hybrid plant

As expected the conversion from PV electrical energy to thermal and again electrical is not efficient at all, giving back less than a quarter of energy originally converted directly by PV, but in some ways it anyways helps.

PV continues to produce during daylight also in the turbine shutdown period, so two kind of capacity factor have been proposed, the one for the whole year and the one for the 8400 hours.

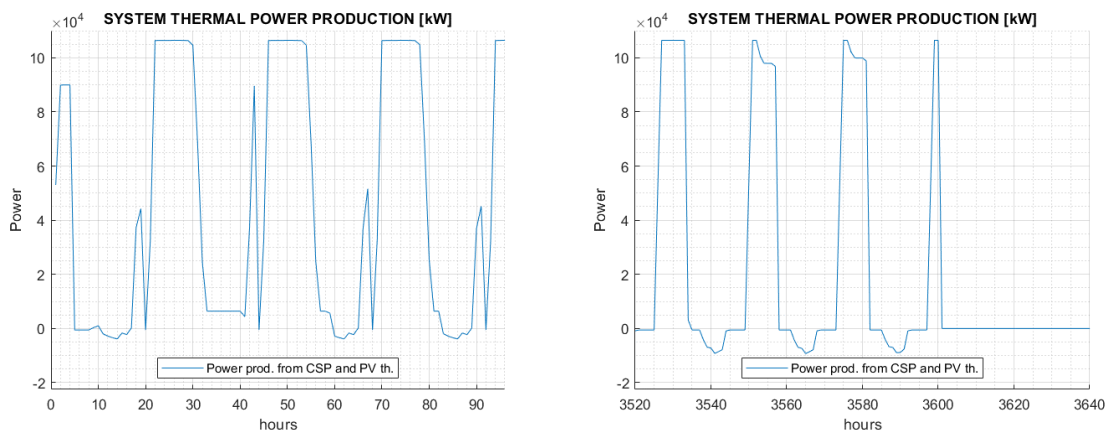


Figure 9-6 Energy produced by thermal storage (CSP + PV) in summer (left) and winter (right)

In Figure 9-6 Energy produced by thermal storage (CSP + PV) is shown the difference in thermal production between seasons, underlining the big effect of number of sun hours during the day. The horizontal line in the figure on the right is due to turbine shutdown.

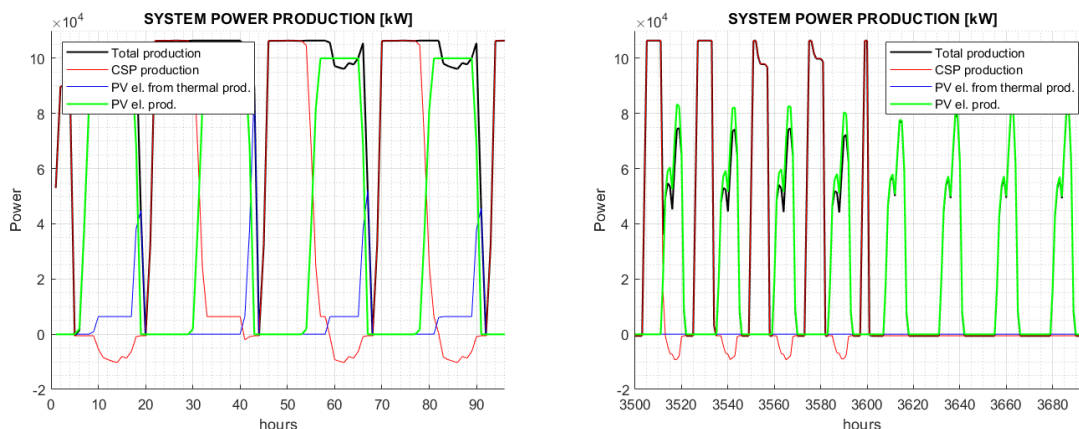


Figure 9-7 Power production in summer (left) and winter (right)

During the summer period the electricity production drop to zero only in few hours of the day, while the most of the day the hybrid plant manage to produce the 106.397 MW expected. PV electricity and thermal energy help to keep the production to constant levels during the whole day, also covering the electricity needs of the CSP plant. During winter, instead, CSP and PV production *are not overlapped*, being the sunlight hours too few to cover the whole day production. During turbine shutdown the PV electric production coincides with total production.

### 9.3 PV + molten salts and Carnot battery

Uniqueness of this plant is the merging of the PV technology with the low cost thermal storage in molten salts. So, ideally it could be a good coupling economically speaking, the point are the differences between the two types of energy in discussion: while electrical energy is

ready to be used, thermal energy needs lot of passages to be converted in the electric energy. It determines a very big amount of losses, mainly due to thermodynamics transformation.

As shown in Figure 9-8, to cover a demand of 106.397 MW for 24h during the sunniest day of the year 750 MW installed are needed. Loosing form 30% to 53% from original production, depending on the period of the year.

This *PV over dimensioning* to fill the demand gap during nighttime is *really exaggerated* due to the super low electric to thermal to electric conversion, needed to store energy and brings to good results in term of production, 596.61GWh/y and 72.86% Capacity Factor, and thanks to losses the overall plant cost increases considerably from the original only PV production cost.

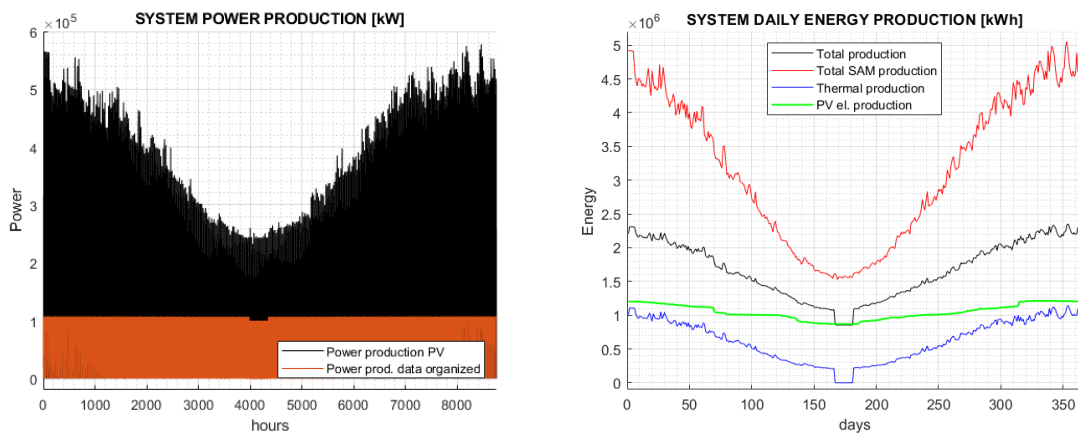


Figure 9-8 PV + molten salt plant production (orange) compared with PV electricity production in SAM (black) (left), Energy production by source (right)

Total final production in more than halved but better distributed during the day, with an effort of thermal source of 48% on the total in summer but only 19% in winter.

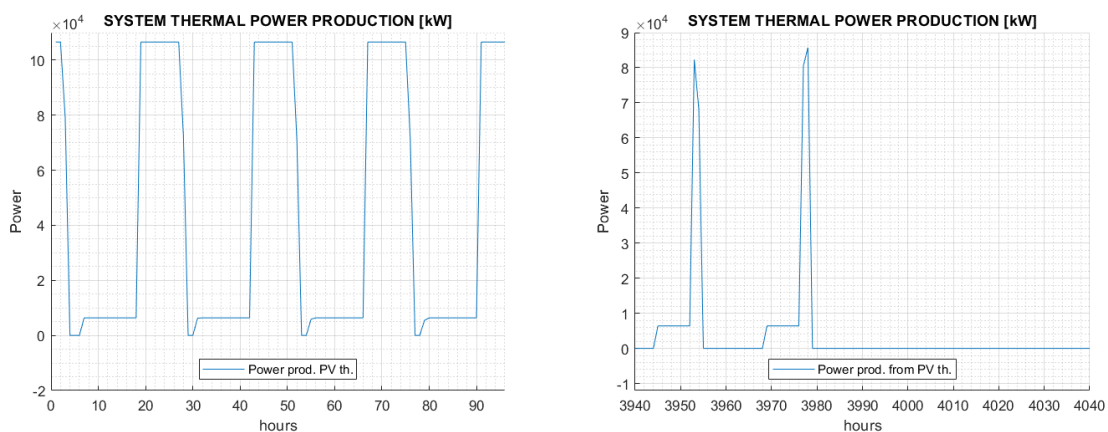


Figure 9-9 Power produced by thermal storage in summer (left) and winter (right)

Flat power production before the peak consist in covering auto consumption.

During winter energy stored is usable only for a *full load period* of *some minutes*.

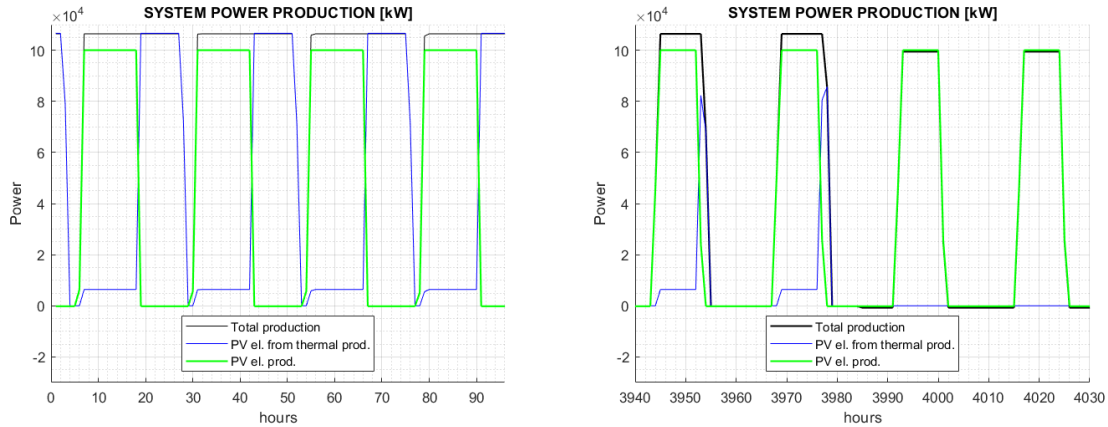


Figure 9-10 Power production in summer (left) and winter (right)

The very advantage of this configuration is the uniformity of the curve shape, managing to produce 106.397 MW the 63.83% of the hours of the year.

The LCOE results almost the same of CSP tower plant but with a 40 % less of land occupied area.

## 9.4 PV + electrical storage

Last but not least the PV plus LMO battery case, that differs from all other cases for two reason: different financial model, but more important, different way of energy storage. Here the storage is in batteries, and so in electrical energy, with little losses in traformation that permits a little over dimensioning of the PV field, with less than half of the occupied land of Carnot battery case.

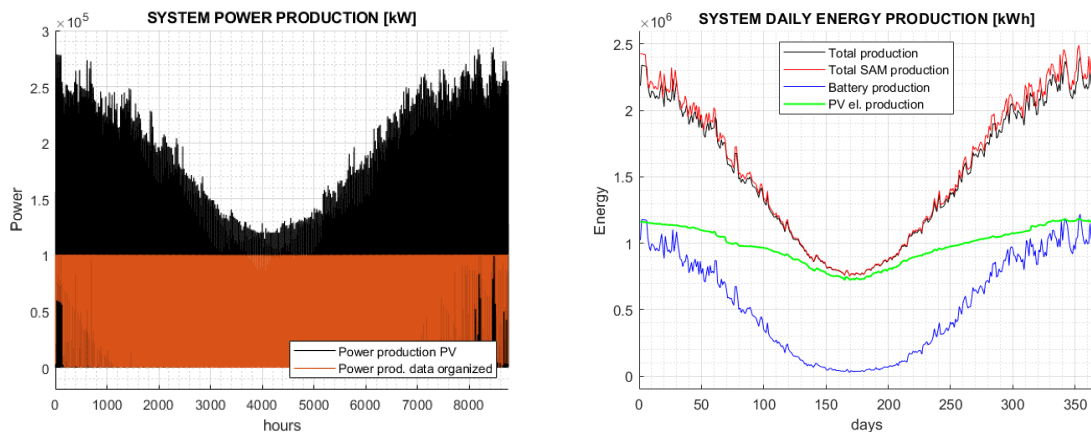


Figure 9-11 PV + LMO batteries production (blue) compared with PV electricity production in SAM (black) (left), Energy production by source (right)

No turbine is present, so no stop period is considered in winter and a full load production of 100 MW.

Total production is really close to SAM data, they only differ in input/output battery efficiency. Battery storage gives a real effort on the total, but with the inconvenience of multiple battery replacement and consequentially a consistent increase of the cost of the plant, that brings to a *negative IRR* and *Net Present Value*.

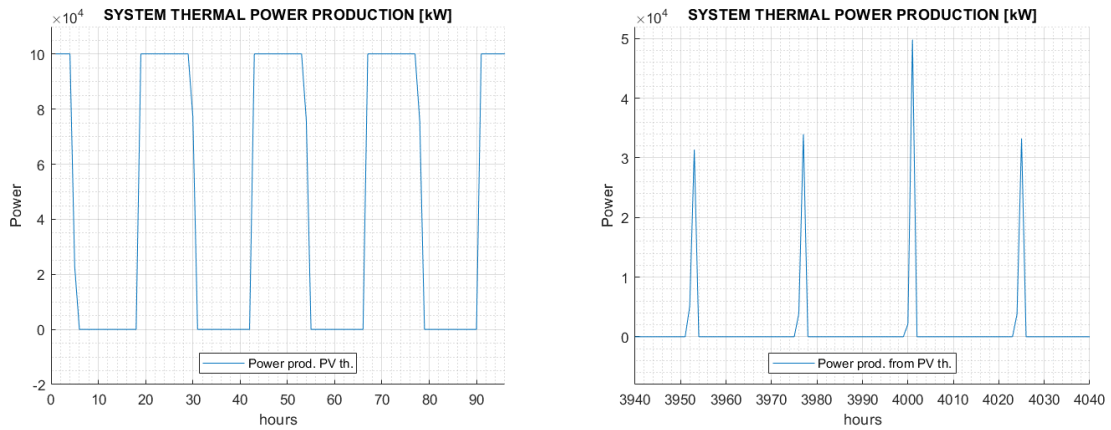


Figure 9-12 Power produced by LMO batteries in summer (left) and winter (right)

Battery contribution have been calculated on *8760 hours period*, that permits a Capacity factor of 63.68 % and a full load work of 55.26%.

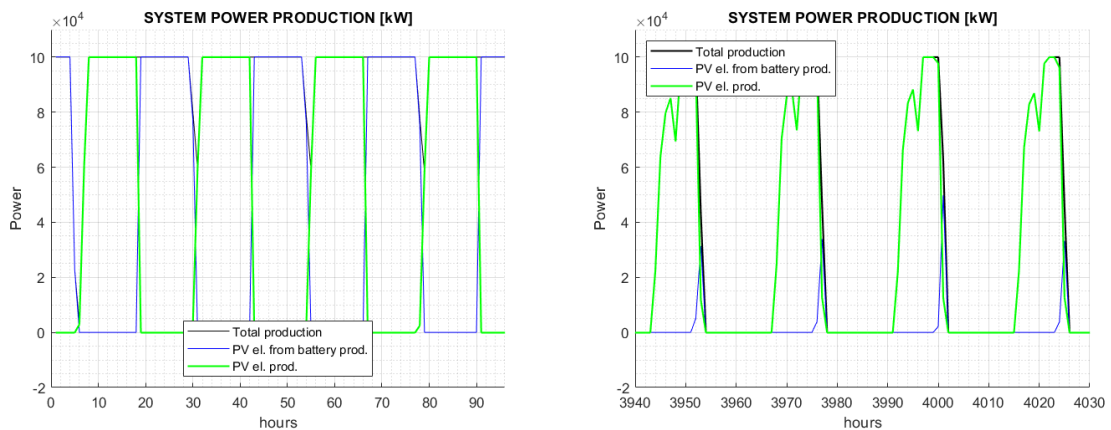


Figure 9-13 Power production in summer (left) and winter (right)

## 9.5 Summarised data output

To conclude are presented the main information summarised in the Table 9-1 and Table 9-2.

	CSP Tower	Tower + PV	PV + Molten Salts	PV + LMO Battery	
CF_8400	70.67	74.70	72.86	/	%
CF_8760	/	72.58	68.11	63.68	%
CF_full_load	39.56	42.26	63.83	55.26	%
Annual Energy (+15 days PV)	593.60	627.45	596.61	/	GWh <sub>el</sub>
	/	635.83	612.04	557.82	
Land Area CSP	5248	2554	/	/	acres
Land Area Modules	/	1143.4	3236	1596.4	acres
Land Area PV field	/	1219.5	3891.9	1920	acres
Total land Area	5248	3773.5	3891.9	1920	acres
LCOE nominal	19.53	15.16	19.68	16.29	¢/kWh
LCOE real	15.51	12.04	15.62	12.94	¢/kWh
PV field	/	235	750	370	MW
CSP field	200	100	/	/	MW

Table 9-1 Resume of main results of the four cases

Best case in term of *LCOE* is as wished the hybrid tower plus PV configuration, thanks to the low cost of power cycle already present, the helping effort of PV during the day and the Carnot battery managing PV excedents.

Hybrid configuration also wins for higher *annual energy* production and *Capacity factor*, second for *Net Capital Cost* but not as distant from the others as the CSP two tower configuration.

Focusing on land area PV plus LMO batteries seems the best solution, but considering also cost, maybe the choice would fall anyway on the hybrid tower plus PV configuration.

Comparing the two towers configuration with the PV plus Carnot battery molten salts, the results are unbelievably similar, the biggest difference can be seen in the *capacity factor* at *full load*, 60% higher for PV configuration, permitting to avoid the duck curve formation at least in summer period, and a land *occupied area* about 40% less of the first configuration.

	CSP Tower	Tower + PV	PV + Molten Salts	PV + LMO Battery	
Net present value	86,202	67,228	68,428	-281,840	k\$
Internal rate of return (IRR)	11.00	11.00	11.00	-5.39	%
IRR at end of project	12.75	13.07 & 12.75	13.03	-0.34	%
Net capital cost	1,367,389	1,035,195	992,460	952,408	k\$
Equity	635,226	474,745	440,822	719,023	k\$
Size of debt	732,162	560,450	551,638	233,384	k\$

Table 9-2 Resume of main financial results of the four cases

Hybrid solution with PV cannot battery plant is in the middle for *size of debt* and *equity*, but also for *Net Present Value*, it also seems the best solution for *Capacity Factor at full load*.

PV plus battery configuration financial results can not be considered with the same eye of other plant, because of its *differet modelization*. Anyway, the *PPA* have been *set as the value obtained by the PV plus molten salts configuration*, and for that reason have been added in the table, to provide an *order of magnitude* of production, charges and costs. According to some experts this configuration is still cheaper than coal in India [69].

Results are in line with the descendent trend of real prices, considering the really bad efficiency chosen as old existing plant, there is hope for future development, that will surely be more effective and efficient if more modern coal plant are decided to be converted too. Also modern study on pilot plants push in that direction with possible efficeincy reaching almost the double of the one considered in this work [37].

## 9.6 Future development

*CSP Parabolic through*, excluded by the study due to its too low oil maximum temperature, could be implemented with the help of PV field and an electrical heater insert after the salt tanks in order to increase the temperature of the source just before to exchange energy with the power cycle HTF, giving it the possibility to be a hybrid conversion solution itself [70].

To increase efficiency, as proposed and studied by some chinese and UK scientists, could be implemented new way of exchange heat between salts and power cycle HTF, in the different pressure levels of the plant and at different temperatures, avoiding waste and *increasing efficiency* [71].

NREL promises in the next release of the software the possibility to *study hybrid configuration*, so another possible evolution could be the verification of the datas with the new implemented tool, and in some years also with the plants already under construction.

The study results are nevertheless influenced by the low efficiency chosen as hypothesis, with new pilot plants those values could be improved gaining further advantage in competitiveness, lowering LCOE. With this possible advantages and more trust in the technology, large scale implementation in high DNI exposition areas is not to be excluded, as for the same reason new kind of incentives and favorable policies, with the idea of considering *stored renewable energy a rich and wise asset* [72].

Last but not least, there are companies that are developing *hybrid heliostats*, converting as PV the visible light and reflecting all the other frequencies, so producing during day and night with the same plant. Hoping results will be waited by this promising solution [73].



# Conclusion

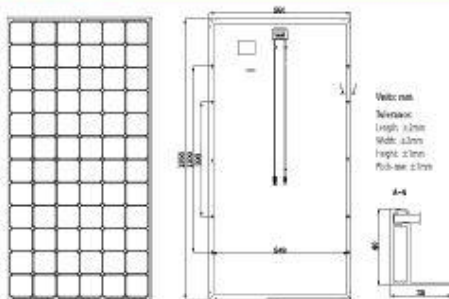
The study cases represent a wide range of possible solutions, all with good advantages and disadvantages. Depending on the aim of the plant realisation and the amount of help that could arrive from different kinds of incentives the solution could end in each solution of the ones proposed. But focusing only on the final purpose of the work, which is the demonstration of the *decrease of LCOE price* and *increase of capacity factor* of the plant in case of an hybrid configuration, the final solution fits with all the hypothesis set at the beginning. LCOE prices that results are in line with actual prices in the market and new policies, visibility and trust in the technology could lower them even more in a soon future, helping to give more credibility and include the new hybrid solution in the arsenal of the future green investors, giving the possibility to put aside fossil fuels and build a renewable driven production world.



# Appendix

## LR6-72PH 360~380M

### Design (mm)      Mechanical Parameters      Operating Parameters



Cell Orientation: 72 (6x12)  
 Junction Box: IP67, three diodes  
 Output Cable: 4mm<sup>2</sup>, 1200mm in length  
 Weight: 22.5kg  
 Dimension: 1956x991x40mm  
 Packaging: 26pcs per pallet

Operational Temperature: -40°C ~ +85°C  
 Power Output Tolerance: 0 ~ 15 W  
 Maximum System Voltage: DC1500V (IEC&UL)  
 Maximum Series Fuse Rating: 20A  
 Nominal Operating Cell Temperature: 45±2°C  
 Application Class: Class A

### Electrical Characteristics Test uncertainty for Pmax: ±3%

Model Number	LR6-72PH-360M		LR6-72PH-365M		LR6-72PH-370M		LR6-72PH-375M		LR6-72PH-380M	
	STC	NOCT	STC	NOCT	STC	NOCT	STC	NOCT	STC	NOCT
Maximum Power (Pmax/W)	360	266.7	365	270.4	370	274.1	375	277.8	380	281.5
Open Circuit Voltage (Voc/V)	47.9	44.7	48.0	44.8	48.3	45.1	48.5	45.3	48.7	45.5
Short Circuit Current (Isc/A)	9.70	7.82	9.74	7.85	9.84	7.93	9.90	7.98	9.99	8.05
Voltage at Maximum Power (Vmp/V)	39.2	36.2	39.3	36.3	39.4	36.4	39.6	36.6	39.8	36.8
Current at Maximum Power (Imp/A)	9.18	7.36	9.29	7.45	9.39	7.53	9.47	7.59	9.55	7.66
Module Efficiency(%)	18.6		18.8		19.1		19.3		19.6	

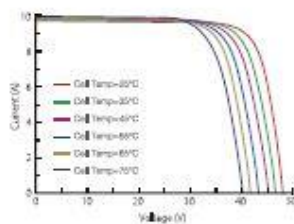
STC (Standard Testing Conditions): Irradiance 1000W/m<sup>2</sup>, Cell Temperature 25°C, Spectra at AM1.5  
 NOCT (Nominal Operating Cell Temperature): Irradiance 800W/m<sup>2</sup>, Ambient Temperature 20°C, Spectra at AM1.5, Wind at 1m/s

### Temperature Ratings ( STC )      Mechanical Loading

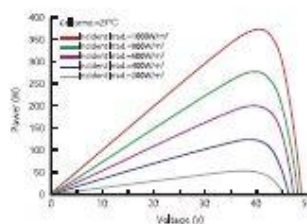
Temperature Coefficient of Isc	+0.057%/°C	Front Side Maximum Static Loading	5400Pa
Temperature Coefficient of Voc	-0.286%/°C	Rear Side Maximum Static Loading	2400Pa
Temperature Coefficient of Pmax	-0.370%/°C	Hailstone Test	25mm Hailstone at the speed of 23m/s

### I-V Curve

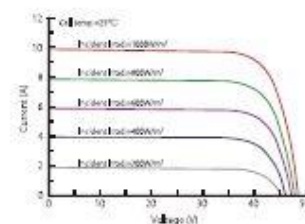
Current-Voltage Curve (LR6-72PH-370M)



Power-Voltage Curve (LR6-72PH-370M)



Current-Voltage Curve (LR6-72PH-370M)



**INGECON**

**SUN**

**PowerStation**  
MV Transformer for 1,500 V Inverter Series

**THREE-PHASE  
OIL-INSULATED  
LV / MV  
TRANSFORMERS**



**Medium Voltage Transformer / Hermetically Sealed Completely Filled**

Ingeeam provides highly performing LV / MV three phase oil-insulated type transformers. Power ratings are available up to 6,400 kVA, with voltage ratings (MV side) from 10 up to 36 kV.

The transformers are classified as per the EIC 60076 standard, offering the following benefits:

- Reduced power losses (EU 548/2014).
- Reduced maintenance needs.
- Suitable both for internal or external use.

The voltage value at the secondary winding (LV side) is compatible with the inverter output voltage: 450V, 540V, 578V, 600V, 615V and 630V.

**STANDARD FUNCTIONS**

- Reduced power losses (EU 548/2014 - Other power losses upon request). Weighted efficiency with standard Euroefficiency\* above 99.1%.
- Electrostatic shield reducing disturbances, distortions and overvoltages.
- DGPT2 / RIS relay.
- Mineral oil insulation.

**FUNCTIONS AVAILABLE UPON REQUEST**

- Natural ester dielectric insulation fluid (fire point > 300 °C)
- Copper windings.
- Other functions available upon request.

\* Euroefficiency calculated with these coefficients: F1(5%)=0.03; F2(10%)=0.06; F3(20%)=0.13; F4(30%)=0.1; F5(50%)=0.48; F6(75%)=0; F7(100%)=0.2

MV Transformer / Hermetically Sealed Completely Filled				
General Information				
Category <sup>1)</sup>	Hermetic mineral oil-insulated transformer (vegetable oil insulated upon request)			
Rated frequency	50 / 60Hz			
Primary voltage regulator	± 2 x 2.5 %			
Insulation class	Primary winding	12 kV. 12 / 28 / 75 kV	17.5 kV. 17.5 / 38 / 95 kV	24 kV. 24 / 50 / 125 kV
	Secondary winding	3.6 kV		
Primary / secondary conductive material	Aluminium / Aluminium (Copper optional)			
Vector group <sup>2)</sup>	Dyn11			
Primary connection	Delta			
Secondary connection	Star + Neutral			
Max. operating temperature	40 °C <sup>3)</sup>			
Max. overtemperature for windings / oil	+75 / +60 K			
No load current	< 1%			
Max. peak starting current	< 15 x In			
Installation	Indoor or outdoor			
Cooling type	ONAN			
Altitude above sea level <sup>4)</sup>	≤ 1000 m			
Short-circuit impedance at 75 °C <sup>5)</sup>	6%			
General features	Terminal board for primary voltage adjustment, lifting lugs, earthing terminal, electrostatic shield and DGPT2 / RIS relay			

	Value	Units
<b>Heliostat ASUP140 v 2.5</b>		
<b>General</b>		
Heliostat Manufacturer / Model	Abengoa / ASUP140 v 2.5	-
Heliostat Width	12.960	m
Heliostat Height	10.940	m
Heliostat Gross Area	141,78	m <sup>2</sup>
Heliostat Solar Effective Aperture Area	138.672 reflective area	m <sup>2</sup>
Mirror Elements per Heliostat	32	-
Mirror dimensions	3210 x 1350	mm
Heliostat Structure Material (i.e. ASTM class and coating)	Carbol Steel: S-275-S355 -JR Galvanized	-
Heliostat Stow Angle	0°	degrees
Heliostat Control System Description	PLC in control box	-
<b>Heliostat Drive / Actuator</b>		
Drive Type (Hydraulic vs. Geared Motor)	Hydraulic mechanism	-
Hydraulic Fluid (if applicable)	Mineral Oil	-
Drive Motor Characteristics (Rated Power, Voltage, Phase, Freq)	0.37/380-400/3/10-50	kW / V / Ph / Hz
Drive Connected Power Load	0.61	kWe
Drive Tracking Power Load	0.24 - 0.61	kWe
Non-Powered Drive Fail-Safe Method and Emergency Power Load (if any, in loss-of-power events)	Defocusing with Solar field UPS	-
Sensor Type	2 axis: Azimuth / Absolute encoder + Elevation/ inclinometer	-
<b>Mirror</b>		
Glass Material	Float glass	-
Mirror Specular Reflectivity	94,8 (average)	%

# Acronyms

AC	Alternate current
CHEST	Compressed Heat Energy Storage
CSP	Concentrated Solar Power
DC	Direct current
DNI	Direct Normal Irradiation
HTF	Heat Transfer Fluid
IEA	International Energy Agency
IET	International Emission Trading
IRENA	International Renewable Energy Agency
LCOE	Levelized Cost Of Energy
LMO	Lithium Manganese Oxide
NREL	National Renewable Energy Laboratory
OECD	Organisation for Economic Co-operation and Development
PTES	Pumped thermal energy storage
PV	Photovoltaic
SAM	System Advisor Model
SAPG	Solar Aided coal-fired Power Generation system
TES	Thermal Energy storage
TOD	Time Of Delivery
UNFCCC	United Nations Framework Conference on Climate Change
WHO	World Health Organization

# Simbology

$c$	Speed of light
$h$	Planck constant
$k_B$	Boltzmann constant
$B$	Beam irradiance
$T$	Temperature
$\lambda$	Wavelength
$\nu$	Frequency
$E_B$	total power emitted per unit area at the surface of a black body
$\sigma$	Stefan–Boltzmann constant
$AM$	Air mass parameter
$I_{tot}$	Total radiation
$I_{dir}$	Direct radiation
$I_{diff}$	Diffuse radiation
$I_{alb}$	Albedo component of total radiation
$I_{DNI}$	Direct normal incident radiation
$\dot{Q}_{rec}$	Thermal power arriving at the receiver
$\dot{Q}_{sun}$	Thermal power arriving from the sun
$\eta_{opt}$	Optical efficiency
$\tau_{glass}$	Glass transmissivity
$\alpha_{rec}$	Receiver absorbtivity
$G_{sun}$	Solar constant
$A_{rec}$	Receiver area
$\dot{Q}_{HTF}$	Thermal power arriving at the HTF
$\dot{Q}_{conv}$	Thermal power due to convection
$\dot{Q}_{rad}$	Thermal power due to radiation
$A_{sf}$	Solar field area
$h$	Convection transfer coefficient
$T_{rec}$	Receiver temperature
$T_{amb}$	Ambient temperature
$\epsilon_{rec}$	attenuation coefficient of the receiver
$CR$	Concentration ratio
$\eta_{th}$	Thermal efficiency
$E_{ph}$	energy transported by a photoelectron

# Bibliography

- [1] «Global Climate Change,» NASA, 28 4 2020. [Online]. Available: <https://climate.nasa.gov/>. [Consultato il giorno 30 4 2020].
- [2] «Air Pollution,» World Health Organization, 2020. [Online]. Available: <http://origin.who.int/airpollution/en/>. [Consultato il giorno 30 4 2020].
- [3] «Paris Agreement,» United Nations Framework Convention on Climate Change, 2020. [Online]. Available: <https://unfccc.int/process-and-meetings/the-paris-agreement/the-paris-agreement>. [Consultato il giorno 30 4 2020].
- [4] «Climate Change Data,» The World Bank, 2019. [Online]. Available: <https://data.worldbank.org/indicator/EG.ELC.RNWX.KH?end=2015&start=1960&view=chart>. [Consultato il giorno 30 4 2020].
- [5] «Renewables,» IEA, 2020. [Online]. Available: <https://www.iea.org/fuels-and-technologies/renewables>. [Consultato il giorno 30 4 2020].
- [6] «Roadmap to 2050,» IRENA, 2018. [Online]. Available: [https://www.irena.org/-/media/Files/IRENA/Agency/Publication/2018/Apr/IRENA\\_Report\\_GET\\_2018.pdf](https://www.irena.org/-/media/Files/IRENA/Agency/Publication/2018/Apr/IRENA_Report_GET_2018.pdf). [Consultato il giorno 30 4 2020].
- [7] «Electric power consumption (kWh per capita),» World Bank, 2019. [Online]. Available: <https://data.worldbank.org/indicator/EG.USE.ELEC.KH.PC>. [Consultato il giorno 1 5 2020].
- [8] «European Commission Launches Green Deal to Reset Economic Growth for Carbon Neutrality,» Europe, 2020. [Online]. Available: <https://sdg.iisd.org/news/european-commission-launches-green-deal-to-reset-economic-growth-for-carbon-neutrality/>. [Consultato il giorno 1 5 2020].
- [9] T. Hamane, «DAY 1 CSP S1 - Evolving Role of CSP with Thermal Energy Storage in National Power Systems. Dispatchable, Renewable and Affordable Power,» in *World Bank's MENA CSP KIP capstone online conference, Concentrating Solar for Power and Heat*, Tunisi, 2020.
- [10] M. Bellizim, «DAY 2 CSP S2 - Case Study on 24h dispatch from RE. DEWA IV CSP\_PV Hybrid (950MW) Project,» World Bank's MENA CSP KIP capstone online conference, Concentrating Solar for Power and Heat, Tunisi, 2020.
- [11] «Atacama Desert,» Comité solar e innovacion energetica, 2019. [Online]. Available: <https://www.comitesolar.cl/english/solar-committee/atacama-desert/>. [Consultato il giorno 11 5 2020].

- [12] «Abengoa Solar,» Abengoa, 2019. [Online]. Available: <http://www.abengoa.cl/web/es/areas-de-actividad/energia-solar/abengoa-solar/>. [Consultato il giorno 11 5 2020].
- [13] Masdar, «Noor Midelt Phase 1,» 2019.
- [14] «Morocco Breaks New Record with 800 MW Midelt 1 CSP-PV at 7 Cents,» Solar Paces, 24 5 2019. [Online]. Available: <https://www.solarpaces.org/morocco-breaks-new-record-with-800-mw-midelt-1-csp-pv-at-7-cents/>. [Consultato il giorno 20 5 2020].
- [15] G. Manzolini, «Solar and biomass power generation,» Polimi, Milan, 2019/2020.
- [16] A. Lucchini, «Heat and mass transfer,» Polimi, Milan, 2019/2020.
- [17] «Air mass (solar energy),» Wikipedia, 14 4 2020. [Online]. Available: [https://en.wikipedia.org/wiki/Air\\_mass\\_\(solar\\_energy\)](https://en.wikipedia.org/wiki/Air_mass_(solar_energy)). [Consultato il giorno 7 7 2020].
- [18] F. C. Fornaroli, «Solar and biomass power generation notes.pdf,» 2020.
- [19] M. A. S. P. Cristina Prieto Rios, «Centrales Solares,» ETSI, Seville, 2019/2020.
- [20] P. Heller, «Introduction to CSP systems and performance,» German Aerospace Center (DLR), Cologne, Germany, 2017.
- [21] J. M. B. J. B. a. T. A. Javier López Carvajal, «Developer view of the CSP evolution,» in *AIP Conference Proceedings 1850, 200002 (2017)*, 27 June 2017.
- [22] P. d. R. N. C. Pere Mir-Artigues, *The Economics and Policy of Concentrating Solar Power Generation*, Springer, 2019.
- [23] «Gemasolar Thermosolar Plant,» Wikipedia, 18 4 2020. [Online]. Available: [https://en.wikipedia.org/wiki/Gemasolar\\_Thermosolar\\_Plant](https://en.wikipedia.org/wiki/Gemasolar_Thermosolar_Plant). [Consultato il giorno 12 5 2020].
- [24] U. D. o. Energy, «2018 Renewable Energy Data Book,» 2018.
- [25] IRENA, «Renewable Energy Capacity Statistics 2020,» 2020.
- [26] J. G.-V. E. O. A. K. A. S. L. F. C. Angel G. Ferndandez, «Mainstreaming commercial CSP systems: A technology review,» Elsevier, Antofagasta, Chile, 2019.
- [27] S. A. P. B. M. B. S. M. W. Chris Deline, «Bifacial PV System Performance: Separating Fact from Fiction and Josh Stein,» NREL, Chicago, 2019.
- [28] S. P. A. Staff, «solar power authority,» 2020. [Online]. Available: <https://www.solarpowerauthority.com/a-history-of-solar-cells/>. [Consultato il giorno 25 5 2020].



- 
- [29] IRENA, «Data&Statistics,» IRENA, 2020. [Online]. Available: <http://resourceirena.irena.org/gateway/dashboard/?topic=3&subTopic=32>. [Consultato il giorno 14 5 2020].
- [30] N. K. f. N. R. E. L. (NREL), «Solar panel,» [Online]. Available: [https://commons.wikimedia.org/wiki/File:ModulePVeфф\(rev200708\).png](https://commons.wikimedia.org/wiki/File:ModulePVeфф(rev200708).png). [Consultato il giorno 30 7 2020].
- [31] A. Casalegno, «Electrochemical Conversion and Storage,» POLIMI, Milan, 2019/2020.
- [32] D. Z. f. L.- u. R. e. (. G. A. C. I. o. E. T. | . T. P. T. Dan Bauer, «Carnot-Batteries,» 2019. [Online]. Available: <https://www.nedo.go.jp/content/100899761.pdf>. [Consultato il giorno 31 7 2020].
- [33] \*. H. J. a. D. B. Wolf-Dieter Steinmann, «Thermodynamic Analysis of High-Temperature Carnot Battery Concepts,» WILEY-VCH Verlag GmbH & Co. KGaA, Weinheim, 2019.
- [34] «VC-Funded Thermal “Battery” is Based on CSP Molten Salt Energy Storage,» SoalrPACES, [Online]. Available: <https://www.solarpaces.org/vc-funded-thermal-battery-based-molten-salt-energy-storage-csp/>. [Consultato il giorno 31 7 2020].
- [35] Michael, «CSP Storage Beyond Sunbelt for Global Energy Transition from Fossil to Renewables Converting Coal Plants into Storage Plants,» 2019.
- [36] «Make Carnot Batteries with Molten Salt Thermal Energy Storage in ex-Coal Plants,» SolarPACES, [Online]. Available: <https://www.solarpaces.org/make-carnot-batteries-with-molten-salt-thermal-energy-storage-from-ex-coal-plants/>. [Consultato il giorno 31 7 2020].
- [37] M. Geyer, «Dispatchable Solar. Complementarity of CSP, Thermal Storage, PV and Batteries,» in *World Bank CSP conference*, Tunisi, 2020.
- [38] L. D. Y. Y. Z. Y. L. Y. Jianxing Wang, «Study on the general system integration optimization method of the solar aided coal-fired power generation system,» Elsevier Ltd, 2018.
- [39] A. L. E. G. Sergio Rech, «Optimum integration of concentrating solar technologies in a real coal-fired power plant for fuel saving,» Elsevier Ltd, 2018.
- [40] F. A. O. M. I. Sorour Alotaibi, «Solar-assisted steam power plant retrofitted with regenerative system using Parabolic Trough Solar Collectors,» Elsevier Ltd, Kuwait, 2020.
- [41] M. B. R. K. Oliver Garbrecht, «Increasing fossil power plant flexibility by integrating molten-salt thermal storage,» Elsevier Ltd, Aachen, Germany, 2017.
- [42] G. B. F. B. L. C. S. C. A. O. D. P. a. A. Z. Linda Barelli, «Dynamic Analysis of a Hybrid Energy Storage System (H-ESS) Coupled to a Photovoltaic (PV) Plant,» energies MDPI, 2018.
- [43] M. L. O. M. a. E. Q. B. Macabebe, «Feasibility Study on Thermoelectric Conversion to Improve Photovoltaic Operation,» Internation Solar Energy Society, 2015.

- [44] A. Insights, «How to accelerate the transition to renewables with Hybrid PV-CSP systems,» 2020.
- [45] S. Kraemer, «CSP Doesn't Compete With PV – it Competes with Gas,» SolarPACES, 11 10 2017. [Online]. Available: <https://www.solarpaces.org/csp-competes-with-natural-gas-not-pv/>. [Consultato il giorno 22 8 2020].
- [46] J. Lowry, *Avoiding Carbon Apocalypse Through Alternative Energy: Life After Fossil Fuels*, Springer, 2017.
- [47] W. Z. W. T. G. v. d. S. M. v. d. B. Bas van Zuijle, «Cost-optimal reliable power generation in a deep decarbonisation future,» Elsevier Ltd, 2019.
- [48] b. o. a. p. w. b. B. H. e. a. 2. - . O. w. d. f. F.-G. c. c. By Maulucioni, «Köppen-Geiger Climate Classification Map,» Wikipedia, [Online]. Available: <https://commons.wikimedia.org/w/index.php?curid=76770997>. [Consultato il giorno 8 7 2020].
- [49] «South Africa,» IEA, [Online]. Available: <https://www.iea.org/countries/south-africa>. [Consultato il giorno 9 7 2020].
- [50] A. d. Toit, «Explaining the Persistence of Rural Poverty in South Africa,» Addis Ababa, 2017.
- [51] «South Africa,» e.i.a., [Online]. Available: <https://www.eia.gov/international/analysis/country/ZAF>. [Consultato il giorno 9 7 2020].
- [52] «Africa,» IEA, [Online]. Available: <https://www.iea.org/regions/africa>. [Consultato il giorno 9 7 2020].
- [53] «Metadata Glossary,» The World Bank Data, [Online]. Available: <https://databank.worldbank.org/metadataglossary/ida-results-measurement-system/series/EN.ATM.PM25.MC.ZS>. [Consultato il giorno 9 7 2020].
- [54] «South Africa Energy Outlook,» IEA, [Online]. Available: <https://www.iea.org/articles/south-africa-energy-outlook>. [Consultato il giorno 9 7 2020].
- [55] «World,» IEA, [Online]. Available: <https://www.iea.org/world>. [Consultato il giorno 9 7 2020].
- [56] «Access to electricity (% of population) - South Africa,» The World Bank , [Online]. Available: <https://data.worldbank.org/indicator/EG.ELC.ACCS.ZS?locations=ZA>. [Consultato il giorno 9 7 2020].
- [57] mineral resources and energy department of South Africa, [Online]. Available: <http://www.energy.gov.za/>. [Consultato il giorno 9 7 2020].

- [58] «KOMATI POWER STATION,» Eskom, [Online]. Available: <http://www.eskom.co.za/sites/heritage/Pages/KOMATIPOWERSTATION.aspx>. [Consultato il giorno 9 7 2020].
- [59] «The revival of Komati,» Eskom, [Online]. Available: <http://www.eskom.co.za/news/Pages/Feb9.aspx>. [Consultato il giorno 9 7 2020].
- [60] «Grootvlei Power Station,» Eskom, [Online]. Available: [http://www.eskom.co.za/Whatweredoing/ElectricityGeneration/PowerStations/Coal/Pages/Grootvlei\\_Power\\_Station.aspx](http://www.eskom.co.za/Whatweredoing/ElectricityGeneration/PowerStations/Coal/Pages/Grootvlei_Power_Station.aspx). [Consultato il giorno 9 7 2020].
- [61] «Camden Power Station,» Eskom, [Online]. Available: [http://www.eskom.co.za/Whatweredoing/ElectricityGeneration/PowerStations/Coal/Pages/Camden\\_Power\\_Station.aspx](http://www.eskom.co.za/Whatweredoing/ElectricityGeneration/PowerStations/Coal/Pages/Camden_Power_Station.aspx). [Consultato il giorno 9 7 2020].
- [62] «Camden Power Station,» Eskom, [Online]. Available: <http://www.eskom.co.za/sites/heritage/Pages/Camden.aspx>. [Consultato il giorno 9 7 2020].
- [63] «Eskom's future CSP plans (to 2030),» Eskom, [Online]. Available: [www.eskom.co.za/AboutElectricity/RenewableEnergy/ConcentratingSolarPower/Pages/Eskom\\_Future\\_CSP\\_Plans.aspx](http://www.eskom.co.za/AboutElectricity/RenewableEnergy/ConcentratingSolarPower/Pages/Eskom_Future_CSP_Plans.aspx). [Consultato il giorno 9 7 2020].
- [64] Eskom, «Transmission Development Plan 2018-2028,» 2017.
- [65] Eskom, «Transmission Development Plan 2019-2029,» 2018.
- [66] «SAM,» NREL, [Online]. Available: <https://sam.nrel.gov/financial-models/utility-scale-ppa.html>. [Consultato il giorno 2020 7 29].
- [67] «wheather data,» climate.onebuilding, [Online]. Available: [http://climate.onebuilding.org/WMO\\_Region\\_1\\_Africa/ZAF\\_South\\_Africa/index.html](http://climate.onebuilding.org/WMO_Region_1_Africa/ZAF_South_Africa/index.html). [Consultato il giorno 6 8 2020].
- [68] «Weather Data,» NREL, [Online]. Available: <https://sam.nrel.gov/weather-data>. [Consultato il giorno 6 8 2020].
- [69] I. B. Lillo, «Instalaciones Fotovoltaicas,» ETSI, Sevilla, 2019.
- [70] A. Insights, «PV + Storage Cheaper than Coal in India».
- [71] W. Platzer, «PV–Enhanced Solar Thermal Power,» Fraunhofer Intitute for Solar Energy Systems, Heidenhofstr, Freiburg, Germany, 2013.
- [72] R. Z. Y. Y. K. P. J. E. O. P. T. Chao Li, «Annual performance analysis and optimization of a solar tower aided coalfired power plant,» Elsevier Ltd., 2019.
- [73] A. Insights, «Policy and Regulatory Considerations in Deploying Storage for Power Systems in Developing Countries,» 2020.

- [74] A. insights, «The present and future of CSP and thermal storage from the European perspective,» 2020.
- [75] A. G. Devineni Gireesh Kumar, «Technological Developments in Direct Grid Connected Power Converters for Solar PV Power Plants,» International Journal of Engineering and Advanced Technology (IJEAT), 2019.